

5th Summer School, Hellenic Astronomical Society, UOI
16-20 September 2024

MHD: solar and stellar activity

Prof. Vasilis Archontis

Department of Physics
University of Ioannina

Overview

- **Topics**

- Magnetic Fields in Astrophysics.

- Magnetic Flux Emergence.

- Eruptions.

- Jets.

- Heating in the Solar Atmosphere.

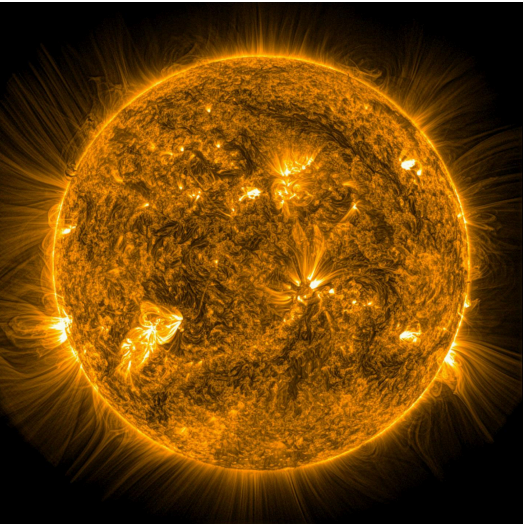
- Flux emergence in F-type stars.

- **Summary**

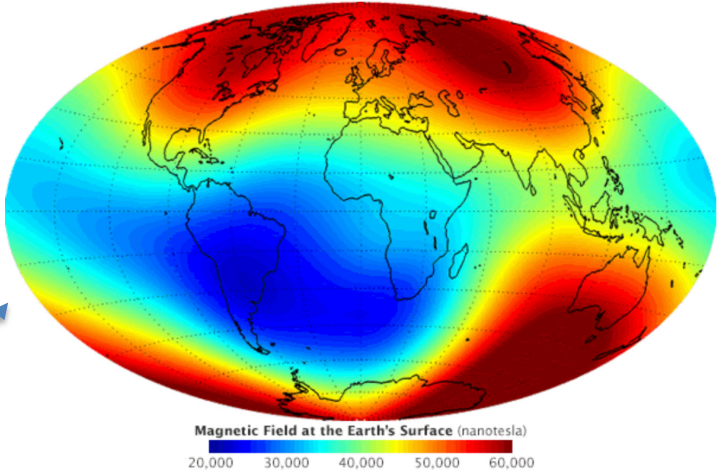
- Recent Advances.

- Future Challenges.

Observed Magnetic Fields in Astrophysics



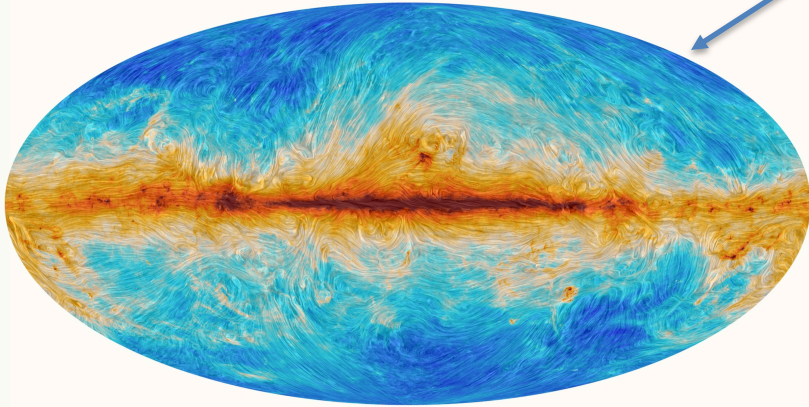
Stars: Our Sun (NASA/SDO)



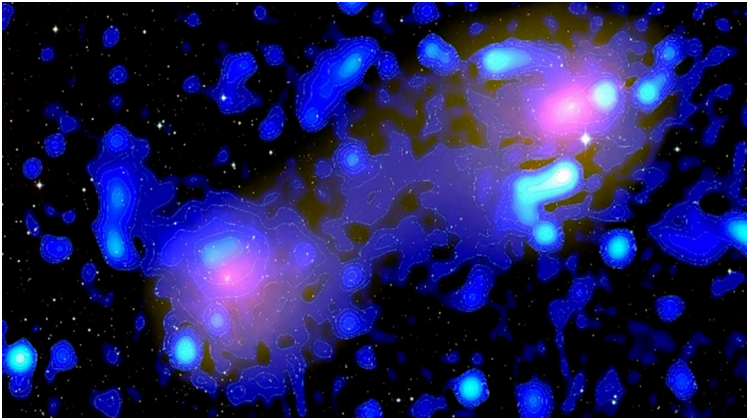
Magnetic Field at the Earth's Surface (nanotesla)
20,000 30,000 40,000 50,000 60,000

Planets: Earth (ESA/Swarm)

Magnetic fields are ubiquitous in Cosmos.



Galaxies: Milky Way (ESA/Planck satellite)



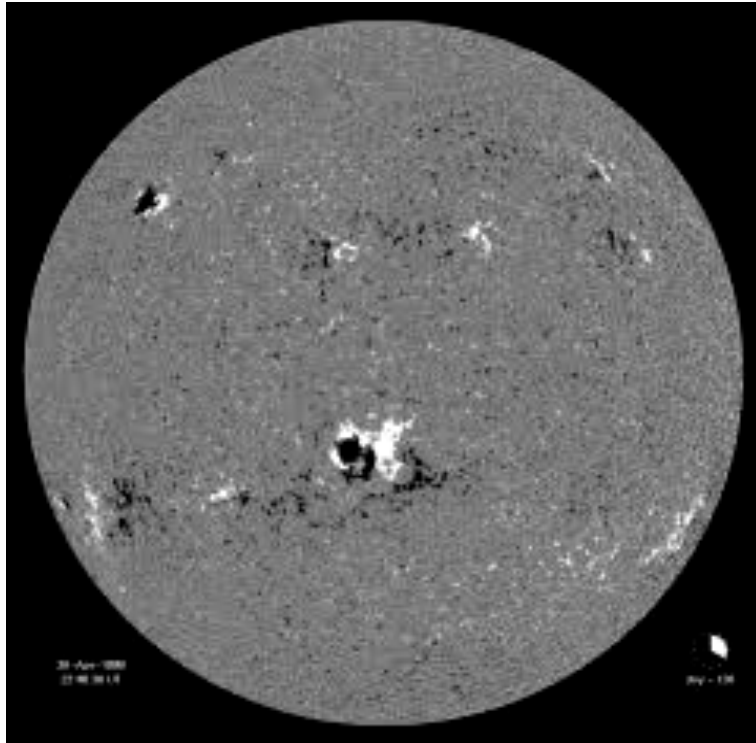
Universe: Between two galaxies (Govoni, F. et.al, 2019, Science)

Magnetic Flux Emergence

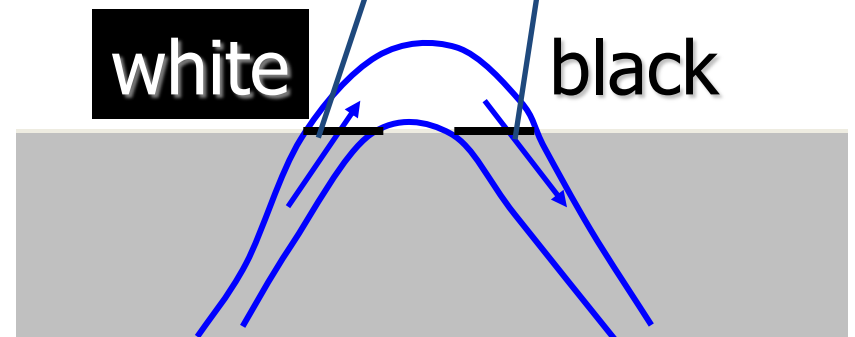
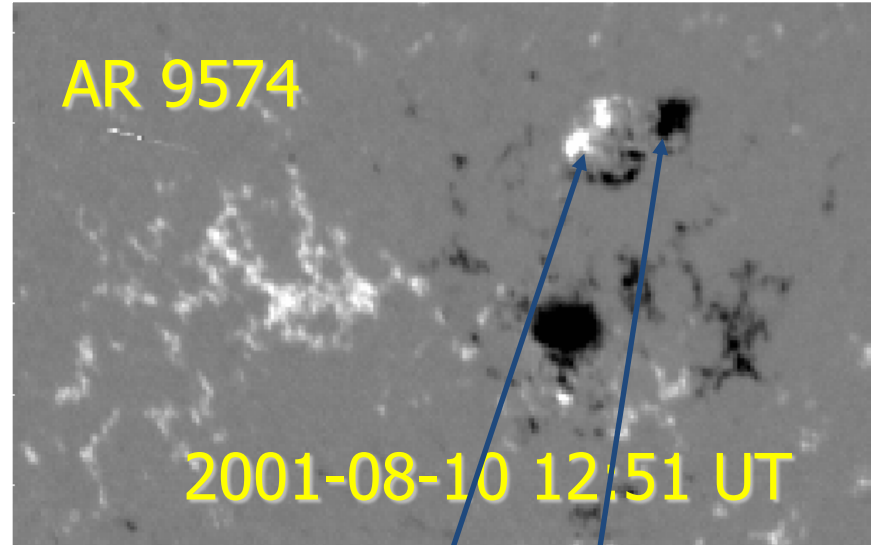
- Observations.
- Flux emergence simulations.
- Emergence at the photosphere.
- Emergence in the corona.
- Comparison to observations.
- Formation of Active Regions.

Magnetic Flux Emergence in the Sun: Observations & Theory.

MFE in a full disk magnetogram.



MDI magnetogram around an Active Region.



Emerging magnetic field forms sunspots

Mechanism of Magnetic Flux Emergence

- **Dynamo** action at/below the base (?) of convection zone.
- **Magnetic buoyancy** acts on the dynamo-generated magnetic field.

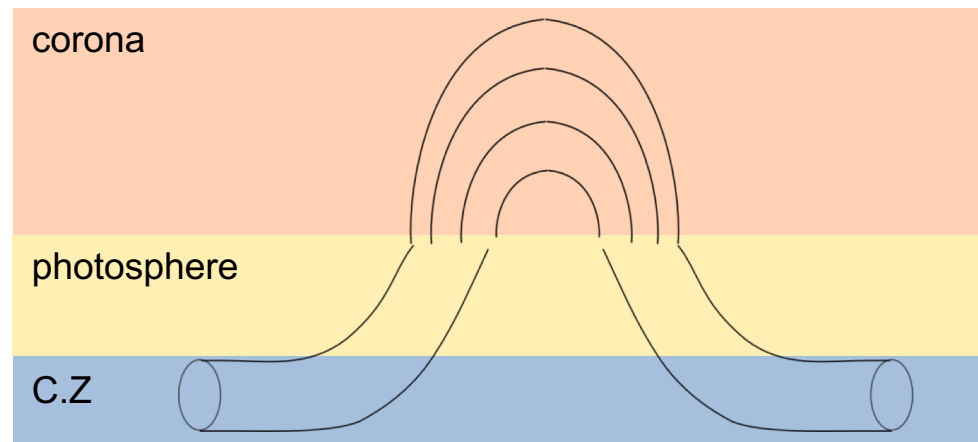
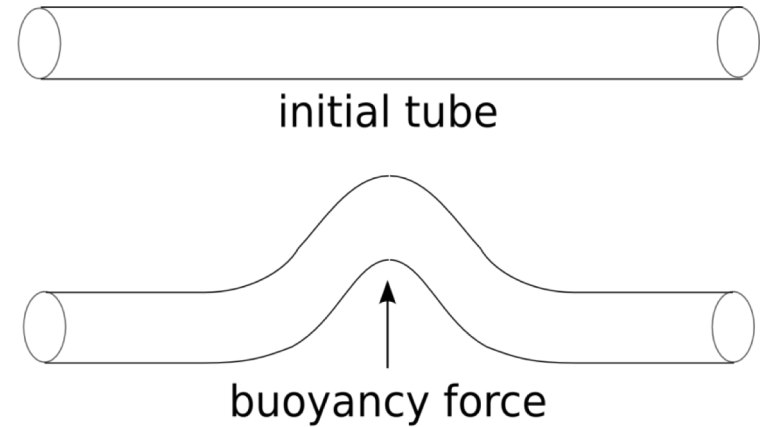
- Total pressure continuous $P_i + (B_i)^2/2\mu = P_e$.
- Thermal equilibrium $T_i = T_e$.
- Then, since $P_i < P_e \rightarrow r_i < r_e$.
- B tube becomes lighter and rises (Parker 1955).

Bipolar regions appear at the photosphere (Fox, 1908).

Twisted structures appear in EFR (Strous & Zwaan, 1999 – Leka et.al, 1996).

Formation of W-loops and arch filament systems (Bruzek, 1967).

Observations of eruptive phenomena, flares, CME's due to flux emergence (Chifor et. al, 2006, Dun et.al 2007, etc.).



Simulations: Type I

- Single flux tube.
- No realistic convection.
- Use MHD (resistive)

Numerical experiments: MHD equations

$$\begin{aligned}\frac{\partial \rho}{\partial t} &= -\nabla \cdot (\rho \mathbf{u}), \\ \frac{\partial (\rho \mathbf{u})}{\partial t} &= -\nabla \cdot (\rho \mathbf{u} \otimes \mathbf{u} + \underline{\underline{\tau}}) - \nabla p + \rho \mathbf{g} + \frac{\mathbf{J}}{c} \times \mathbf{B}, \\ \frac{\partial e}{\partial t} &= -\nabla \cdot (e \mathbf{u}) - p \nabla \cdot \mathbf{u} + Q_{\text{Joule}} + Q_{\text{visc}},\end{aligned}$$

Mass,
momentum and
energy conservation eqs.

$$\begin{aligned}\frac{\partial \mathbf{B}}{\partial t} &= -c \nabla \times \mathbf{E}, \\ \mathbf{E} &= -\frac{\mathbf{u}}{c} \times \mathbf{B} + \eta \frac{\mathbf{J}}{c^2}, \\ \mathbf{J} &= \frac{c}{4\pi} \nabla \times \mathbf{B},\end{aligned}$$

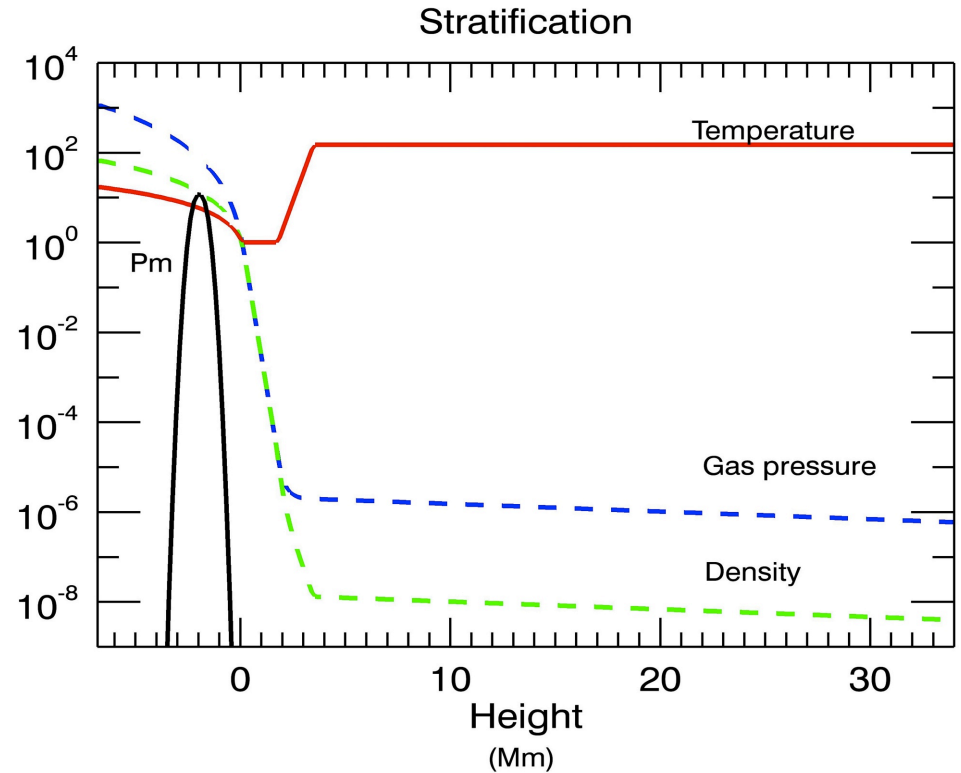
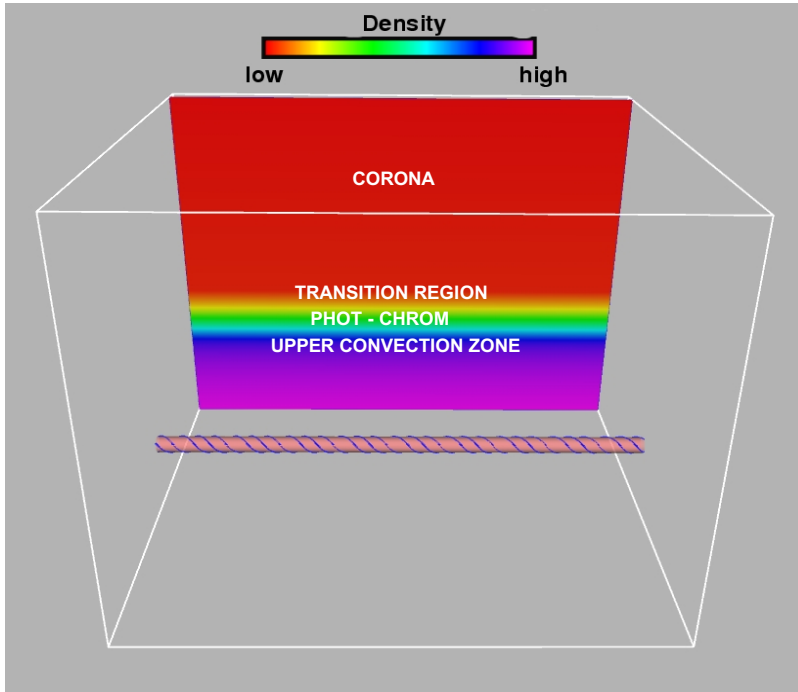
Faraday,
Ohm and
Ampere's law.

$$p = \rho T \frac{\mathcal{R}}{\bar{\mu}},$$

EOS.

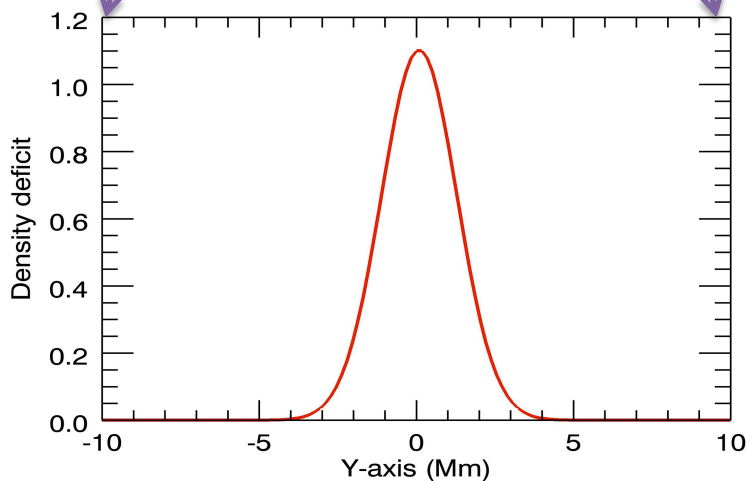
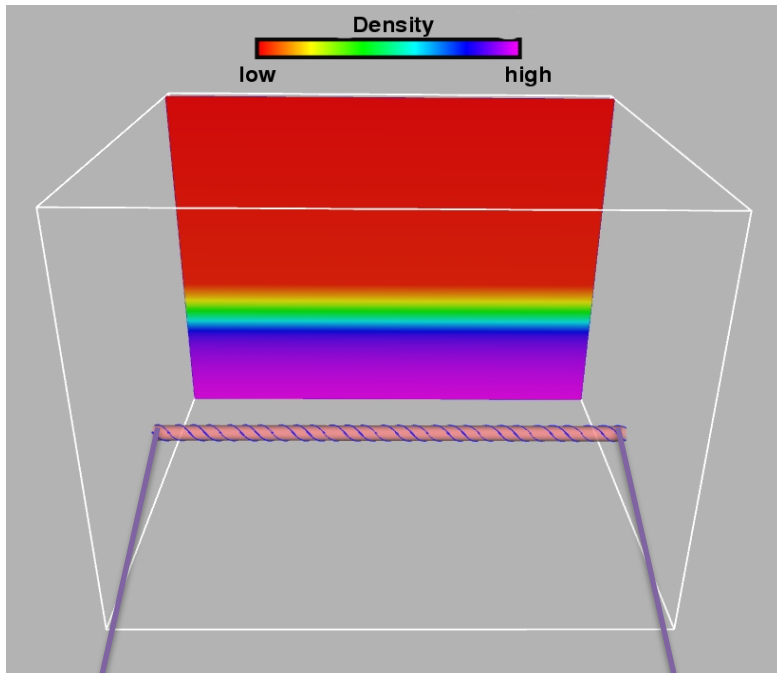
Thermodynamics: ideal gas, no heat conduction, no radiative cooling.

Magnetic Flux Emergence: Simulations



- Stratified (plane-parallel) atmosphere.
- Magnetic flux tube (twisted).
- Density deficit \rightarrow buoyancy.
- Ambient magnetic field.
- Atmosphere, magnetic field(s).
- Large density and pressure contrast.
- Hydrostatic equilibrium.
- 3D resistive MHD (Lare3d code).

Initial Conditions



Flux tube magnetic field

$$\mathbf{B} = (0, B_{\theta}(r), B_y(r))$$

$$B_y = B_0 e^{-r^2/R^2}, \quad B_{\theta} = \alpha r B_y$$

Coronal magnetic field

$$B_c = B_c(z) (\cos\phi, \sin\phi, 0)$$

Density deficit

$$\frac{\rho_m}{\rho_b} = \frac{p_m}{p_b} e^{-y^2/\lambda^2},$$

Parameters

$$\text{Radius } (R) = 425 \text{ Km},$$

$$\text{Twist } (\alpha) = 0.1 - 0.4,$$

$$B_0 = 3 - 4 \text{ kG},$$

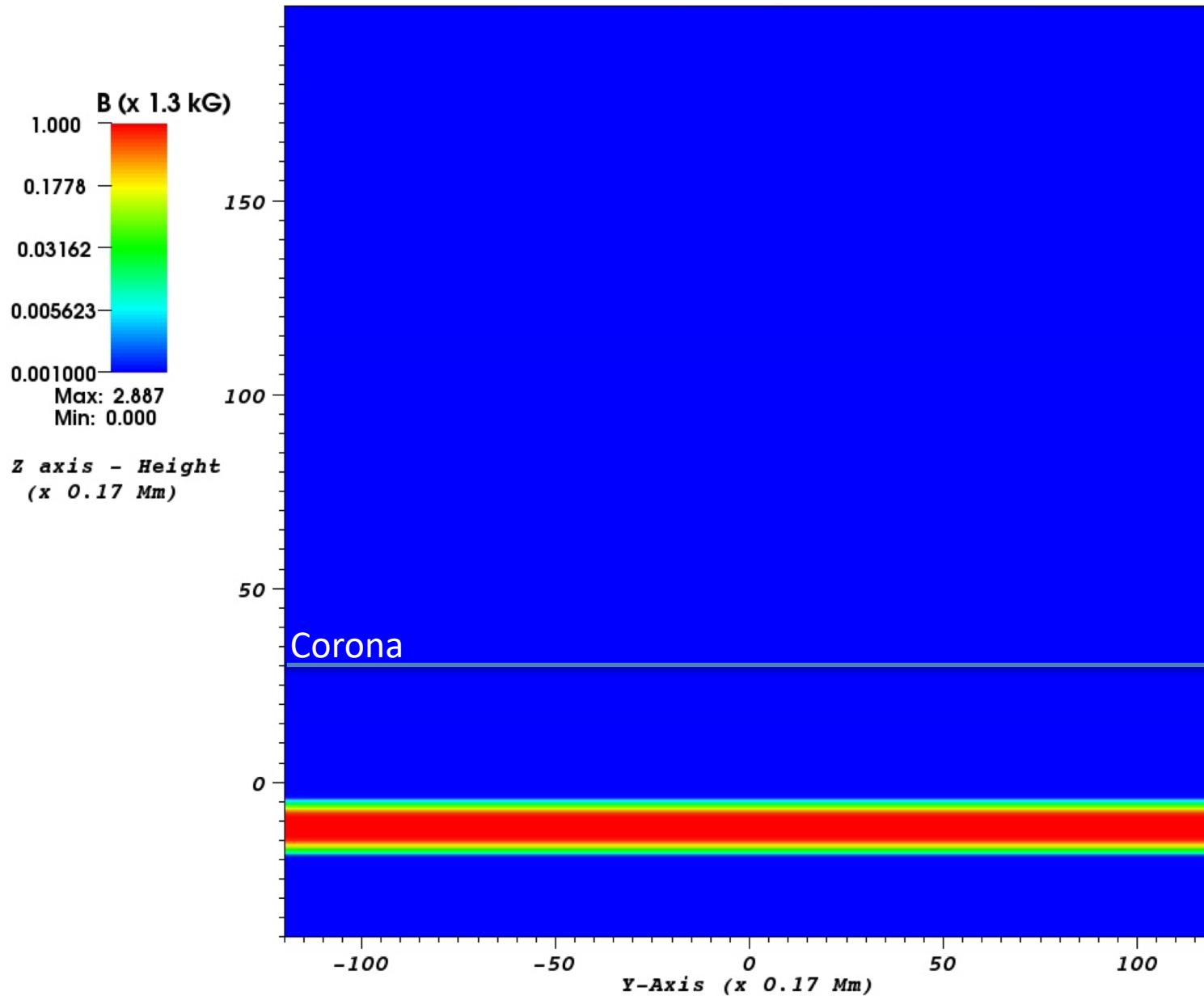
$$B_c(z) = 10 \text{ G},$$

$$\text{Buoyant part } (\lambda) = 3 - 4 \text{ Mm},$$

$$\text{Deficits} : \rho_m, p_m,$$

$$\text{Background plasma} : \rho_b, p_b$$

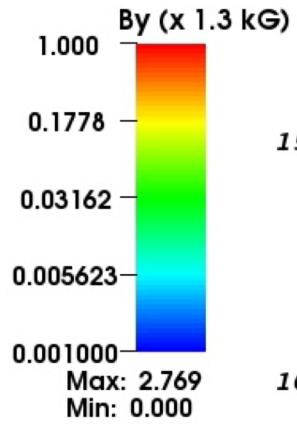
B_y (along the tube)



168 min (total)

Time=0

B_y (cross section / mid-plane)



Z axis - Height
(x 0.17 Mm)

150

100

50

Corona

0

-100

-50

0

50

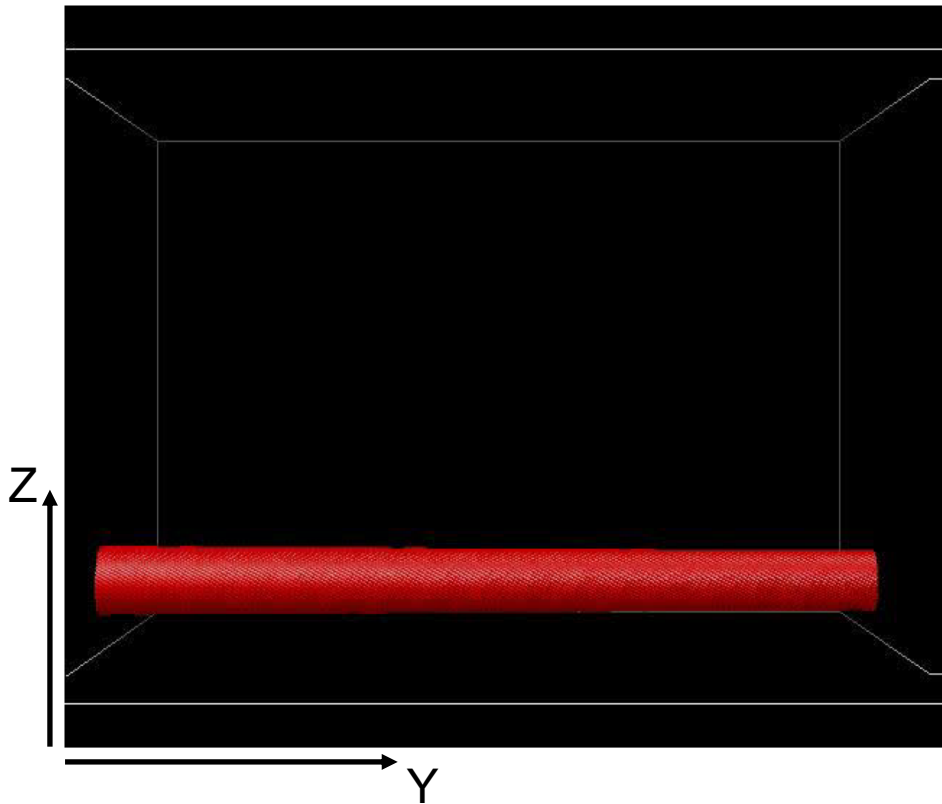
100

X-Axis (x 0.17 Mm)

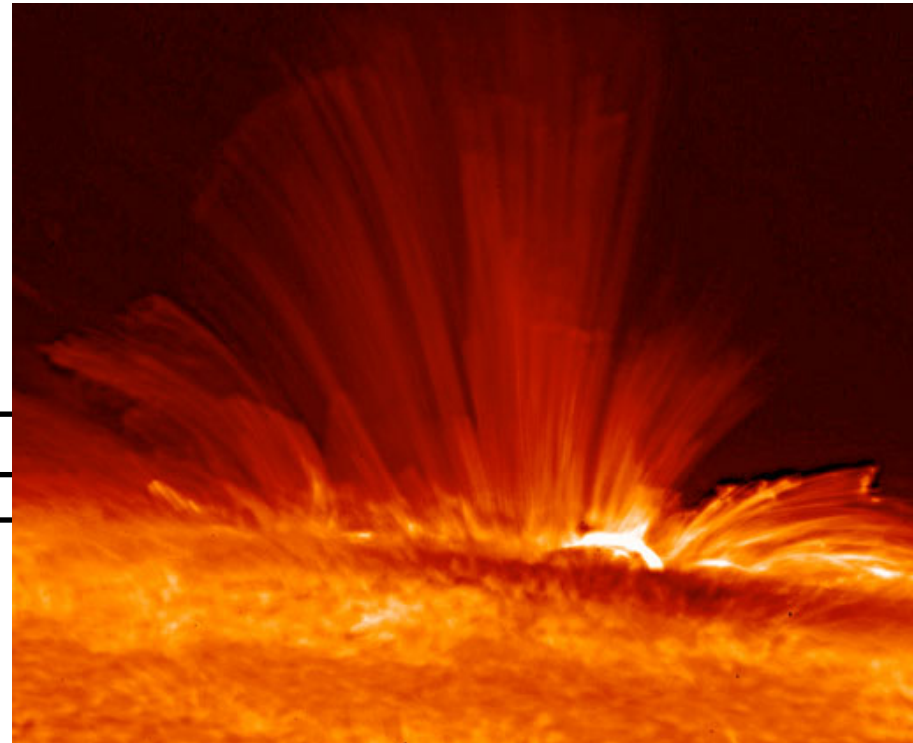


168 min (total)

3D Emergence, Formation of Coronal Loops



- The tube is more buoyant in the middle.
- Fieldlines expand in three directions.
- Strongly azimuthal nature at the top.
- Fan-like shape of the expanding field.



Velocities:

$V_{\text{rise_init}}$: $V_z \sim 2$ km/sec

$V_{\text{max}} \sim 14$ km/sec

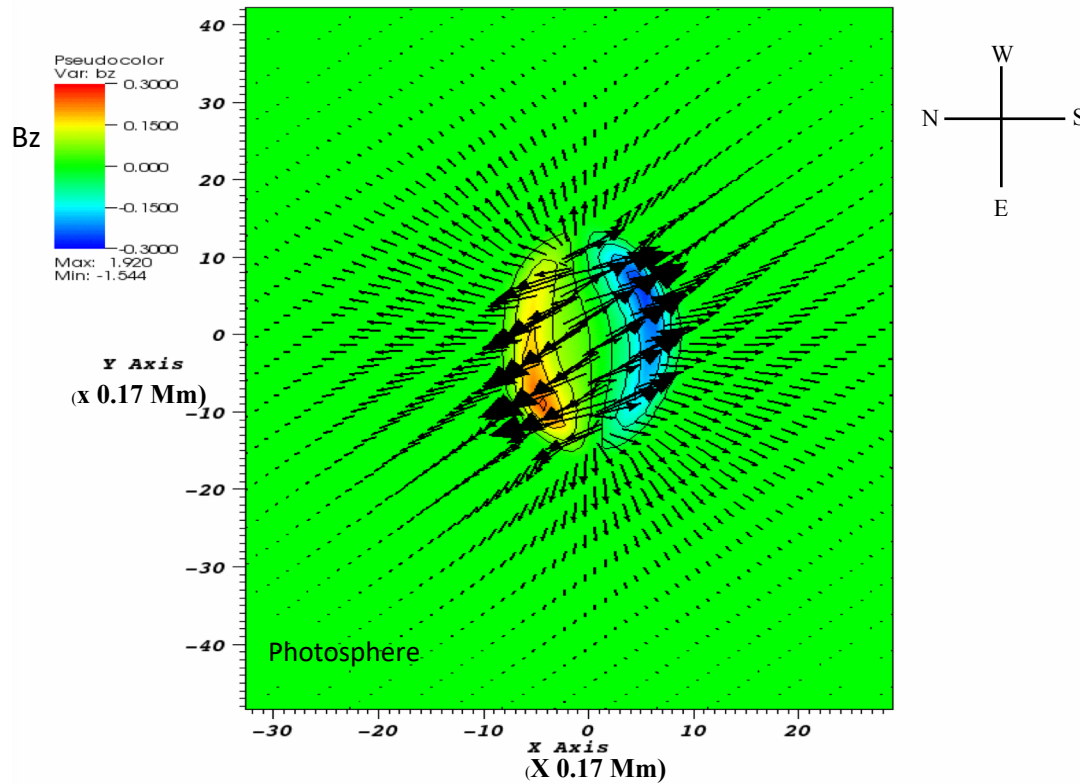
$V_x \sim 47$ km/sec

$V_y \sim 34$ km/sec

$V_{\text{downf}} \sim 20$ km/sec

Parametric study: e.g. Archontis, et.al. A&A (2004)

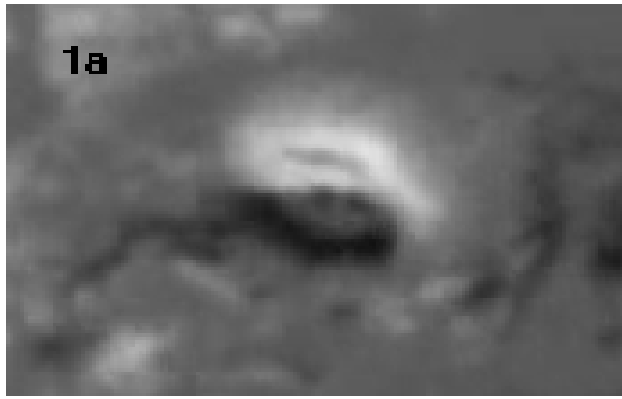
Formation of Magnetic Bipoles and “Tails”



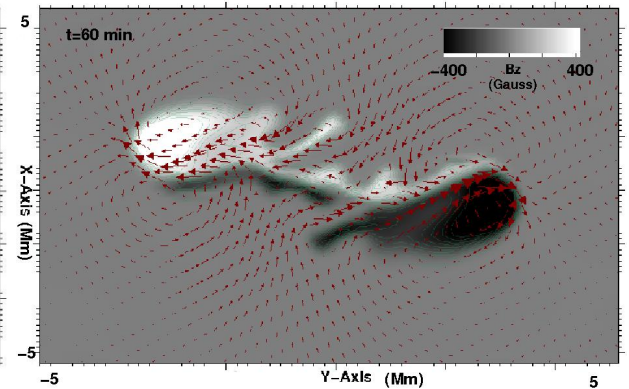
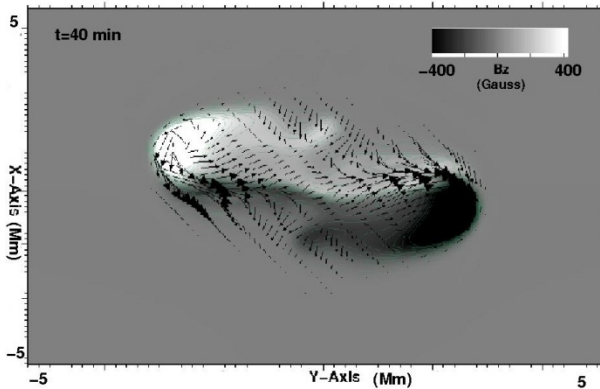
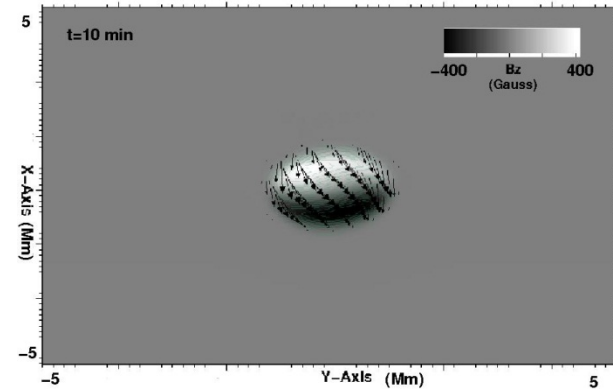
- $V_{\text{rise}}=1.7$ km/sec, $t=12.5$ min.
- Formation of a bipolar region.
- $B \sim 600\text{G}$ at the photosphere.
- Formation of ‘**tails**’ on both sides of PIL.
- Organized **shear** velocity flow along the PIL.
- **Inflow** in the transverse direction.

Observations (NOAA AR 10808) vs. Simulations

Observations



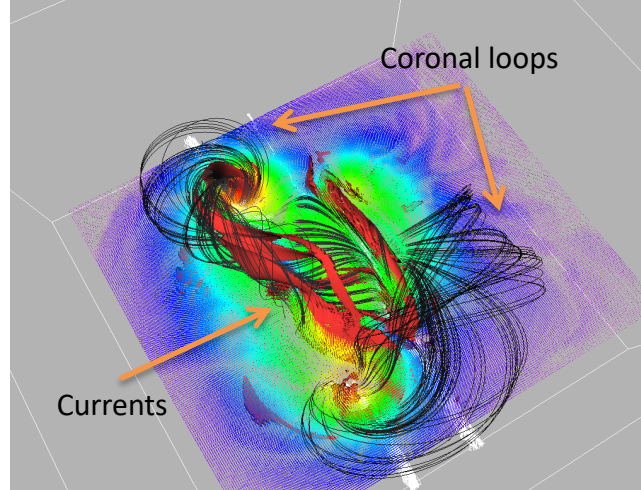
Simulations



Magnetic 'tails': a twisted flux tube is emerging from below (Archontis & Hood, A&A (2010)).

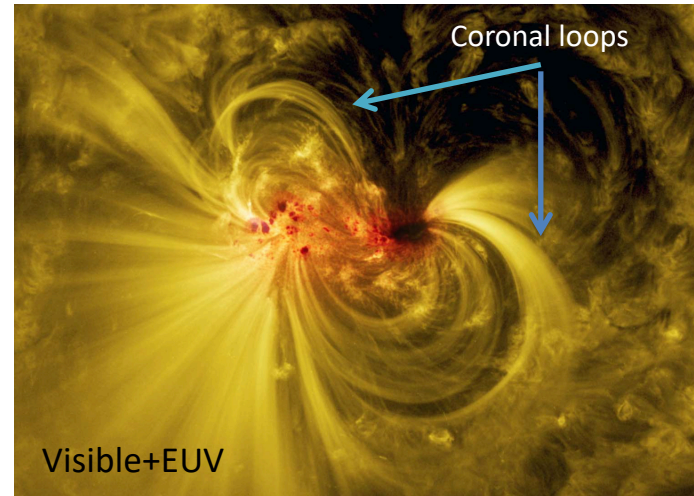
Formation of ARs and sigmoids

Simulations: Archontis & Hood, ApJL (2008)

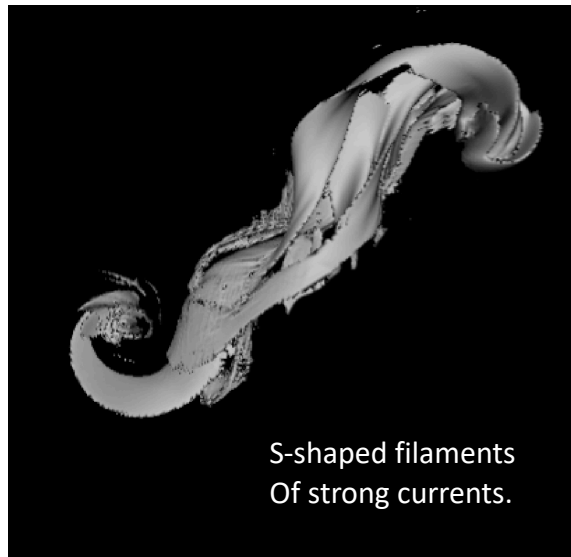


ARs

Observations: AR12665 2017 (NASA/SDO)

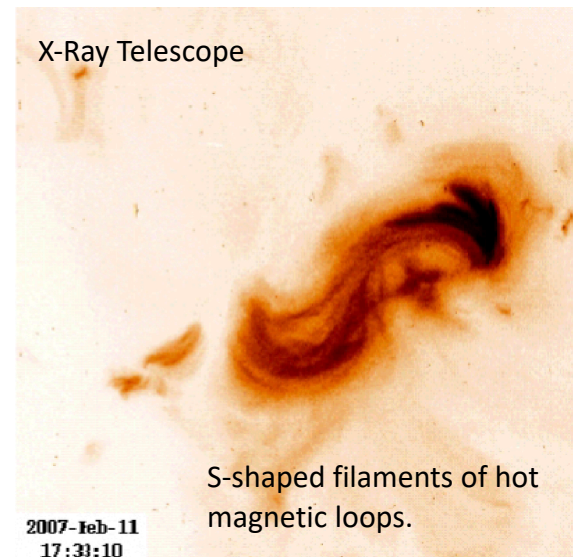


Simulations: Archontis, V. et.al, ApJ (2009)



Sigmoids

Observations: McKenzie & Canfield, ApJ (2008)

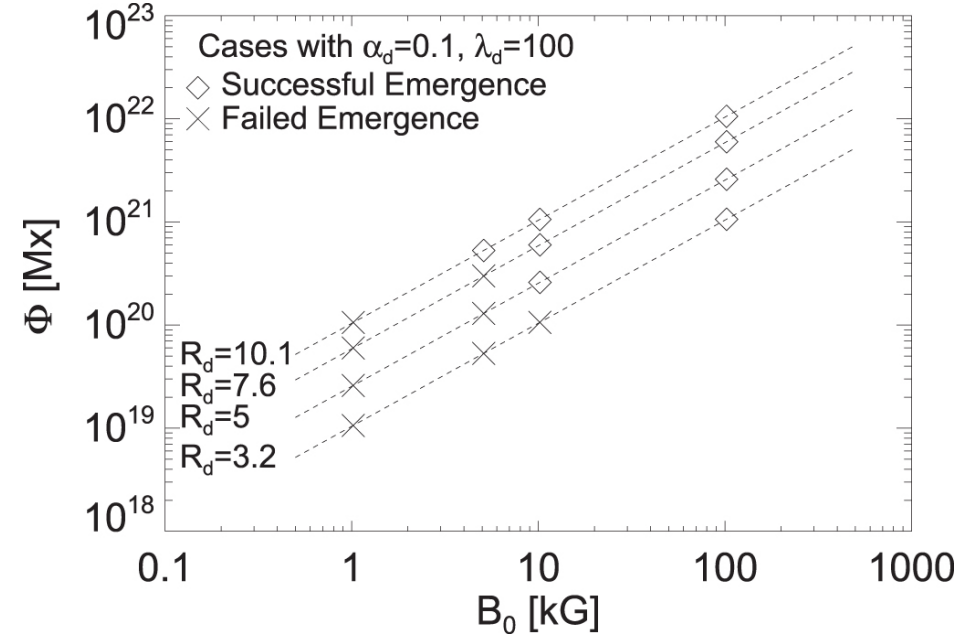


Simulations: Type II

- Single flux tube.
- Parametric study.
- Failed vs. successful emergence.
- MHD (resistive).

Parametric study I

Case	B_{0d} ($\times B_c$)	R_d ($\times H_c$)	λ_d ($\times H_c$)	α_d ($\times H_c^{-1}$)	Φ (Mx)
1*	3.4	3.2	100	0.1	1.1×10^{19}
2*	3.4	5	100	0.1	2.6×10^{19}
3*	3.4	7.6	100	0.1	6.0×10^{19}
4*	3.4	10.1	100	0.1	1.1×10^{20}
5*	17	3.2	100	0.1	5.3×10^{19}
6*	17	5	100	0.1	1.3×10^{20}
7*	17	7.6	100	0.1	3×10^{20}
8	17	10.1	100	0.1	5.3×10^{20}
9*	34	3.2	100	0.1	1.1×10^{20}
10	34	5	100	0.1	2.6×10^{20}
11	34	7.6	100	0.1	6.0×10^{20}
12	34	10.1	100	0.1	1.1×10^{21}
13	340	3.2	100	0.1	1.1×10^{21}
14	340	5	100	0.1	2.6×10^{21}
15	340	7.6	100	0.1	6.0×10^{21}
16	340	10.1	100	0.1	1.1×10^{22}



B_{0d} (B-tube's strength), $B_c=300$ G.

R_d (radius of tube), $H_c=180$ km.

λ_d (length of buoyant part of the tube).

a_d (twist).

Φ (tube's initial flux).

Cases with constant λ_d and a_d .

The initial magnetic flux Φ cannot indicate directly whether the magnetic structure will emerge or not to the surface.

Parametric study II

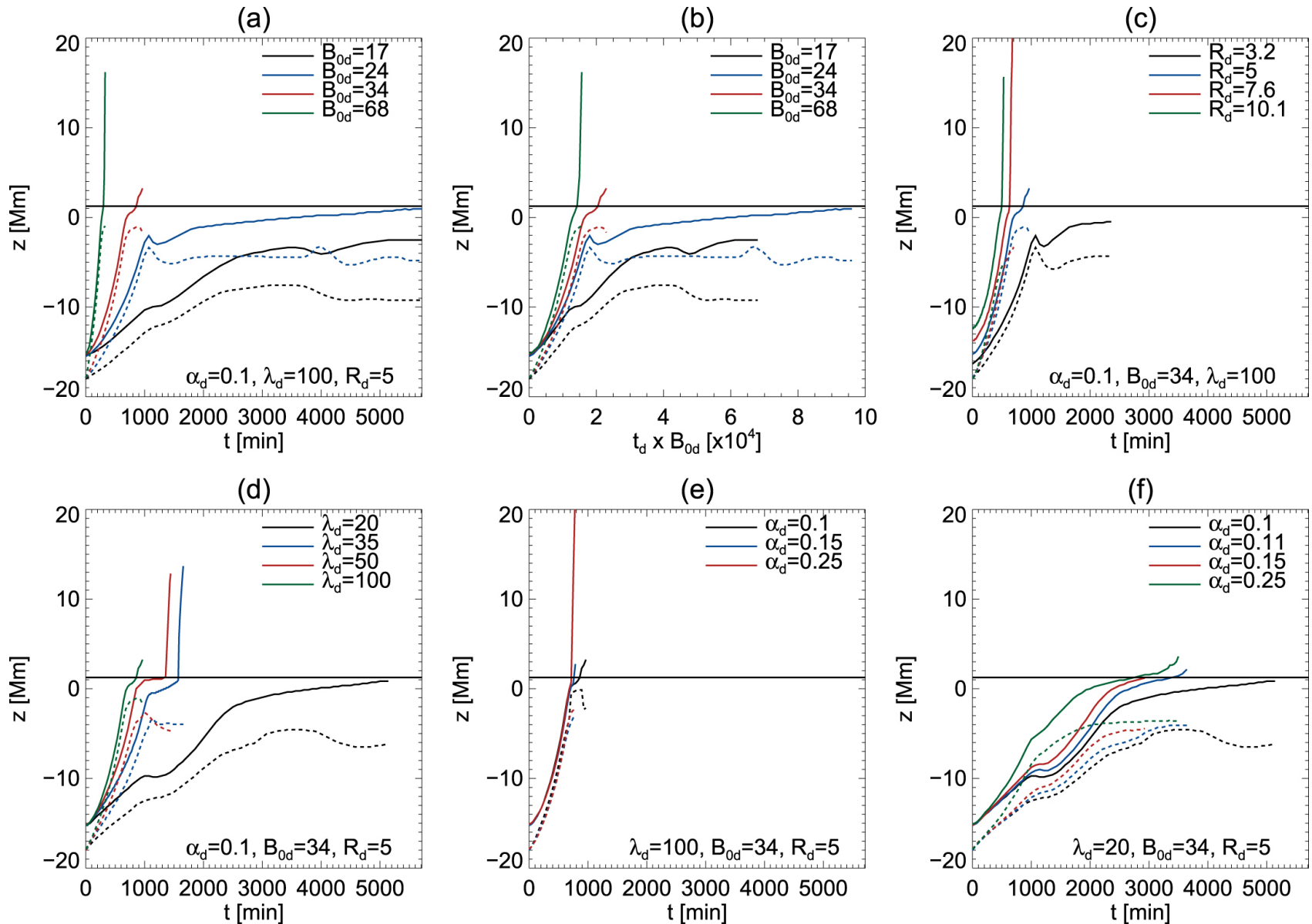
Case	B_{0d} ($\times B_c$)	R_d ($\times H_c$)	λ_d ($\times H_c$)	α_d ($\times H_c^{-1}$)	Φ (Mx)
1*	17	5	100	0.1	1.3×10^{20}
2*	24	5	100	0.1	1.8×10^{20}
3	34	5	100	0.1	2.6×10^{20}
4	68	5	100	0.1	5.1×10^{20}
5	34	3.2	100	0.1	1.1×10^{20}
6	34	7.6	100	0.1	6.0×10^{20}
7	34	10.1	100	0.1	1.1×10^{21}
8*	34	5	20	0.1	2.6×10^{20}
9	34	5	35	0.1	2.6×10^{20}
10	34	5	50	0.1	2.6×10^{20}
11	34	5	100	0.15	2.6×10^{20}
12	34	5	100	0.25	2.6×10^{20}
13	34	5	20	0.11	2.6×10^{20}
14	34	5	20	0.15	2.6×10^{20}
15	34	5	20	0.25	2.6×10^{20}
16*	34	3.2	50	0.1	1.1×10^{20}
17*	44	5	10	0.1	3.4×10^{20}
18*	24	5	20	0.1	1.8×10^{20}
19*	24	5	20	0.25	1.8×10^{20}
20	24	7.6	100	0.1	4.3×10^{20}
21*	17	7.6	100	0.1	3.0×10^{20}

Change all parameters.

Keep only $\Phi=10^{20}$ - 10^{21} Mx.

* = "failed" emergence.

Parametric study II



Conclusions

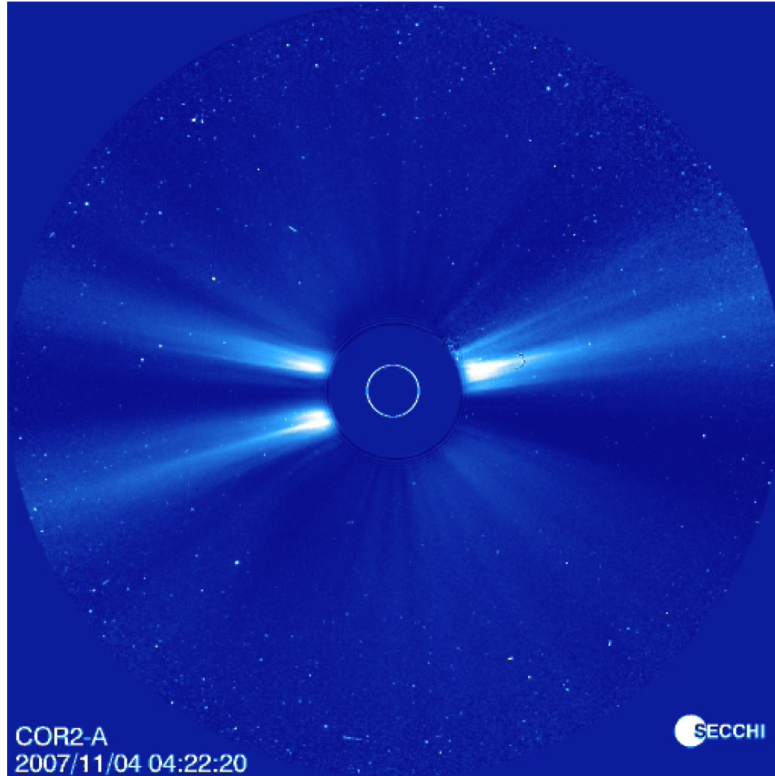
- Magnetic flux alone is not sufficient to estimate whether the magnetic field will emerge, especially below 10^{21} Mx.
- The magnetic field is more efficiently transferred upward when B_0 or R increases. In most cases, this also applies to the twist.
- A highly curved flux tube (small λ) with low twist emerges less efficiently than a lower curvature flux tube (large λ) with similar twist.
- In a highly curved flux tube, increasing the twist does not necessarily lead to efficiency of the emergence. There are cases where a more strongly twisted flux tube can eventually bring less magnetic field closer to the photosphere than a more weakly twisted flux tube.
- Tubes with initially high- B_0 (weak- B_0) may fail (succeed) to emerge to the photosphere, depending on their geometrical properties.

Eruptions

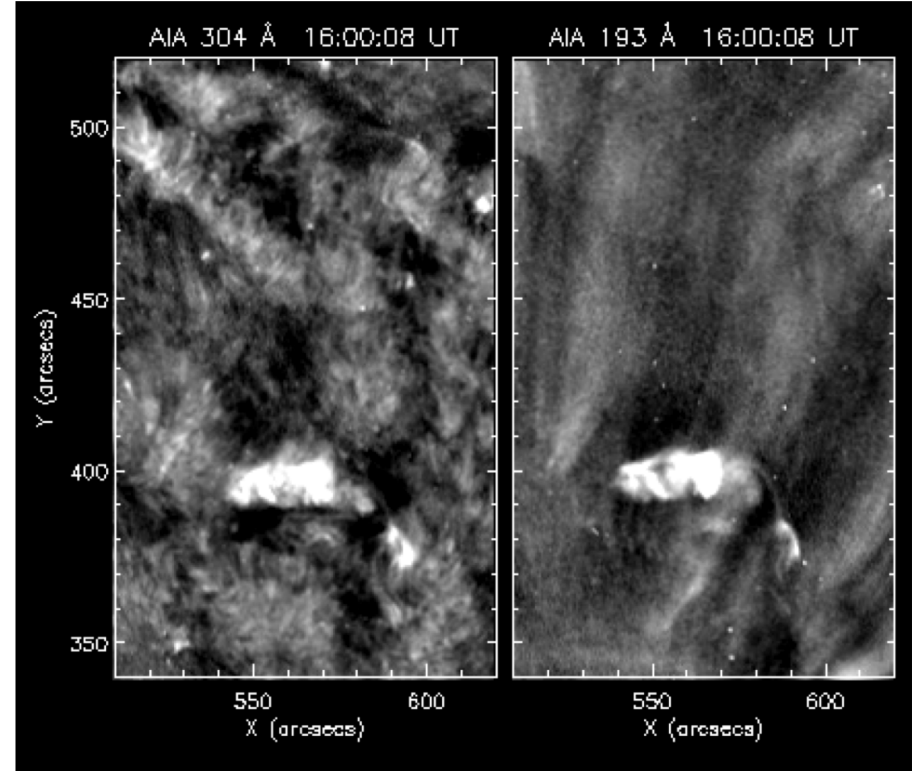
- Observations.
- Theoretical interpretation.
- Simulations.
- Formation of erupting flux ropes.
- Connection to CMEs.

Observations: Eruptions on various scales

Coronal Mass Ejections

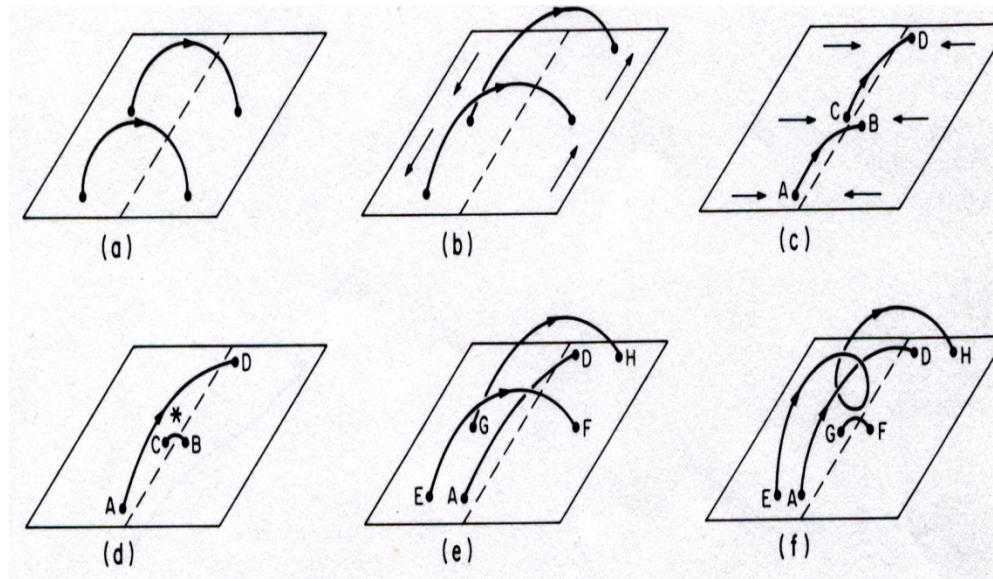


Small-scale filament eruptions



- Huge explosions, billion tons of plasma into space.
- Space weather, Sun-Earth connection.
- High-speeds (\sim up to 10^4 km/s).
- Flux-rope-like structure.
- Erupting cool material, a few Mm size.
- Simultaneous hot and cool emission (EUV, H α).
- Wide jet (200-300 km/sec).

Theory: Formation of (erupting) filaments



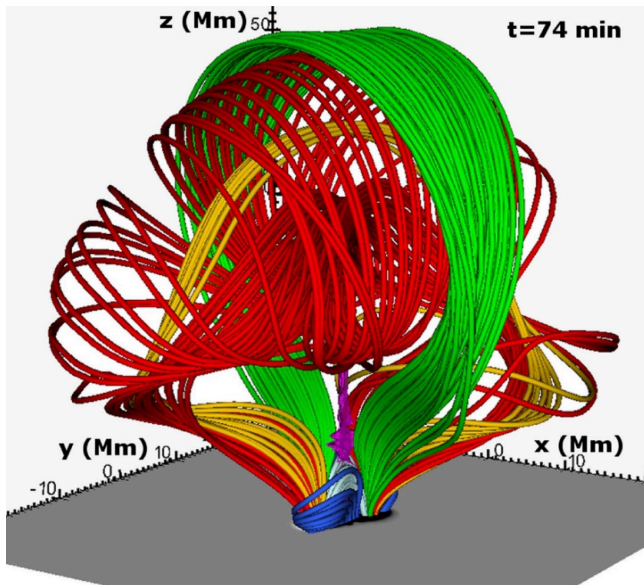
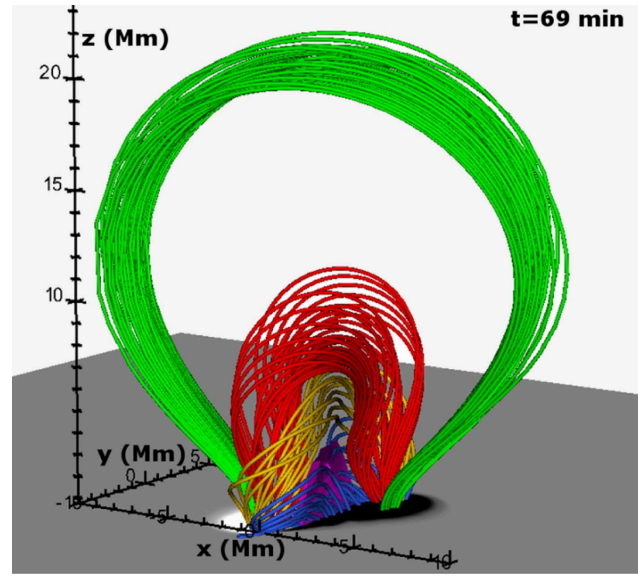
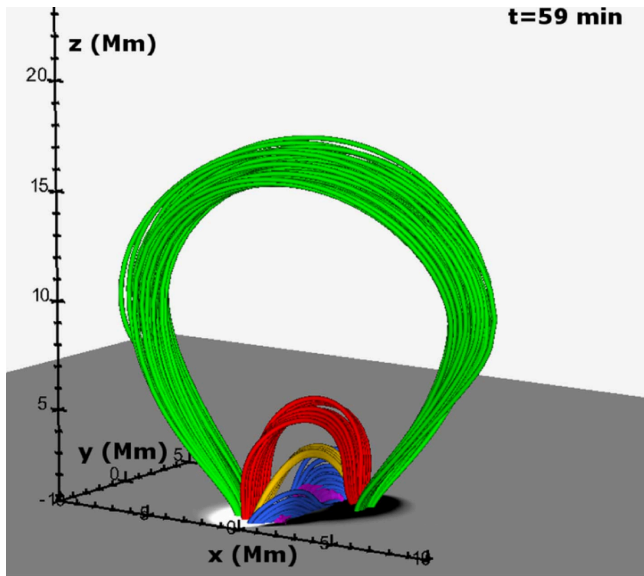
A. van Ballegooijen and P. Martens (1989)

Shearing motion + Convergence + Reconnection

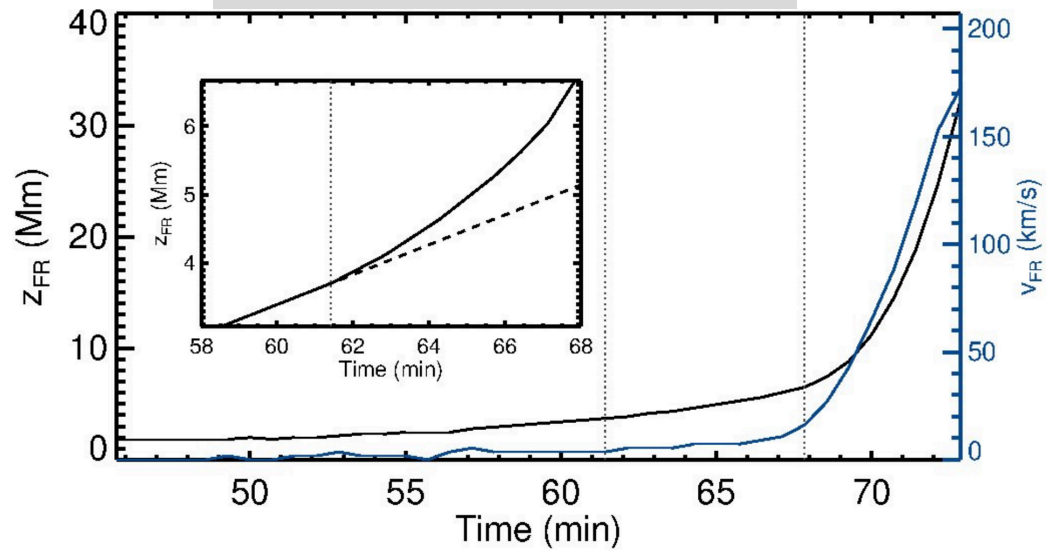


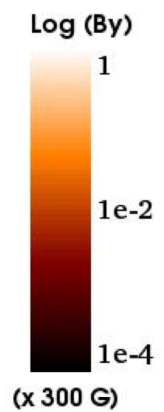
Current sheets, longer loops and helical magnetic field structures, which might erupt.

Simulations: Formation of (erupting) flux-ropes

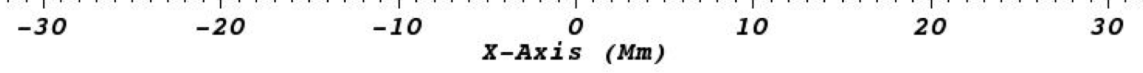
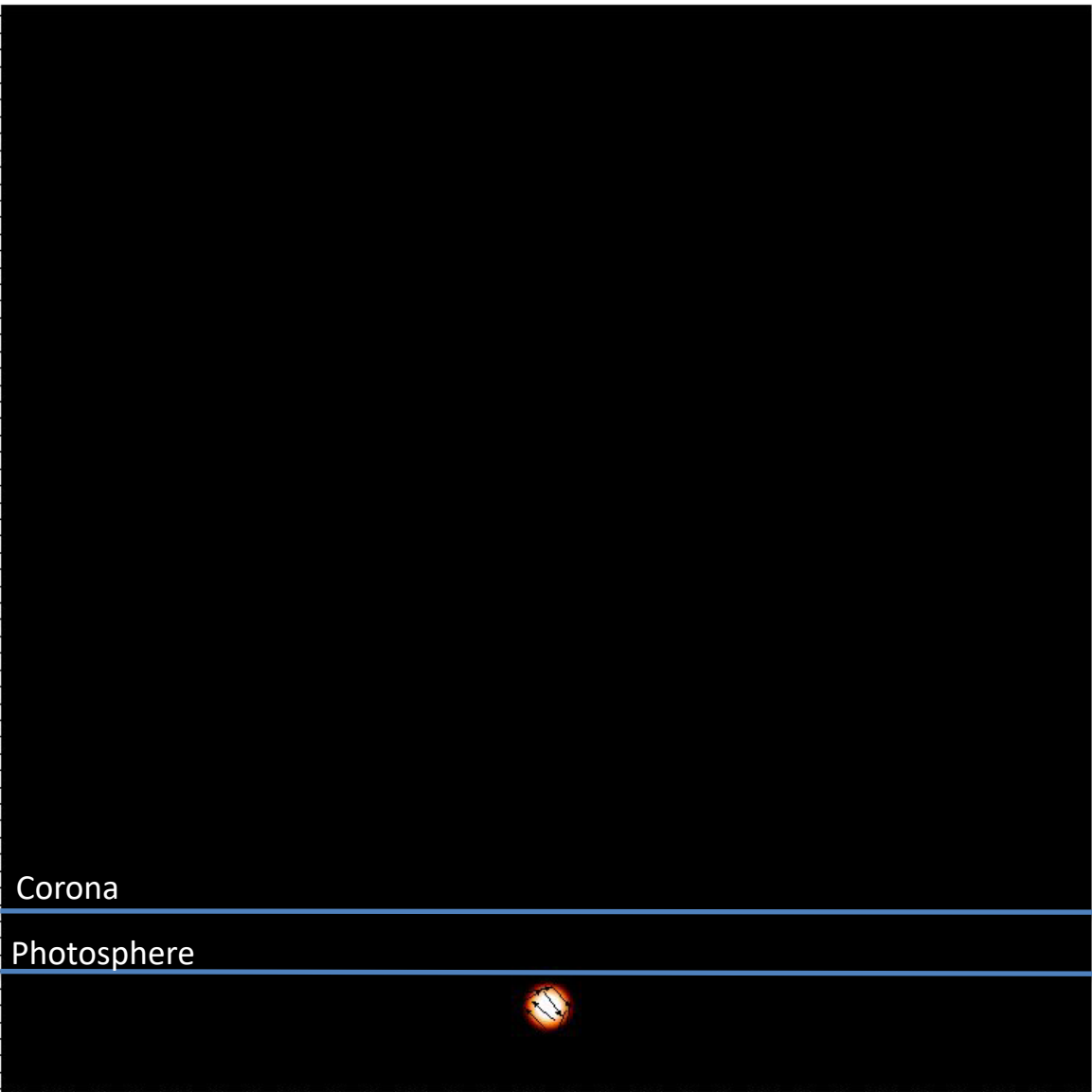
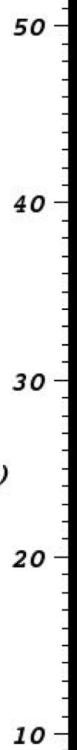


Syntelis, Archontis, Tsinganos, ApJ, (2017)





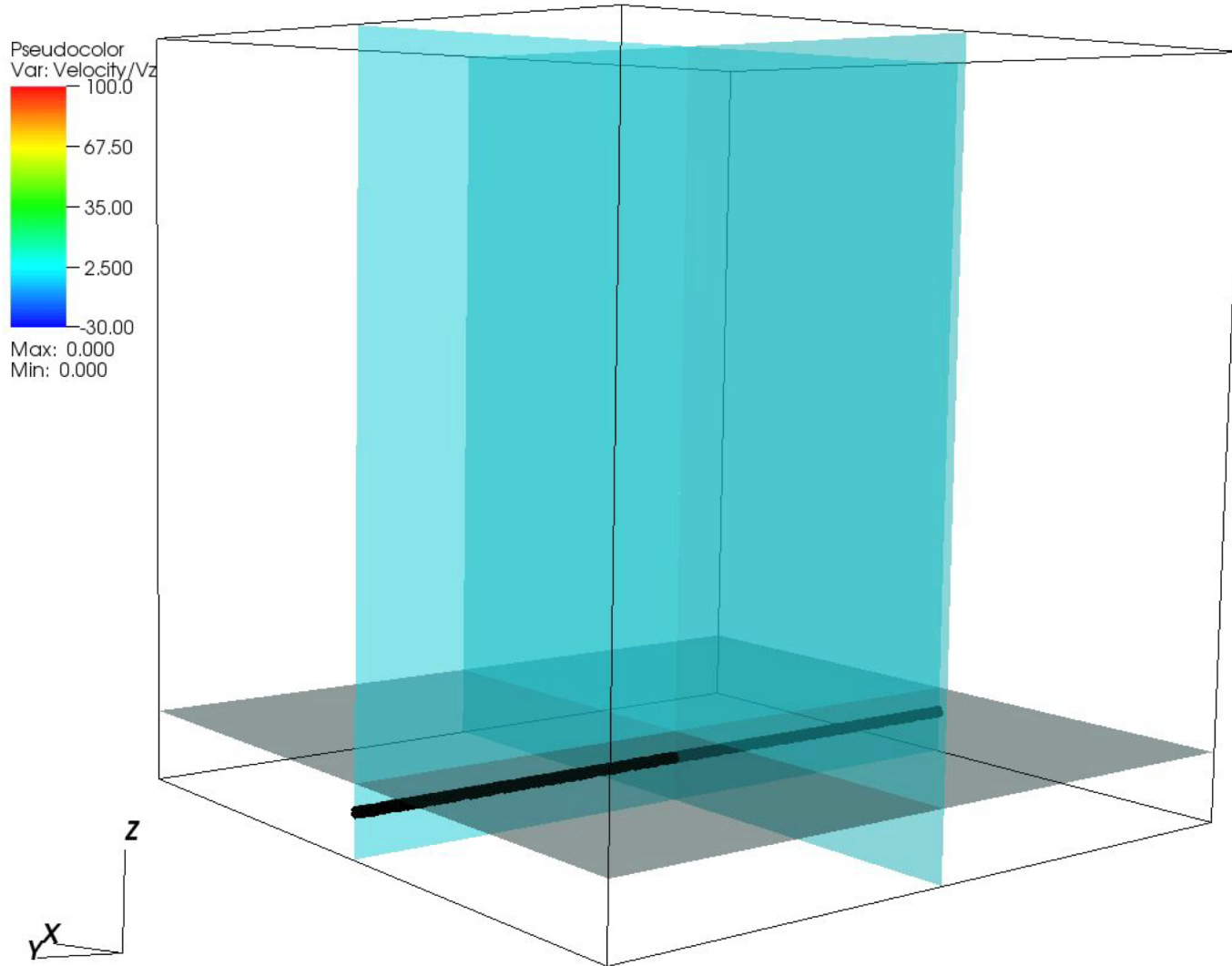
Y-Axis (Mm)



135 minutes (in total)

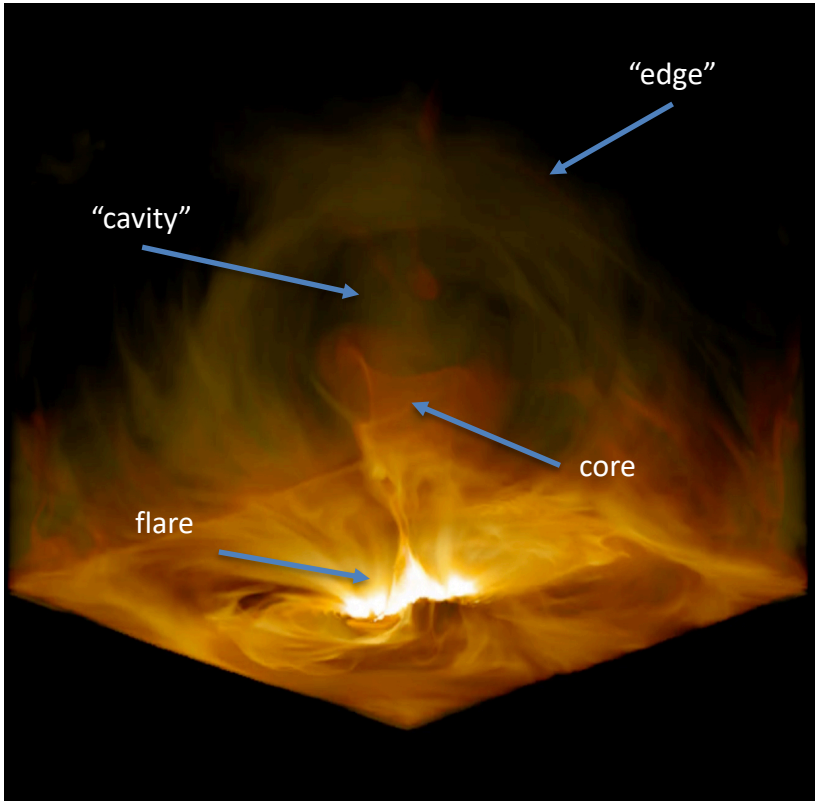
DB: 0000.cfd
Cycle: 0 Time:0

Vertical velocity (Vz)



Simulations: Eruptions of CME-like structures

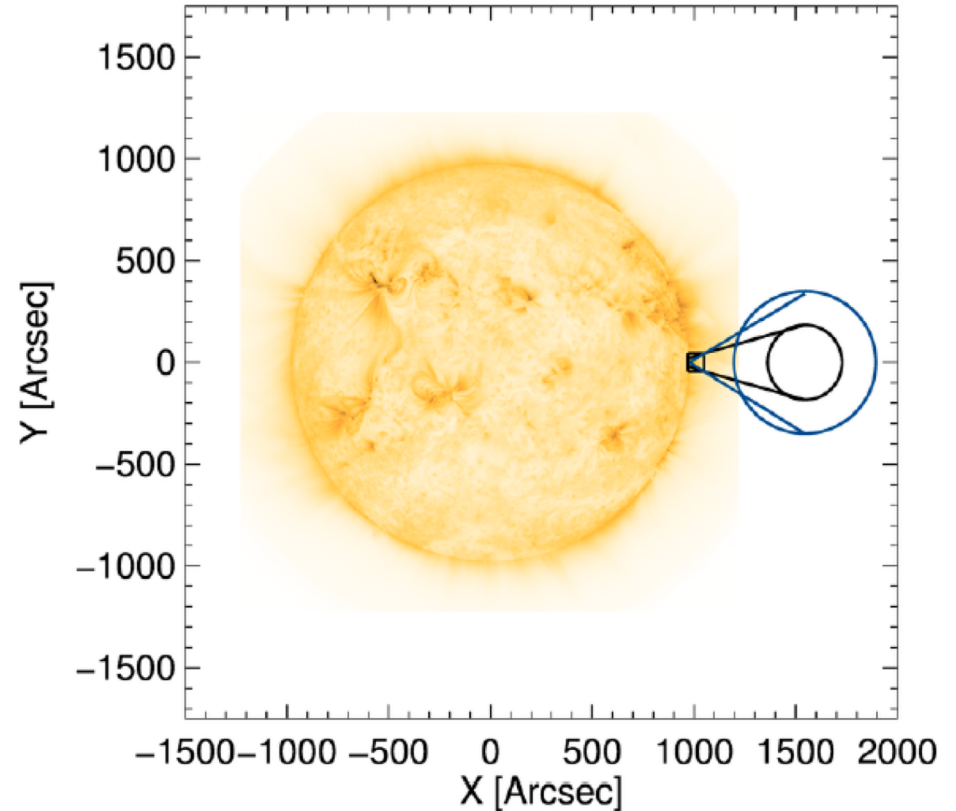
Simulations: synthetic images of eruptions



- AIA 170A + AIA 304A
- Dense plasma in the core.
- Hot and cool erupting plasma.
- Flare (5×10^6 K).

Nindos, et.al, ApJ, 808, 117, (2015)

Simulations: extrapolated size of the eruptions



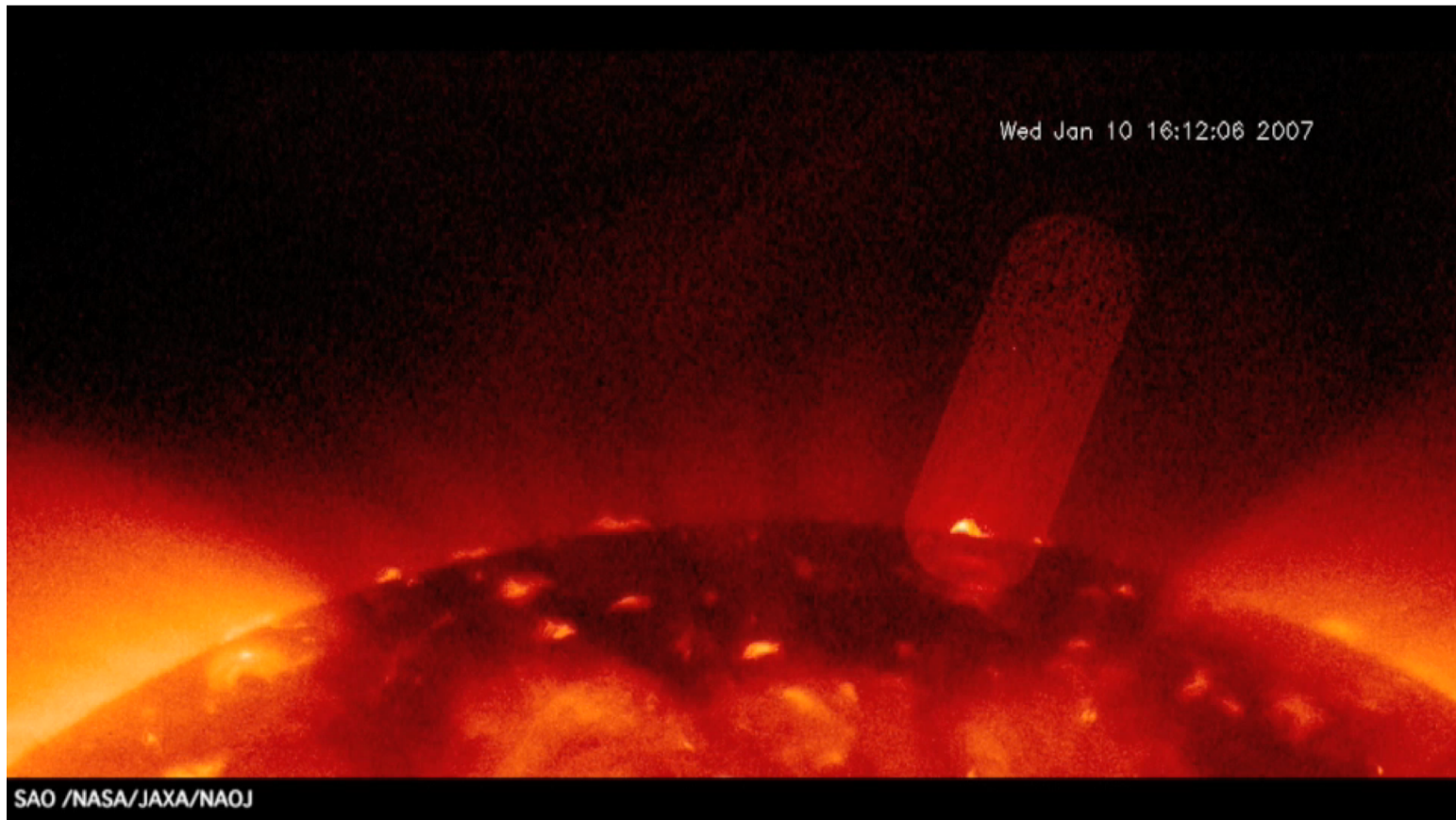
- Extrapolation at $0.6 R_{\odot}$.
- Length of the flux rope ~ 100 Mm
- Energy $\sim 10^{28}$ erg
- Small CMEs.

Syntelis, Archontis, Tsinganos, ApJ, (2017)

Jets

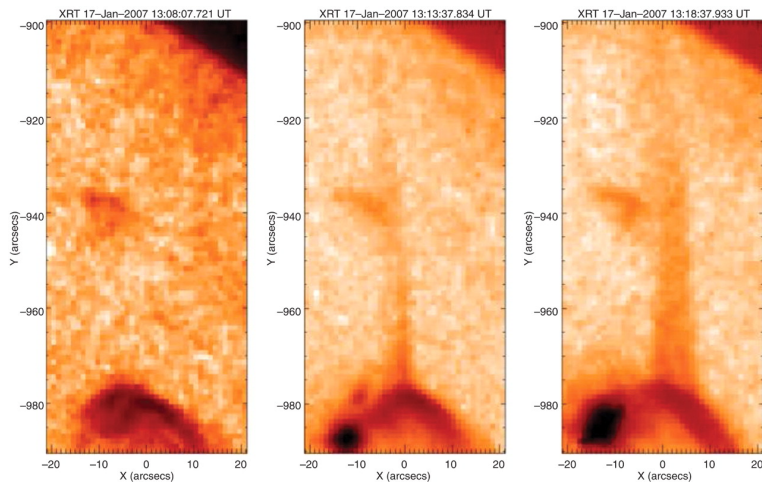
- Observations.
- Theory, mechanism.
- Simulations.
- A new class of (eruption-driven) jets.
- New numerical models.

Observations: X-Ray jets (XRT/Hinode)



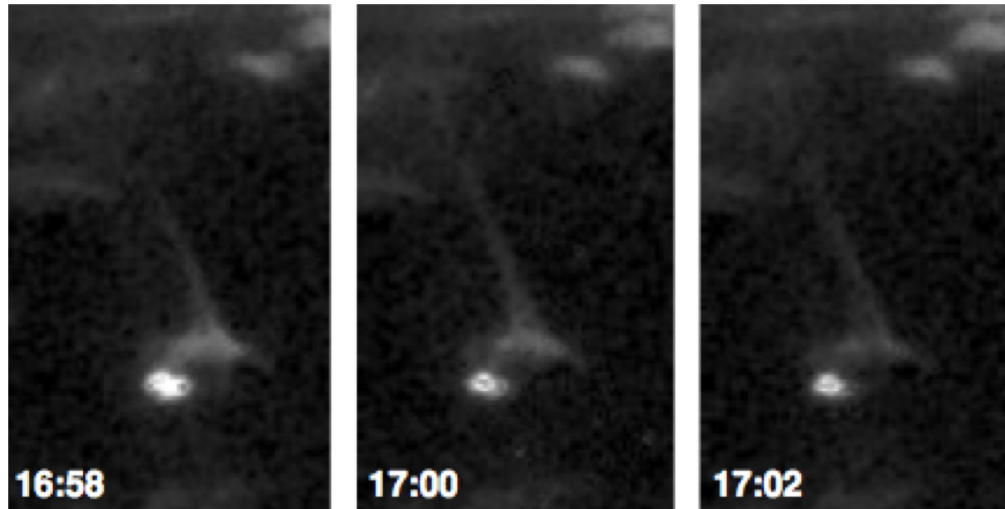
- Ubiquitous appearance.
- Fast ejection of hot, collimated, plasma outflow.
- Mechanism ?
- Contribution to solar wind ?

Observations: Progression of X-Ray jets



Helical jet, 2007 June 7, Patsourakos et.al. (2008)

North polar coronal hole, 2007 Jan. 17, Cirtain et.al. (2007).



North polar coronal hole, 2008 Sept. 22, Moore et.al. (2010).

Key features.

- Column of hot plasma is shoot up into the corona.
- Inverted, Y-shape configuration.
- Flaring BP located off to the side of the jet.
- Vertical jet spire, migrates away from the BP.

Recent review on solar coronal jets
Raouafi, N.E et.al. (2016).

Theory: Mechanism of (X-Ray) jets.

Shibata et.al., PASJ, (1992).

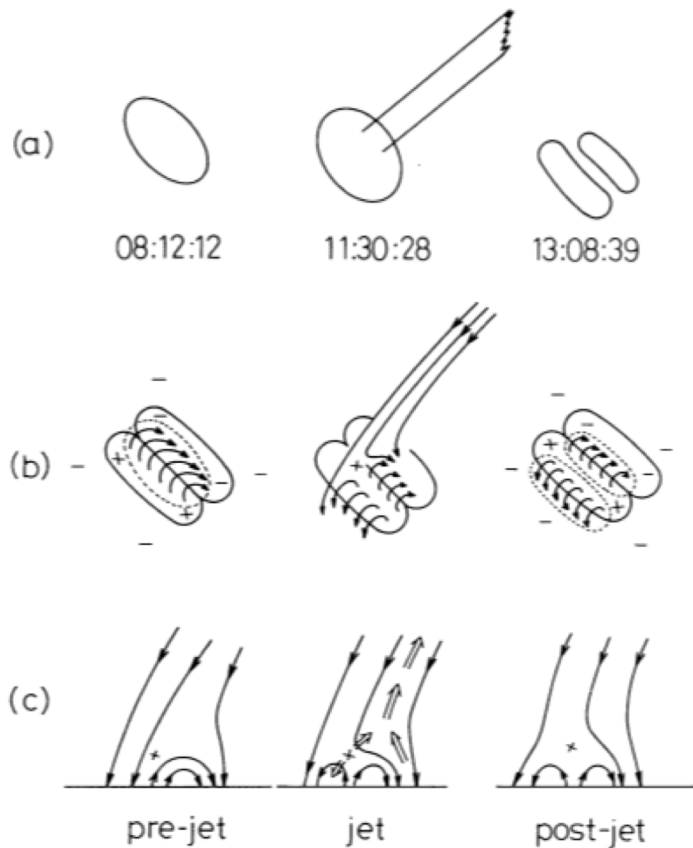
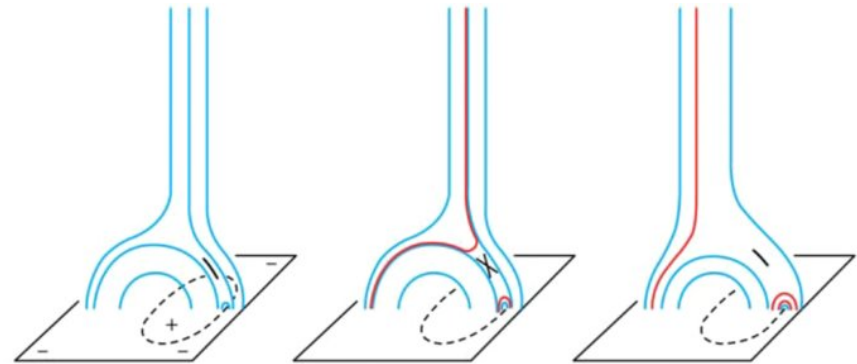


Fig. 5. Schematic picture of the possible physical situation of the 1991 November 12 jet. (a) Cartoons of the SXT image of the active regions and jets for pre-jet, jet, and post-jet stages. (b) Magnetogram data and the birds-eye view of the inferred magnetic field line configuration. (c) Side view of the magnetic reconnection occurring between the emerging flux and the pre-existing coronal field.

Moore et.al., ApJ, (2010).

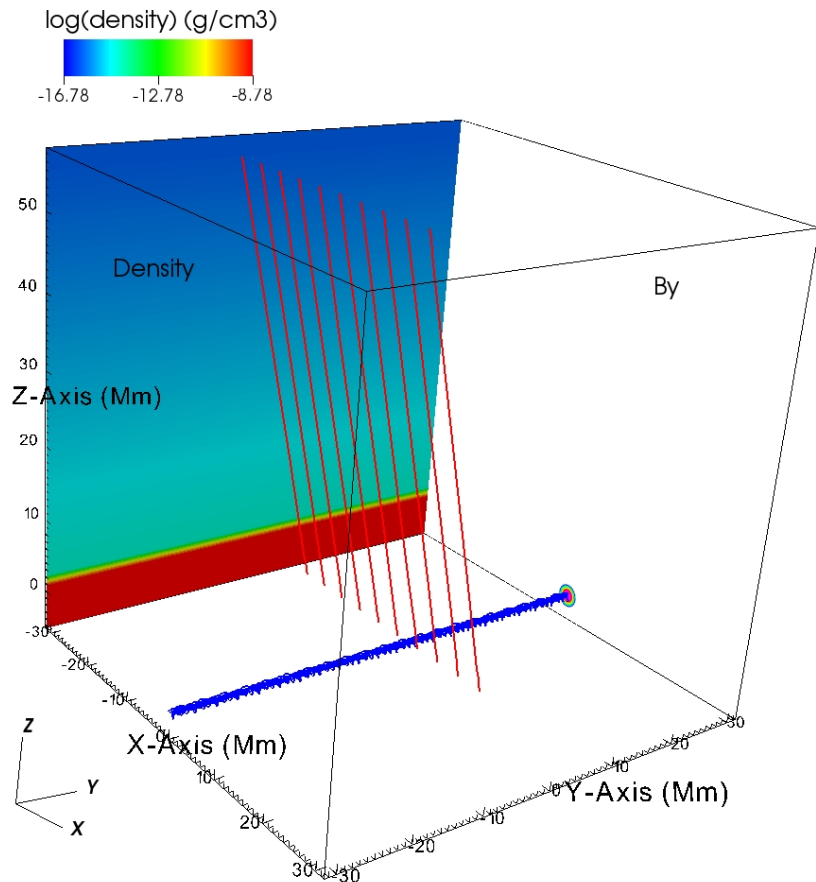


'Standard' jets.

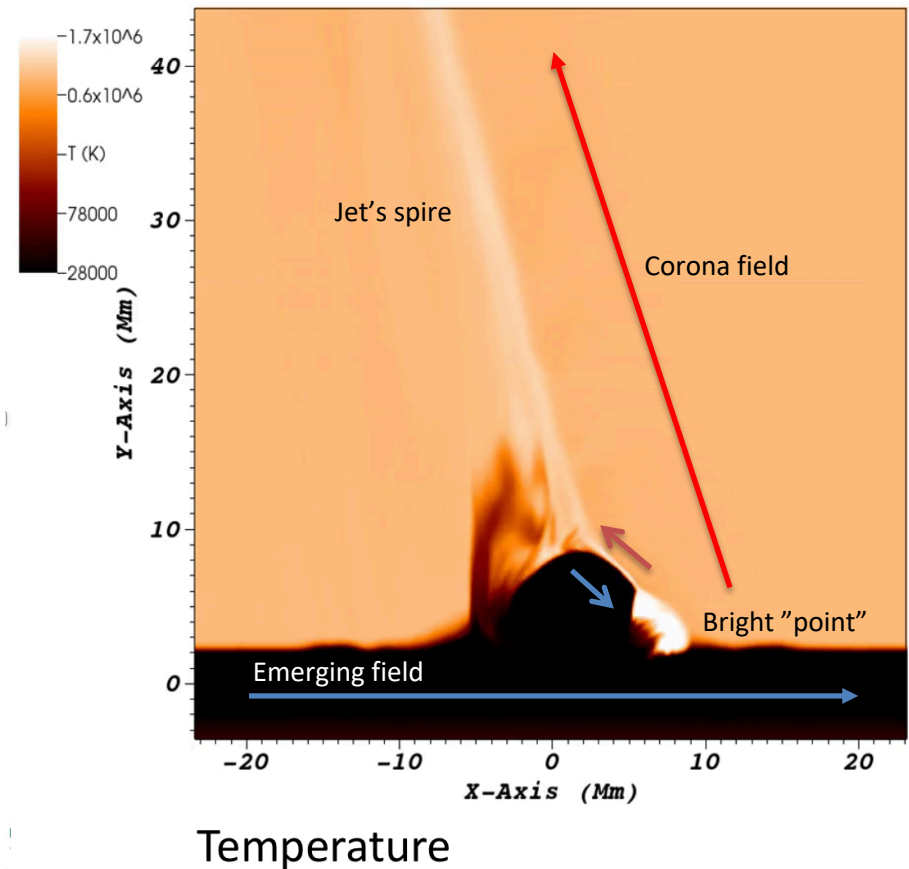
- Emerging arch + 'open' ambient field.
- 'External' reconnection.
- X-ray jet + 'bright' point (arcade).
- Little or no emission in cooler lines.

Simulations: Jets via flux emergence

3D Simulations: flux emergence into magnetized corona

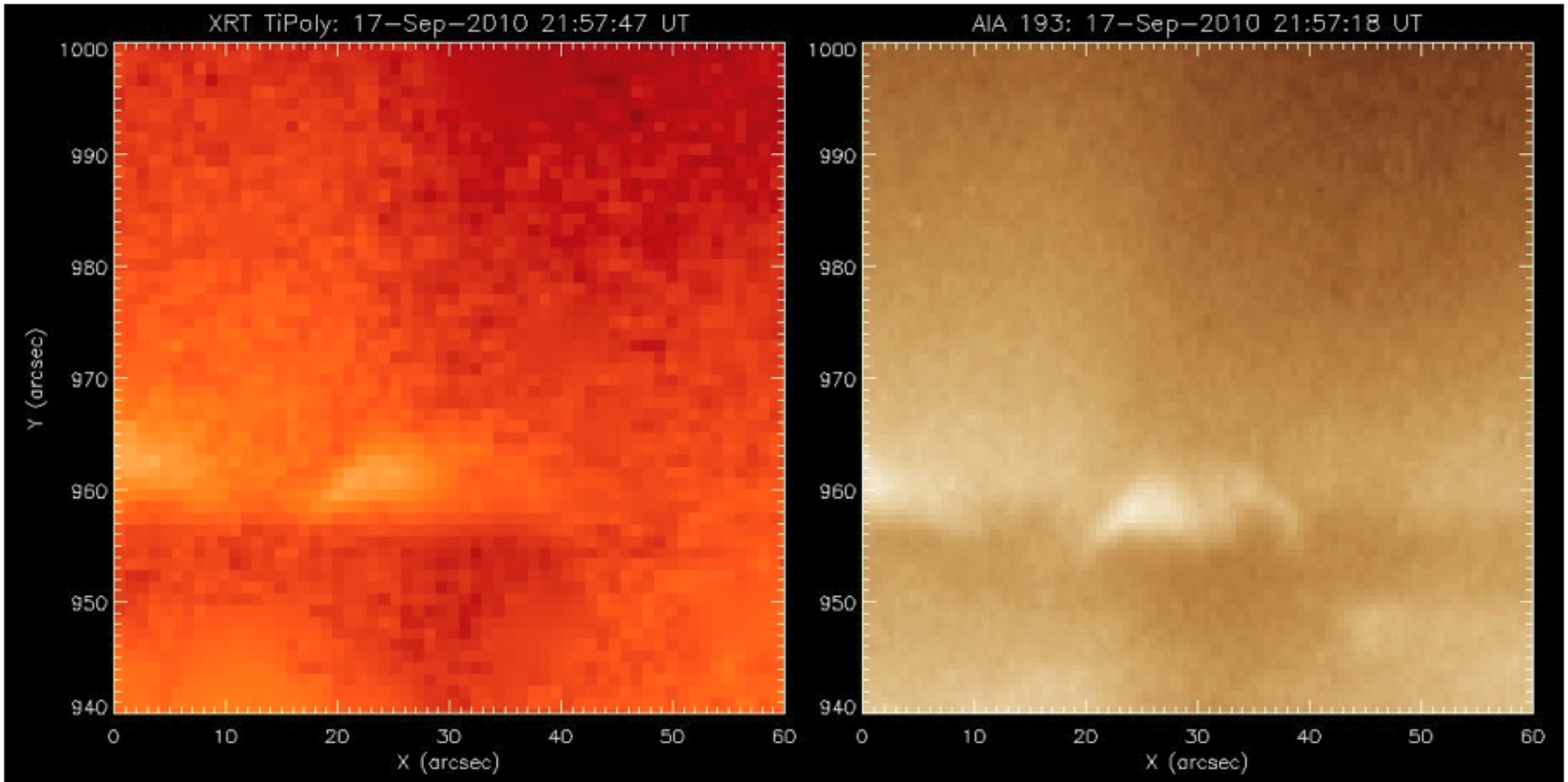


3D Simulations: comparison to observations



Archontis et.al., ApJ, (2013).

Recent observations: Small-scale (mini) filaments drive jets?

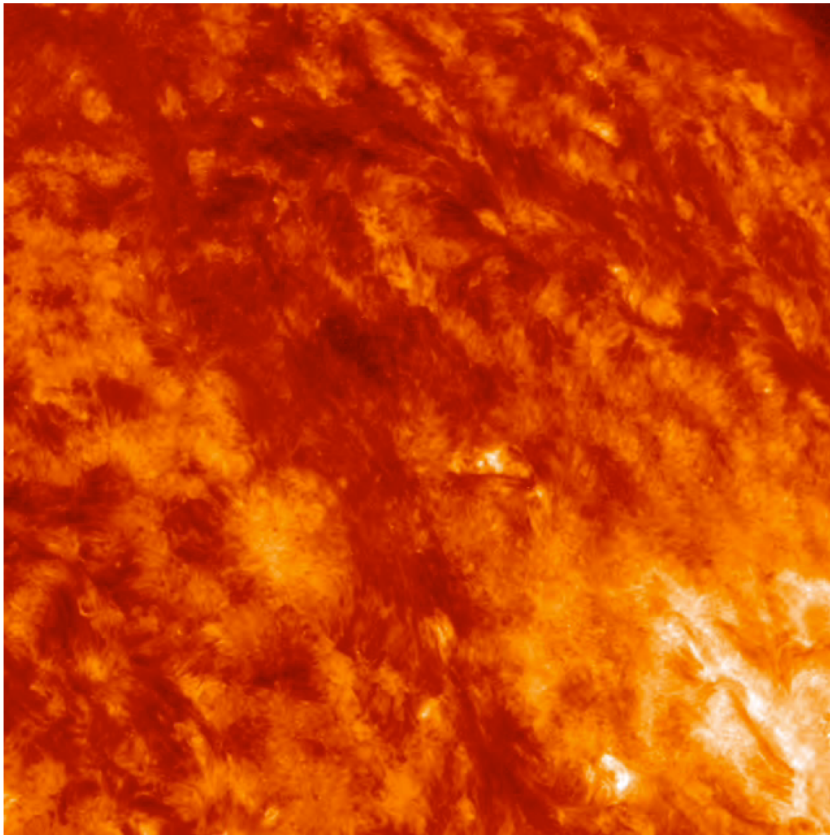


Soft X-ray (Hinode/XRT, TiPoly filter)

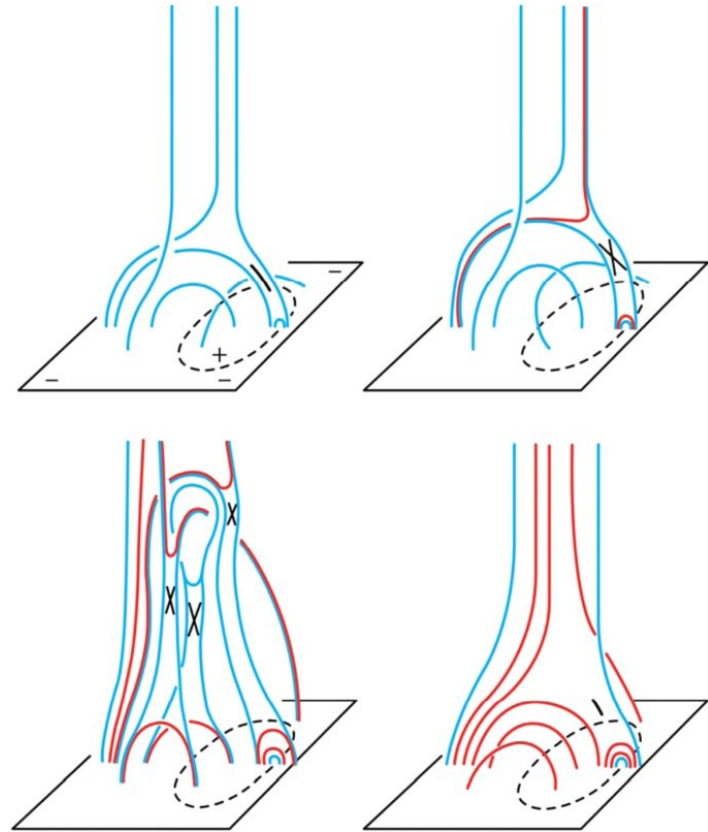
EUV (SDO/AIA 193 A)

Sterling, A. et.al., Nature, (2015).

Recent observations: small-scale (mini) filaments drive jets?



SDO/AIA 304 A (4/4/2013)

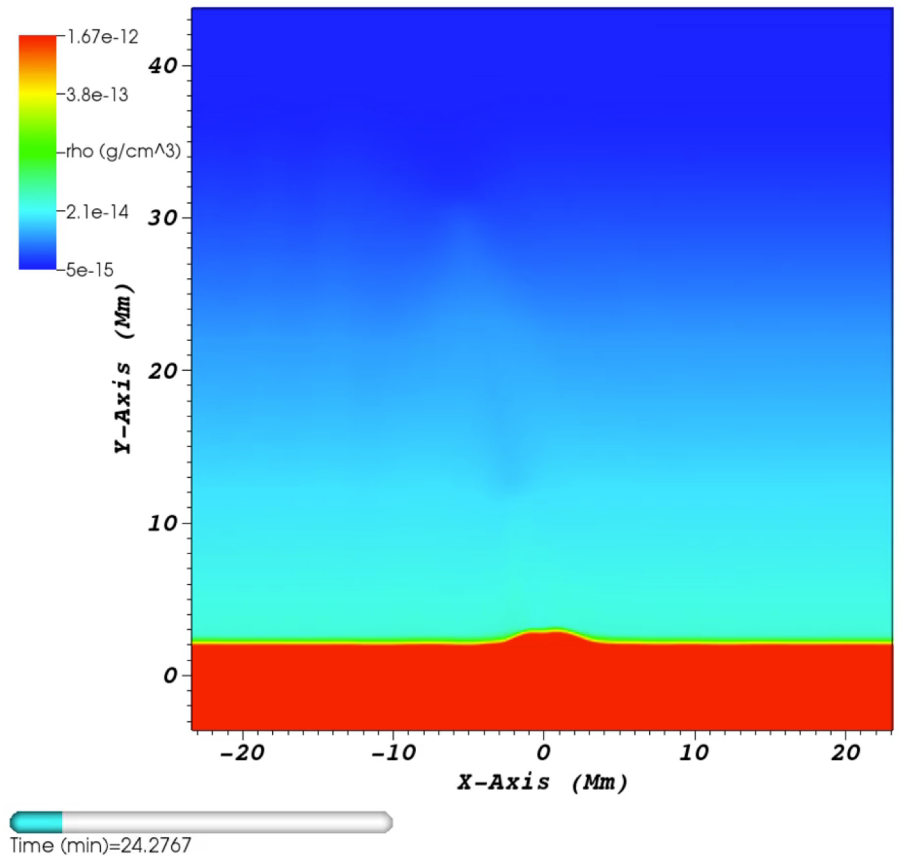
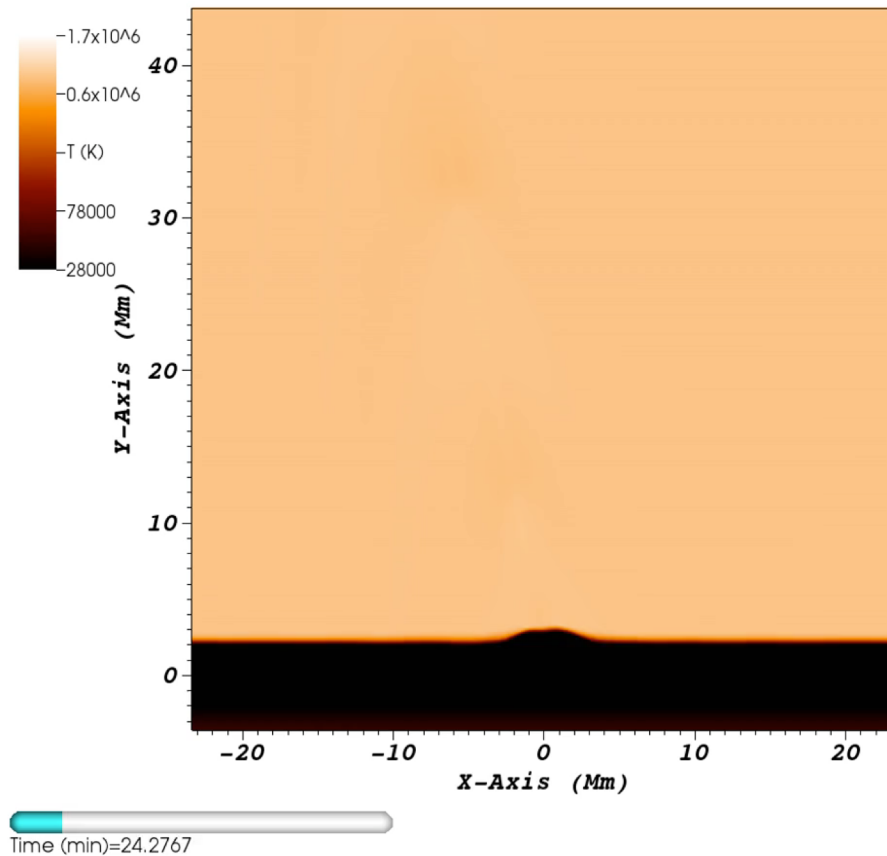


Moore et al., ApJ, (2010).

'Blowout' jets.

- Eruption of the field.
- 'External' & 'Internal' reconnection.
- Wider jet channel.
- Hot and cool emission.
- Brightening on arcades.

Simulations: First model to explain eruption-driven jets.

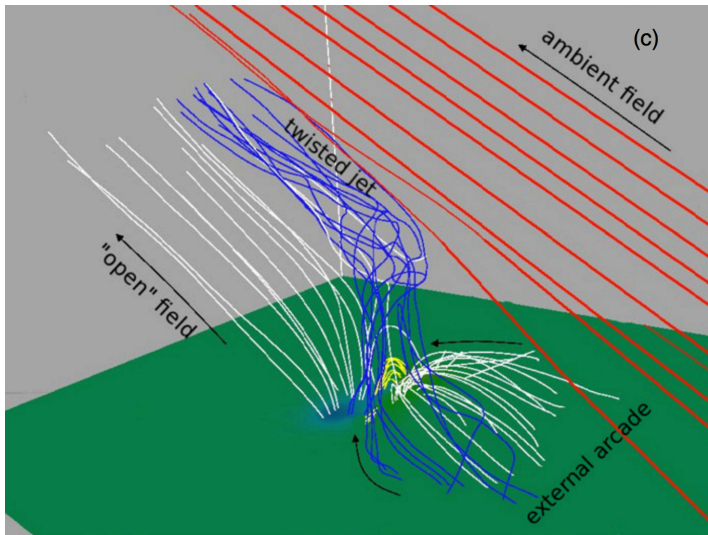
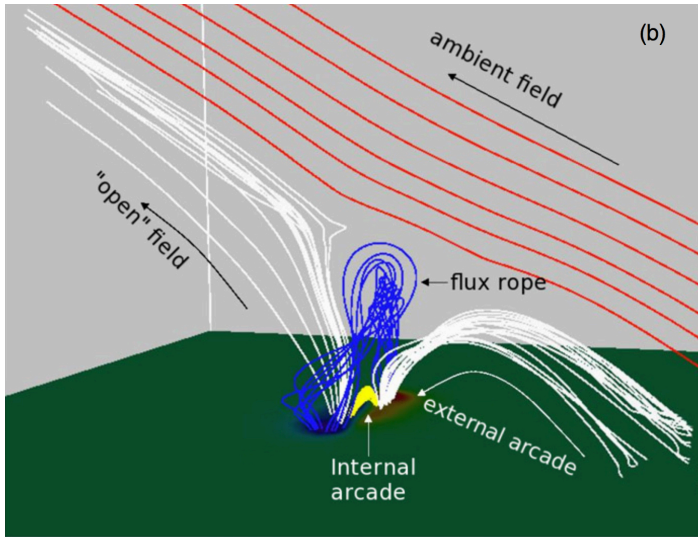


Model explains the key observed features:

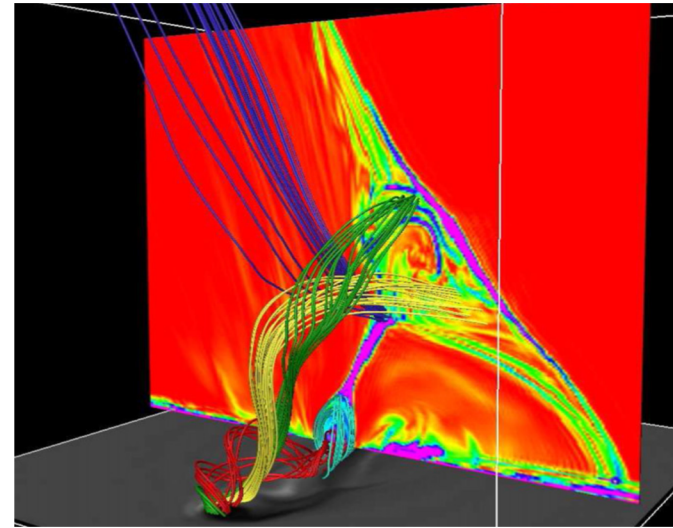
- Hot and cool emission along the jet.
- Spire of the jet is much wider.
- Bright point underneath the jet.

Archontis, V. & Hood, A., ApJL, (2013).

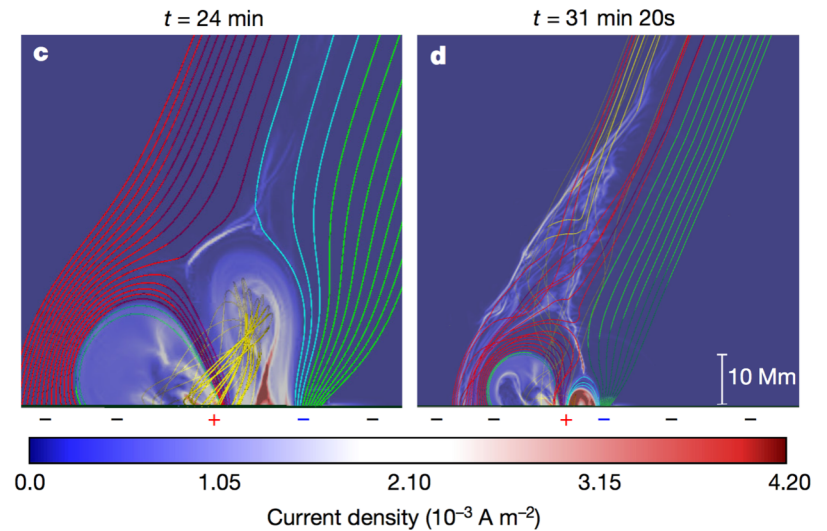
Simulations: Eruption of flux ropes drive jets.



Archontis, V. & Hood, A., ApJL, (2013).



Moreno-Insertis, F., V. & Kalsgaard, K., ApJ, (2013).

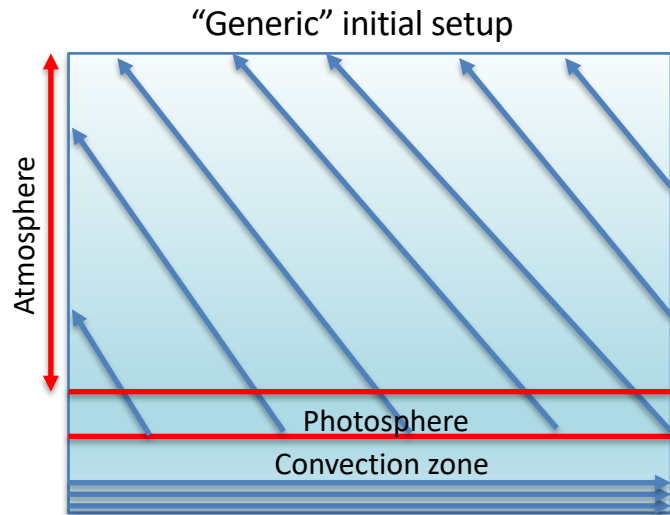


Wyper, Antiochos & DeVore, Nature, (2017).

Heating in the solar atmosphere

- R-MHD flux emergence experiments.
- Multi-scale magnetic activity.
- Nano-flares.
- IRIS “bombs”.

Multi-scale emergence of magnetic flux driven by convection.



Bifrost code.

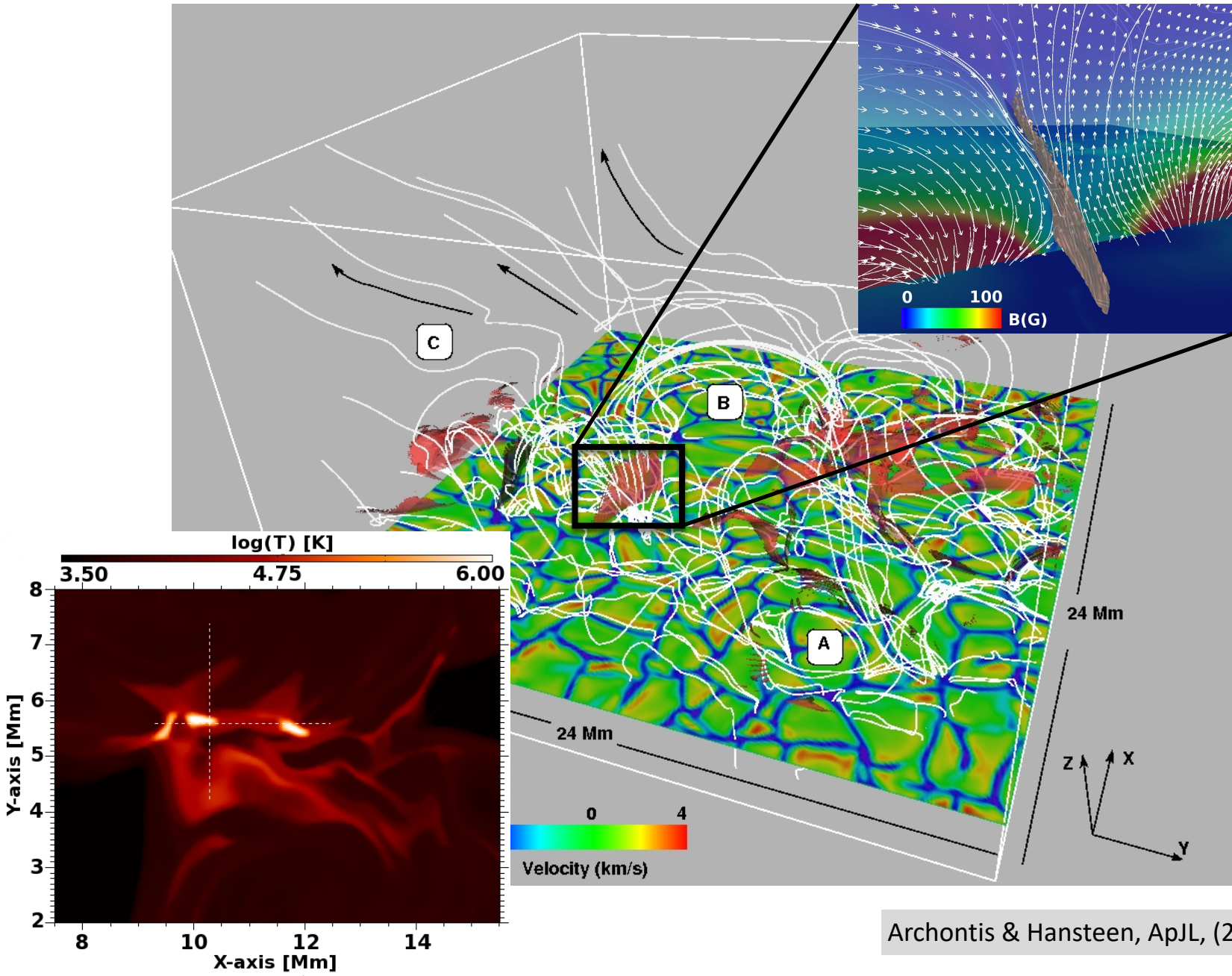
Synergy: Oslo, St. Andrews, UOI

Convection ~ 3 Mm, domain $24 \times 24 \times 17$ Mm.

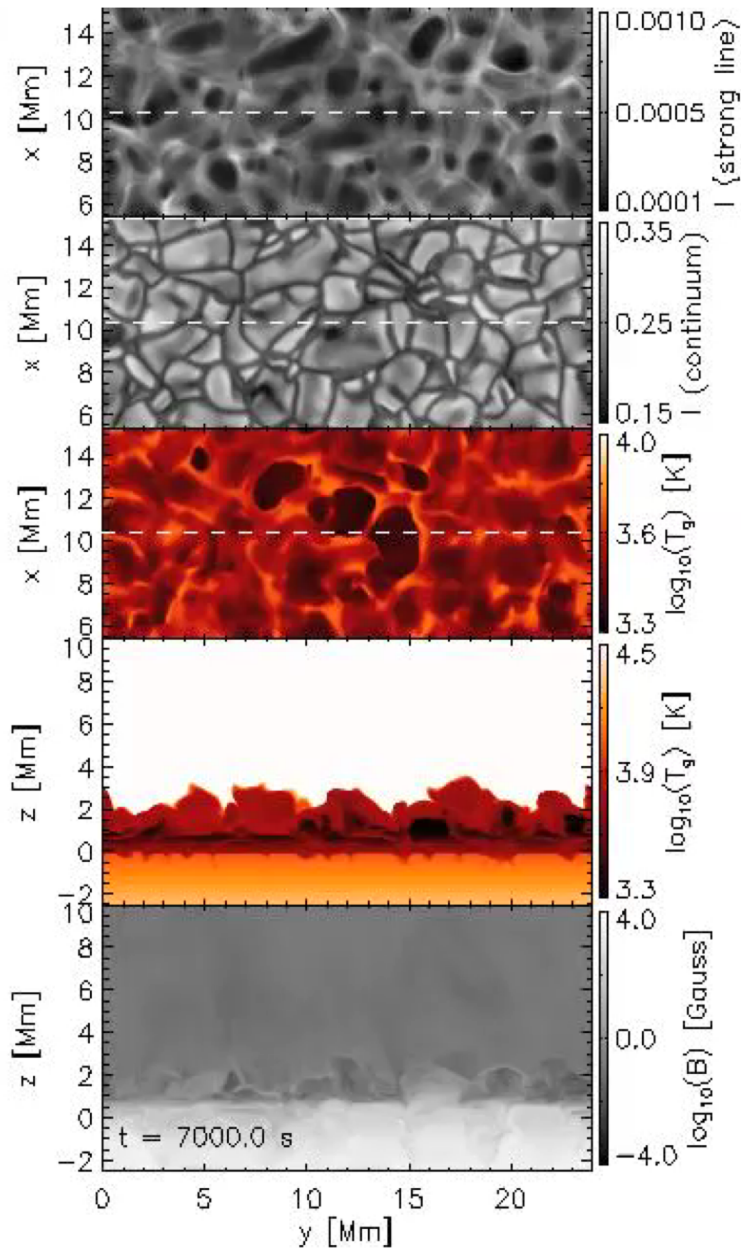
Injection of magnetic flux (sheet) at the bottom boundary, $B_y = 3.4$ kG.

Results: Emerging field with a sea-serpent magnetic field configuration, formation of Ellerman bombs, UV bursts, nano/micro flares and heating.

Simulations: Multi-scale magnetic flux emergence.



Simulations: Flaring and heating



These experiments reveal:

- 1. Current sheet fragmentation.**
- 2. Small-flare structure and heating.**

Lifetime: 30s -3min.

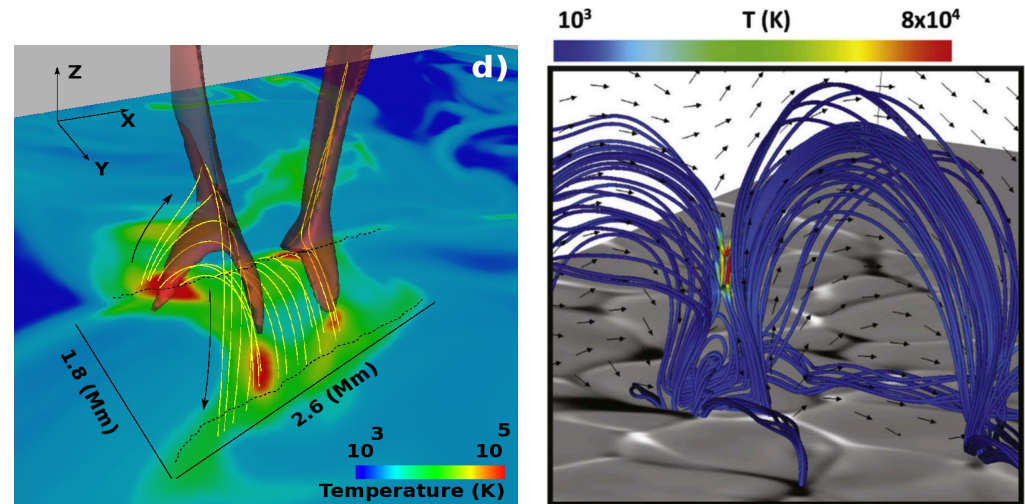
Occurrence rate: $\sim 4 \times 10^{-20} \text{ s}^{-1} \text{ cm}^{-2}$.

Total heating: 1-6 MK.

Average energy flux: $1.2 \times 10^6 - 7 \times 10^7 \text{ erg s}^{-1} \text{ cm}^{-2}$.

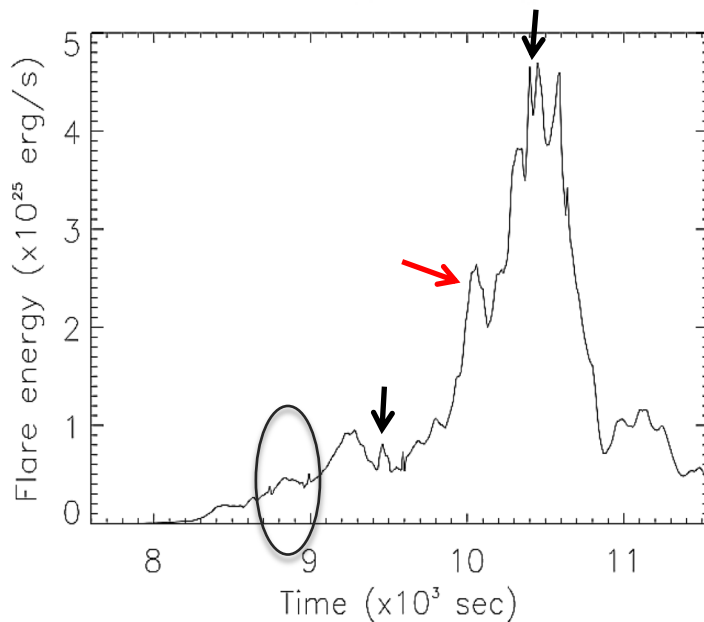
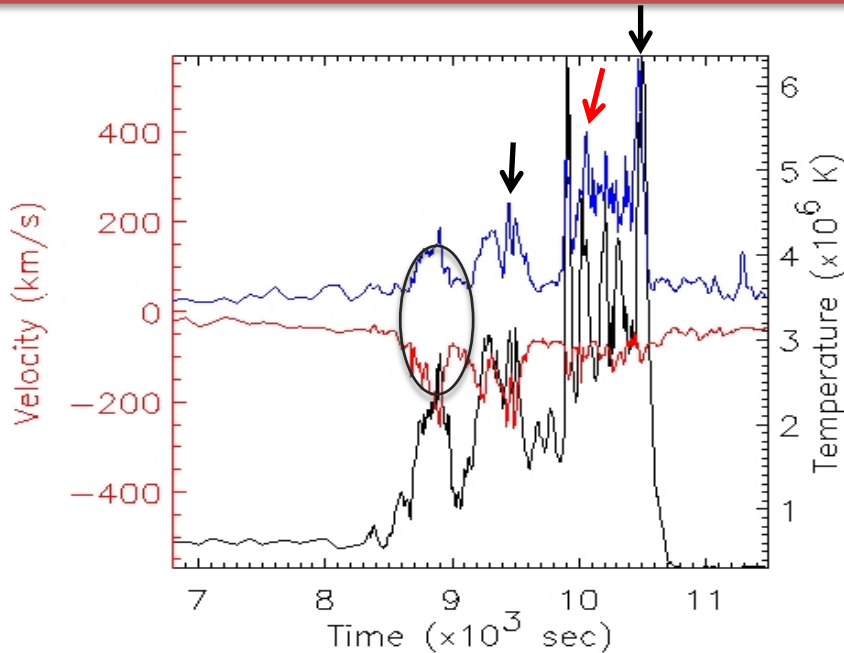
- 3. IRIS “bombs”.**

Hot explosions (up to 10^5 K) in the cool (10^4 K) lower atmosphere of the Sun.



Archontis & Hansteen, ApJL, (2014)
Hansteen, Archontis, et.al., ApJ (2017)

Temperature, vertical velocity (V_z) and energy.

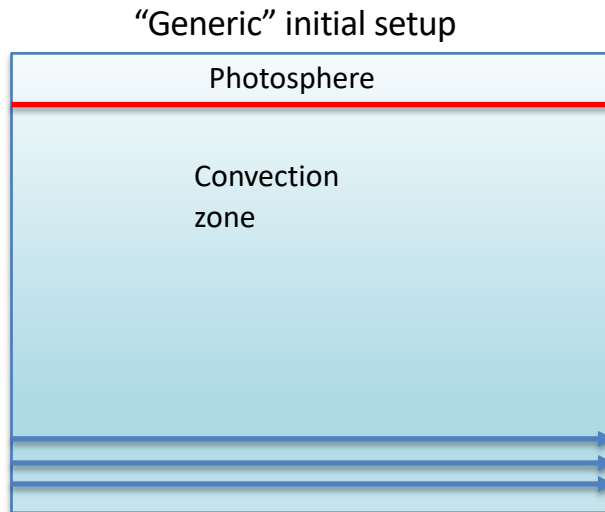


- Plasma heating (1-6 mK) by small flares.
- Reconnection-driven acceleration.
- Heating-Energy: good correlation.
- Short-lived bursts of energy.
- \uparrow Superposition of small flares (10^{25} - 10^{26} erg).
- \uparrow "Individual" energy emissions $\sim (10^{27})$ erg.
- Lifetime of small flares: 30 s – 3 min.
- Flares at various heights.
- ~ 20 flares in 38 min.
- For coronal flares: average energy flux $\sim 2.1 \times 10^6 - 10^7 \text{ erg s}^{-1} \text{ cm}^{-2}$.

Simulations: Type IV

- Flux sheet.
- Realistic convection, deep.
- Focus on small- and large-scale dynamics.
- Pores and ARs.

Multi-scale emergence of magnetic flux driven by convection.



Bifrost code.

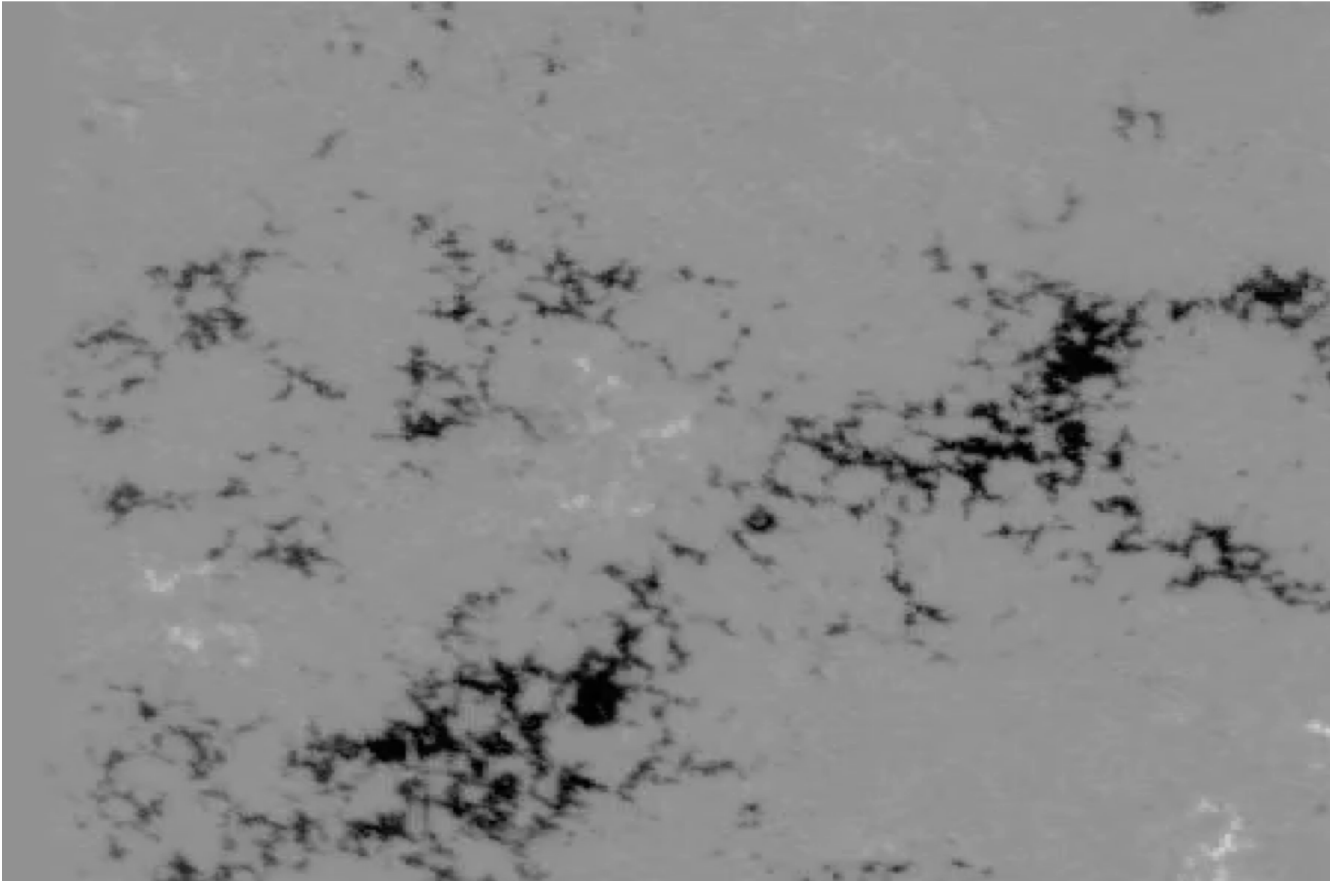
Synergy: Oslo, St. Andrews

Convection ~ 8 Mm, 73×73 Mm horizontal,
4 supergranules.

Injection of magnetic flux (sheet) at the
bottom boundary, $\Phi - 10^{21}$ Mx.

Preliminary results: Emerging field with a sea-serpent configuration, formation of pores and small/ephemeral AR, through systematic coalescence of like polarities and cancellation of opposite polarities on small scales.

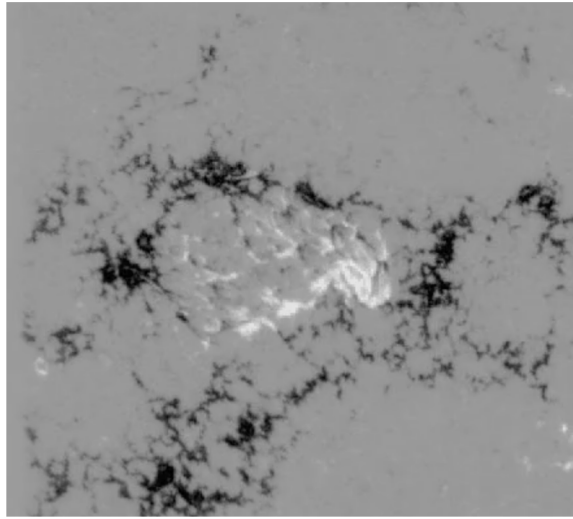
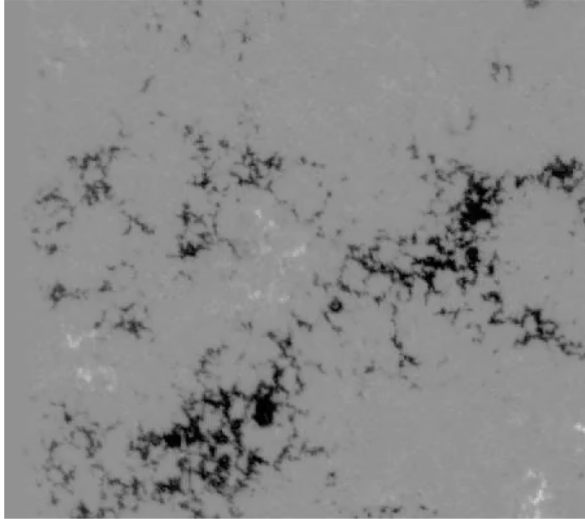
Observations: formation of sunspots and AR(s).



1-2 December 2006, SOT e.g. Harra, L., *et.al.* Solar Physics (2012)

Small-scale flux emergence, formation of pores, sunspots, ARs.

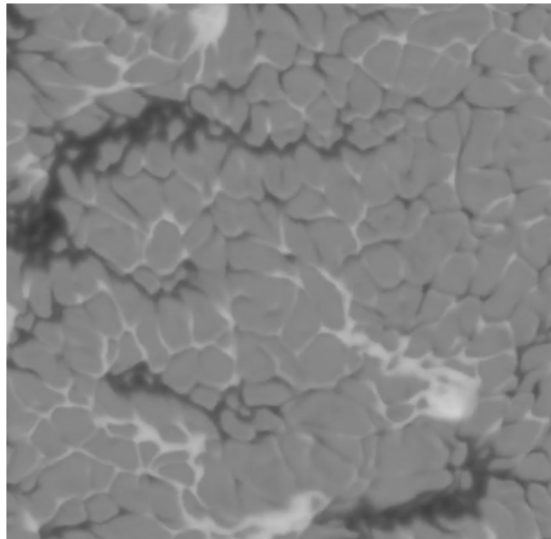
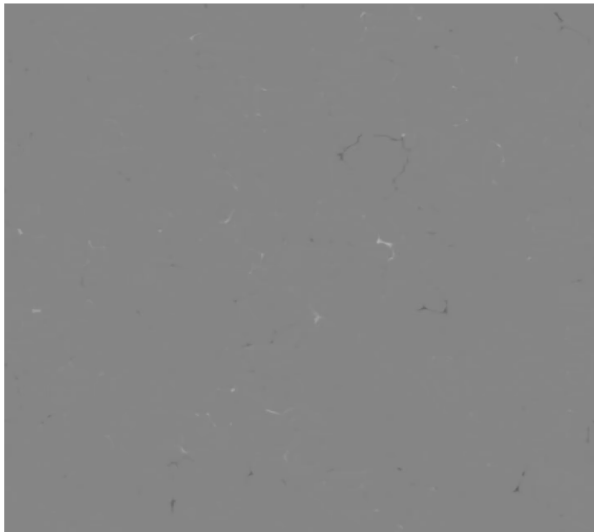
Observations



Magnetogram.
Hinode/SOT (2006)

Magara, T., ApJL, 2008

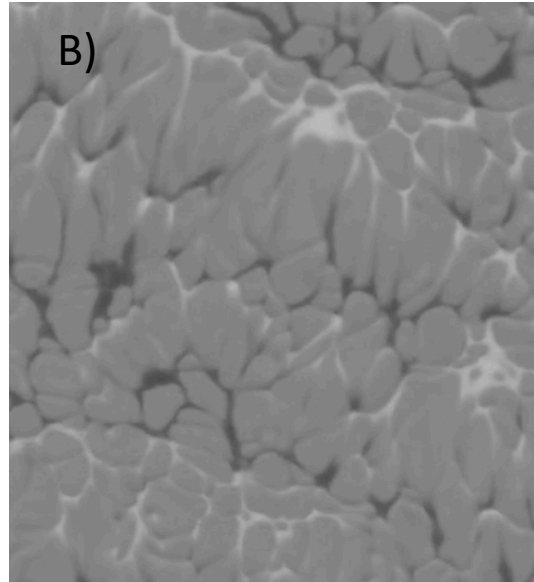
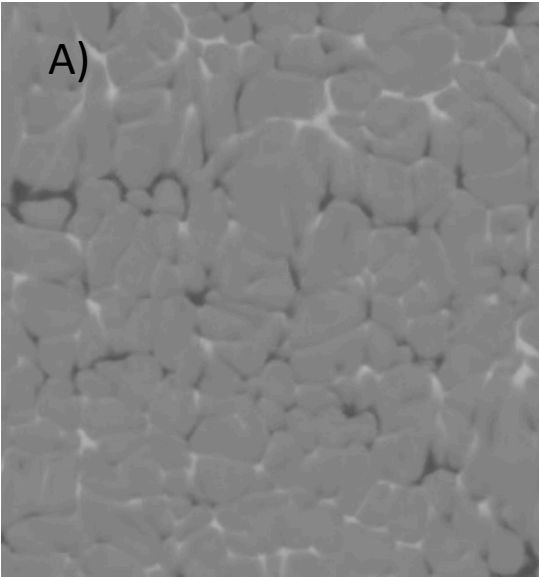
Simulations



“Magnetogram”.
Bifrost simulations.

*Work in progress (Boris
Gudiksen)*

Multi-scale flux emergence with deeper convection.



Close-up, $\sim 35 \times 40$ Mm.

$B_z \sim (-3.5 - 3.5)$ kG.

Formation of pairs of pores on various locations.

~ 25 hours (solar).

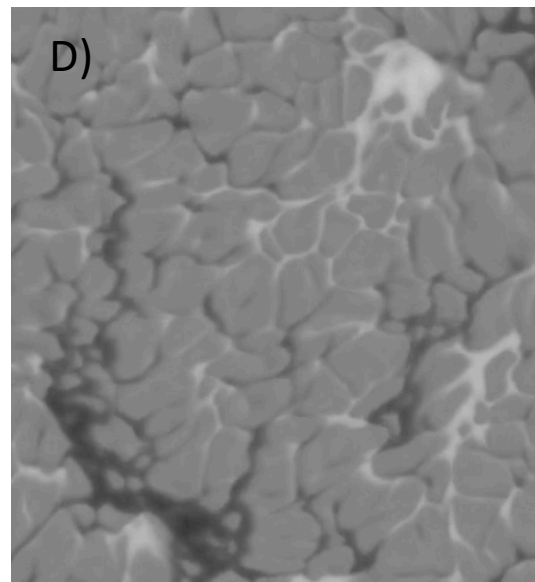
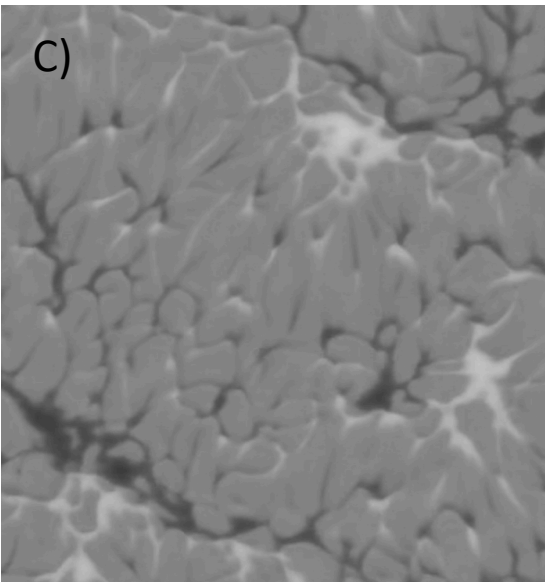
Questions

Nature of pores?

Connection to sub-surface field?

Connection to super-granules?

Formation of sunspots?

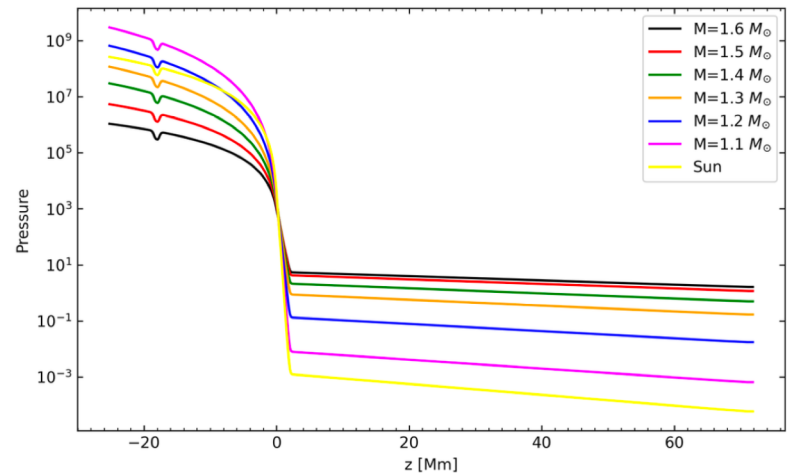
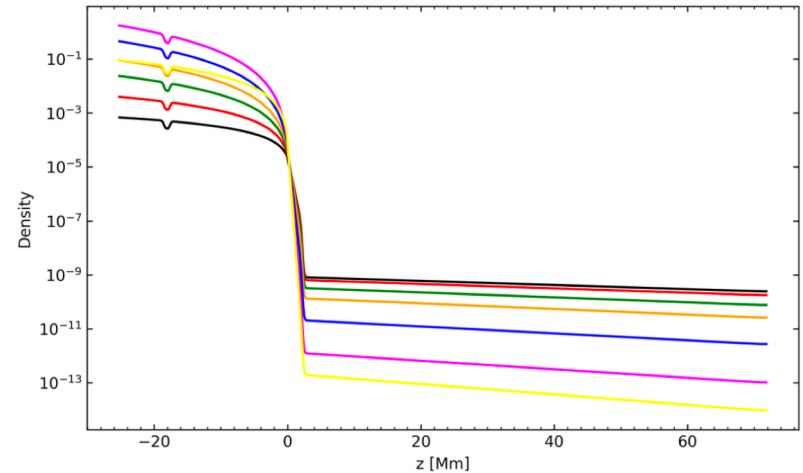


Flux emergence in F-type stars

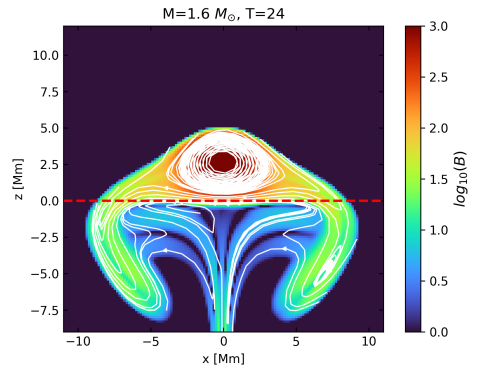
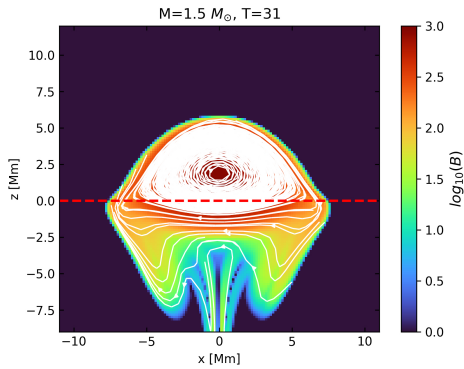
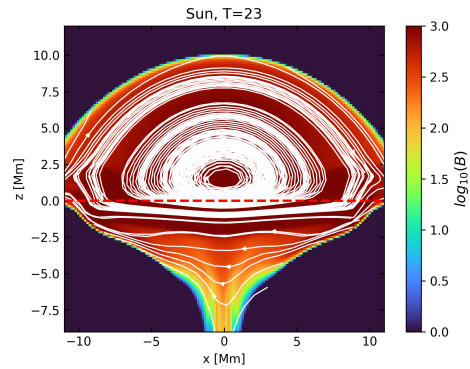
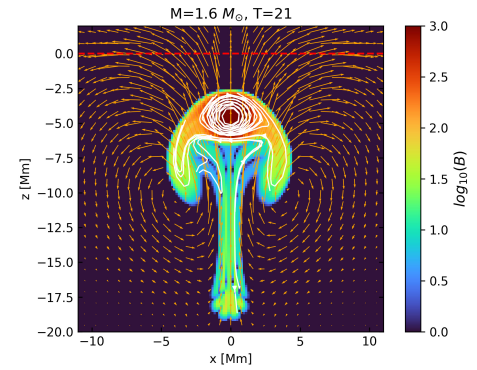
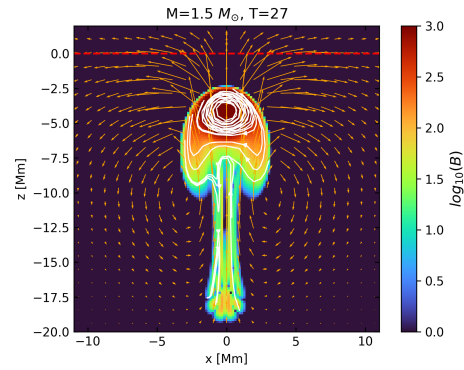
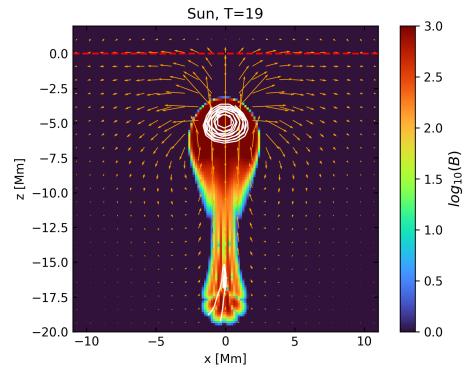
- First, new results
- ERC synergy with Paris/Saclay.

Initial Conditions

- Numerical experiments use Lare3D (Arber et al. 2001)
- Cartesian Box $600 \times 600 \times 600$ grids ($[-48.6, 48.6] \times [-48.6, 48.6] \times [-25.2, 72]$ Mm)
- We simulate F-stars with masses varying from $M=1.1 M_{\odot}$ to $M=1.6 M_{\odot}$
- Density profile of the stellar interior is defined by a stellar evolution code ASH
- A magnetic flux tube is placed at -18 Mm and rise due to buoyancy (Similar to Archontis et al. 2004, Fan et al. 2009, Syntelis et al. 2015, 2017 etc.)
- Our goal is to simulate the flux emergence process of a magnetic flux tube under a different stratification resembling the conditions in F-stars



Flux Emergence Phase



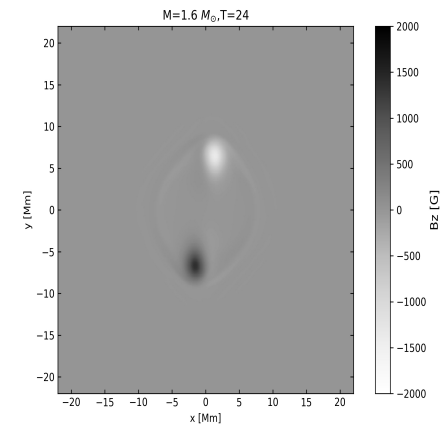
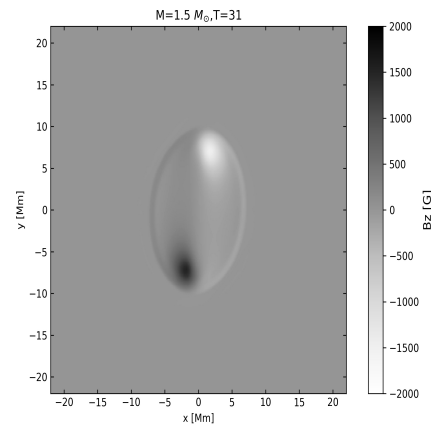
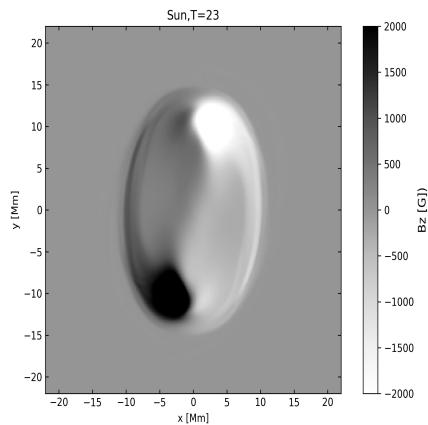
No Vortex motion for smaller Stars and the Sun

Intense Vortex motion around flux tube axis

Stellar Active regions

Classical Sigmoidal formation at the PIL

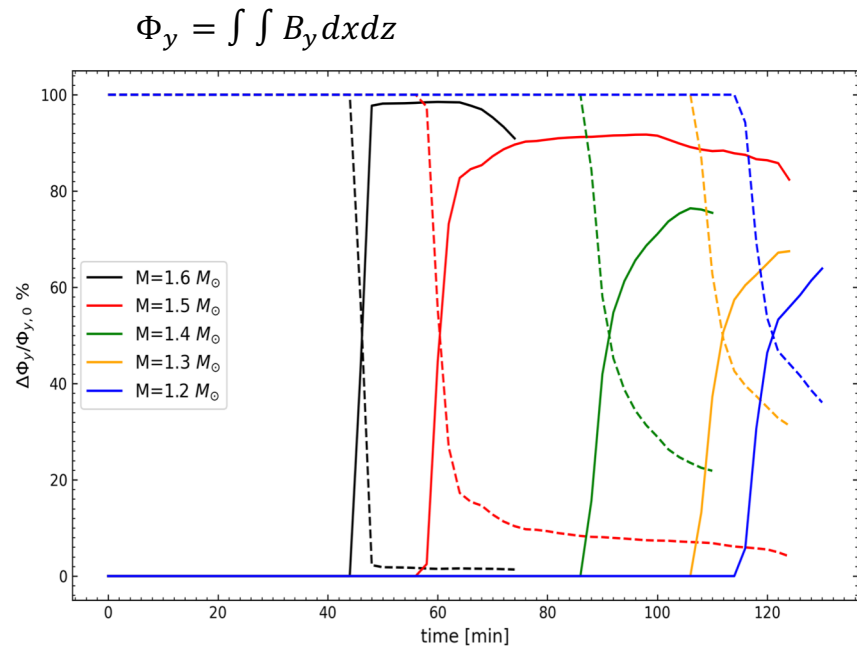
Circular spots appearing with no sigmoidal or PIL forming



PIL formed similar to the Sun but no sigmoidal shape -> PIL roughly straight and stretched

Axial Flux above and beneath the Photosphere

- Larger stars reach the photosphere faster
- Larger stars emerge almost 100% of their B_y flux
- B_y flux is important for the creation and eruption of flux ropes



1) Solid line -> Percentage of B_y flux emerging above the photosphere
2) Dashed line -> Percentage of B_y flux beneath the photosphere

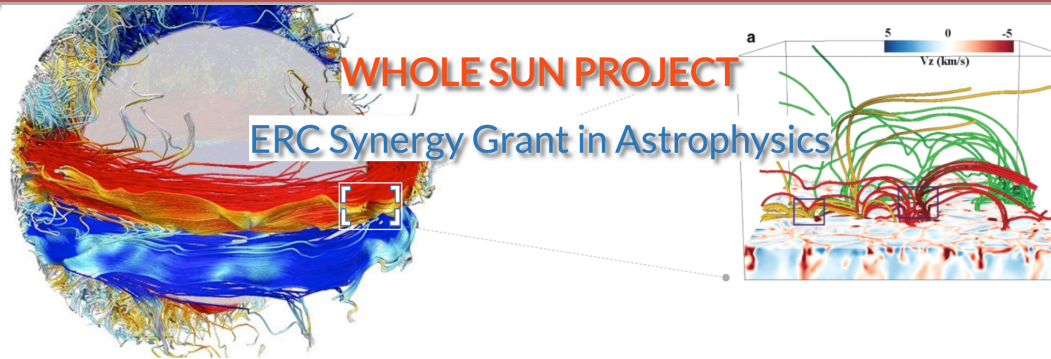
Summary

- Recent advances.
- Future Challenges.

Recent Advances

- **A unified model for solar jets.**
 - A new mechanism for "standard jets"
 - The ultimate connection between "standard" and "blowout" jets.
 - Collaborators: Dr. Syntelis, Dr. Tibor Torok, Dr. A. Sterling, Dr. R.J.Moore.
 - Status: under submission.
- **R-MHD models of flux emergence towards the formation of pores/sunspots.**
 - Self-consistent formation of pores attached to supergranulation
 - Collaborators: Prof. Boris Gudiksen.
 - Status: under submission.
- **Global dynamo and flux emergence.**
 - Coupling of ASH code with Lare3D code to study emergence of dynamo fields.
 - Collaborators: Prof. Sacha Brun, Dr. Alexei Borrison.
 - Status: to be submitted.
- **Flux emergence in other stars.**
 - Use existing flux emergence models in F-type stars
 - Collaborators: Prof. Sacha Brun, Dr. Alexei Borrison, Dr. Rui Pinto.
 - Status: to be submitted.

Future Challenges

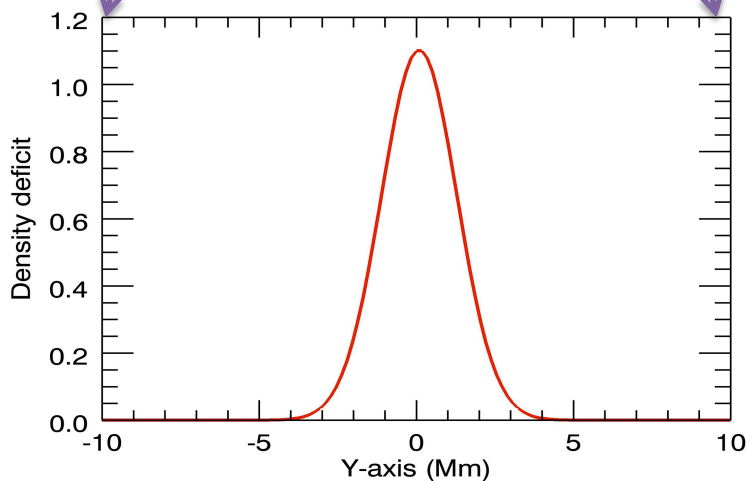
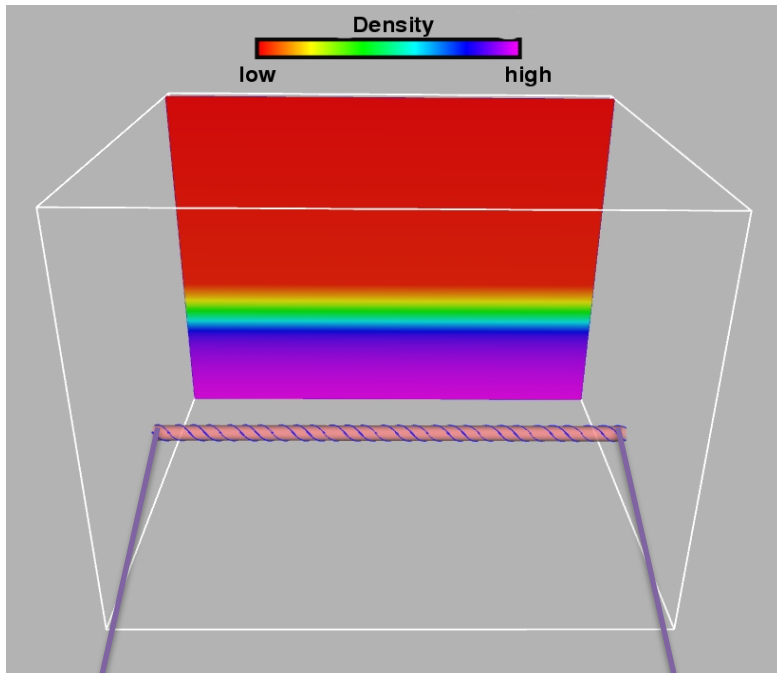


- **Coupling global-dynamo with flux emergence into the solar atmosphere.**
How does the dynamo-generated field emerge to form ARs ?
- **Kinetic effects on Radiative-MHD models of solar magnetic fields.**
Particle acceleration on current sheets (flares, jets, eruptions)
- **Magnetic and Thermodynamical coupling:**
Between the solar interior and outer atmosphere.
On the nature of eruptive and/or explosive events.
- **Space Weather.**
Incorporate Solar wind into the models.
Sun-Earth connection.
- **Build of Globus/Dispatch code(s).**
Study the “Whole Sun” using one global code on exa-scale supercomputers.
Study the Solar-Stellar connection.

THANK YOU !

EXTRAS

Initial Conditions



Flux tube magnetic field

$$\mathbf{B} = (0, B_\theta(r), B_y(r))$$

$$B_y = B_0 e^{-r^2/R^2}, \quad B_\theta = \alpha r B_y$$

Coronal magnetic field

$$B_c = B_c(z) (\cos\phi, \sin\phi, 0)$$

Density deficit

$$\frac{\rho_m}{\rho_b} = \frac{p_m}{p_b} e^{-y^2/\lambda^2},$$

Parameters

$$\text{Radius } (R) = 425 \text{ Km},$$

$$\text{Twist } (\alpha) = 0.1 - 0.4,$$

$$B_0 = 3 - 4 \text{ kG},$$

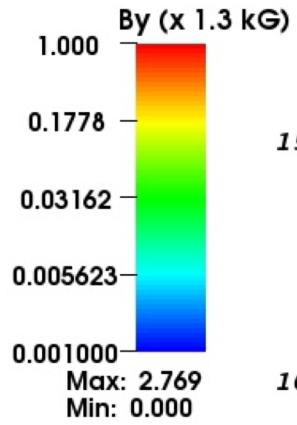
$$B_c(z) = 10 \text{ G},$$

$$\text{Buoyant part } (\lambda) = 3 - 4 \text{ Mm},$$

$$\text{Deficits} : \rho_m, p_m,$$

$$\text{Background plasma} : \rho_b, p_b$$

B_y (cross section / mid-plane)



Z axis - Height
(x 0.17 Mm)

150

100

50

Corona

0

-100

-50

0

50

100

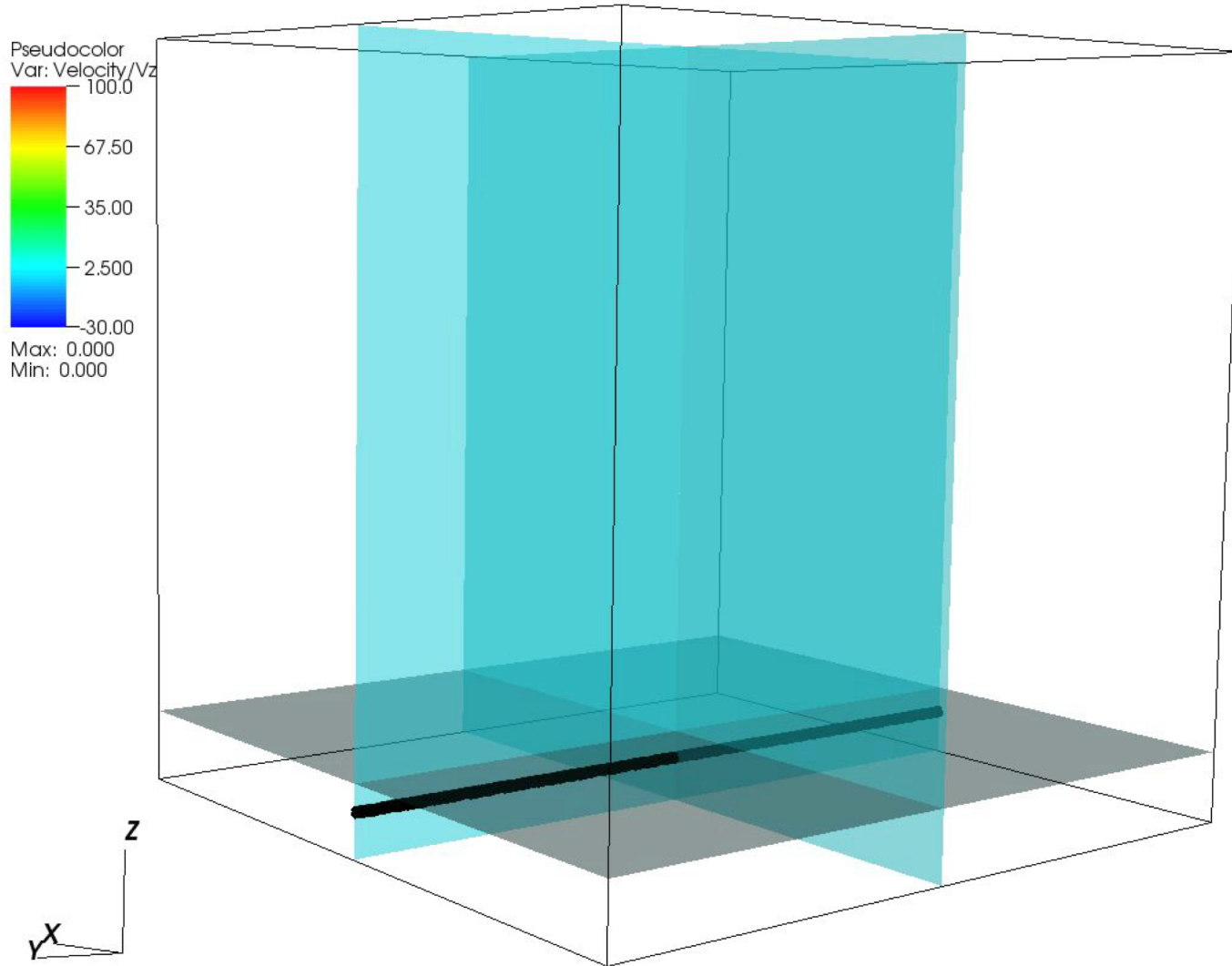
X-Axis (x 0.17 Mm)



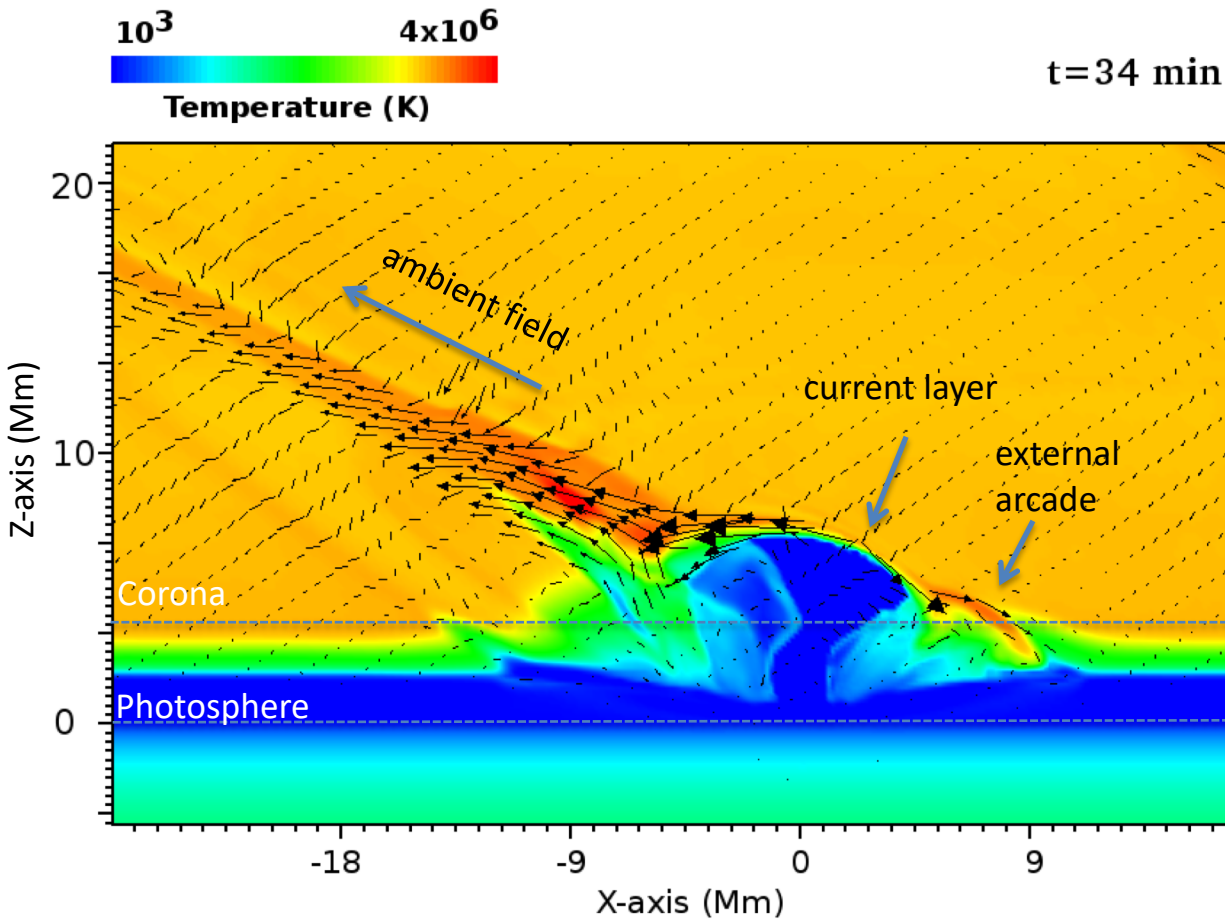
168 min (total)

DB: 0000.cfd
Cycle: 0 Time:0

Vertical velocity (Vz)



'Standard' jets – Temperature.



Oblique – Φ varies.

$B_{\text{tube}}=5 \text{ kG}$, $B_{\text{amb}}=5\text{-}10 \text{ G}$

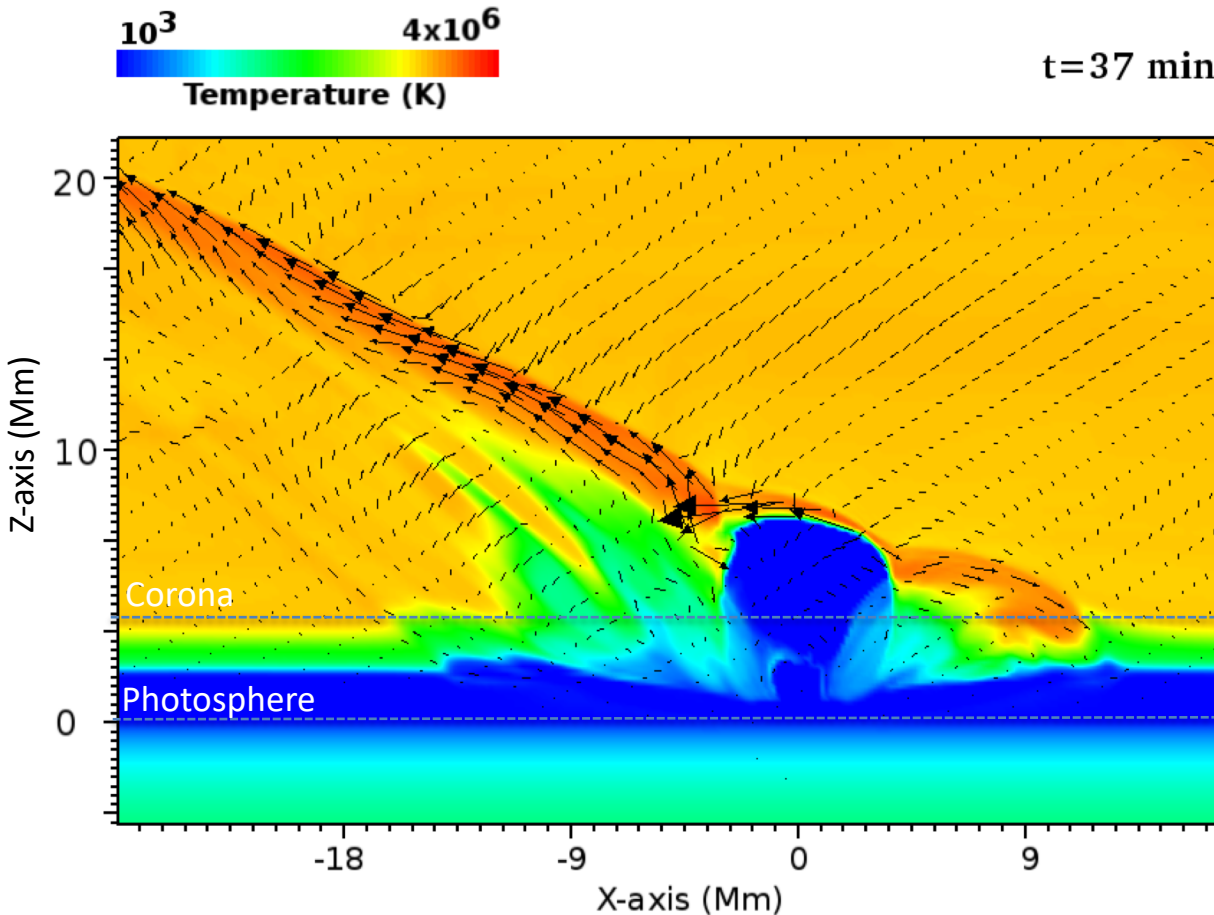
High $|J|$ - reconnection.

Pair of high velocity outflows:
(200-300 km/sec)

Inverse Y or λ configuration.

Heating:
(jets 4-8 mK, arcade $\sim 10 \text{ mK}$).

'Standard' jets – Temperature.



Oblique – $\Phi=135$ deg.

$B_{\text{tube}}=5.1$ kG, $B_{\text{amb}}=4.4$ G

High $|J|$ - reconnection.

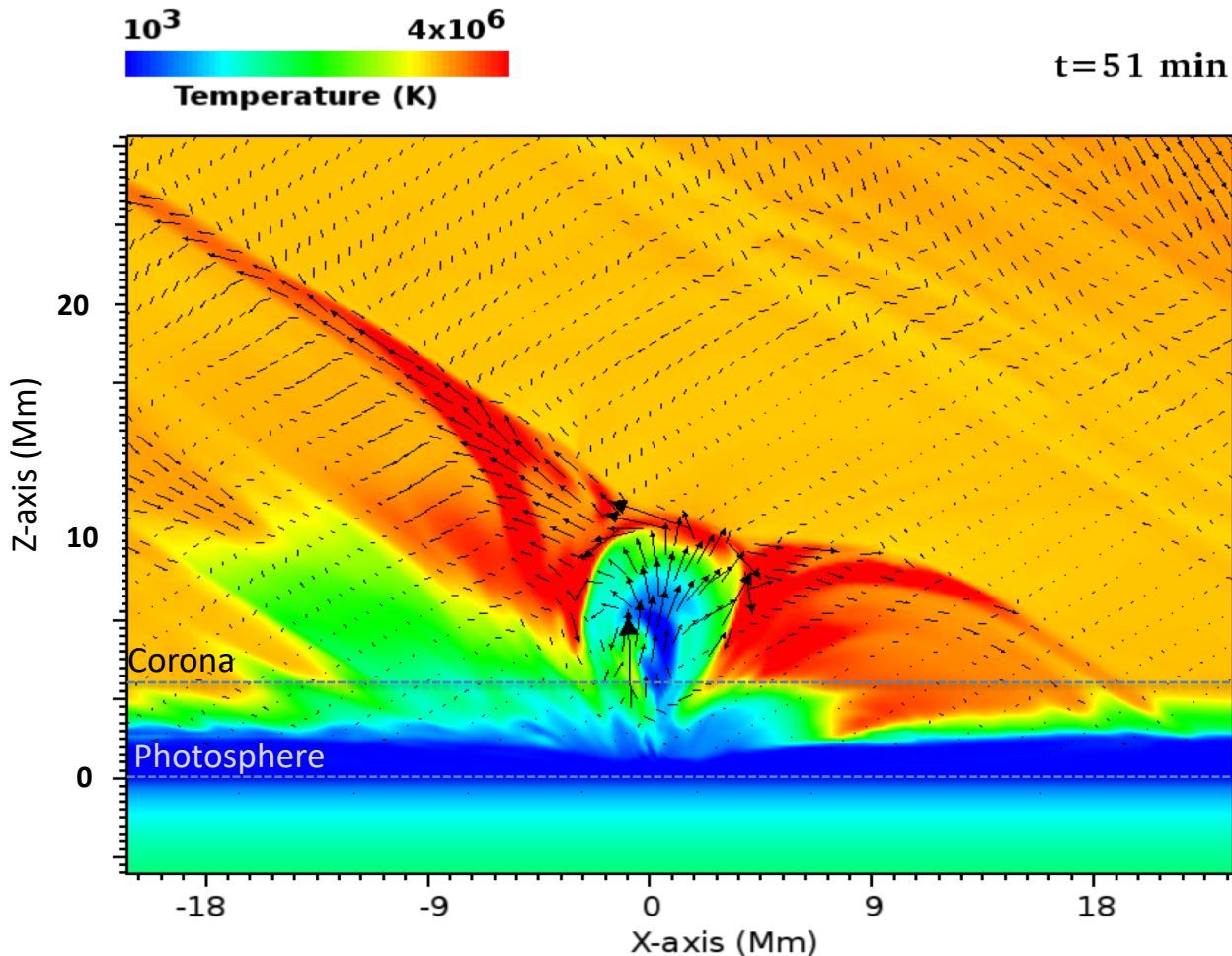
Pair of high velocity outflows:
(200-300 km/sec)

Inverse Y or λ configuration.

Heating:
(jets 4-8 MK, arcade ~ 10 MK).

- More elongated spire.
- Wider external arcade.

'Blowout' jet driven by eruption - Temperature



$t = 51$ min

Eruption of flux rope.

Internal arcade (5-10 mK).

Upflow/jet (400-500 km/sec).

More external reconnection.

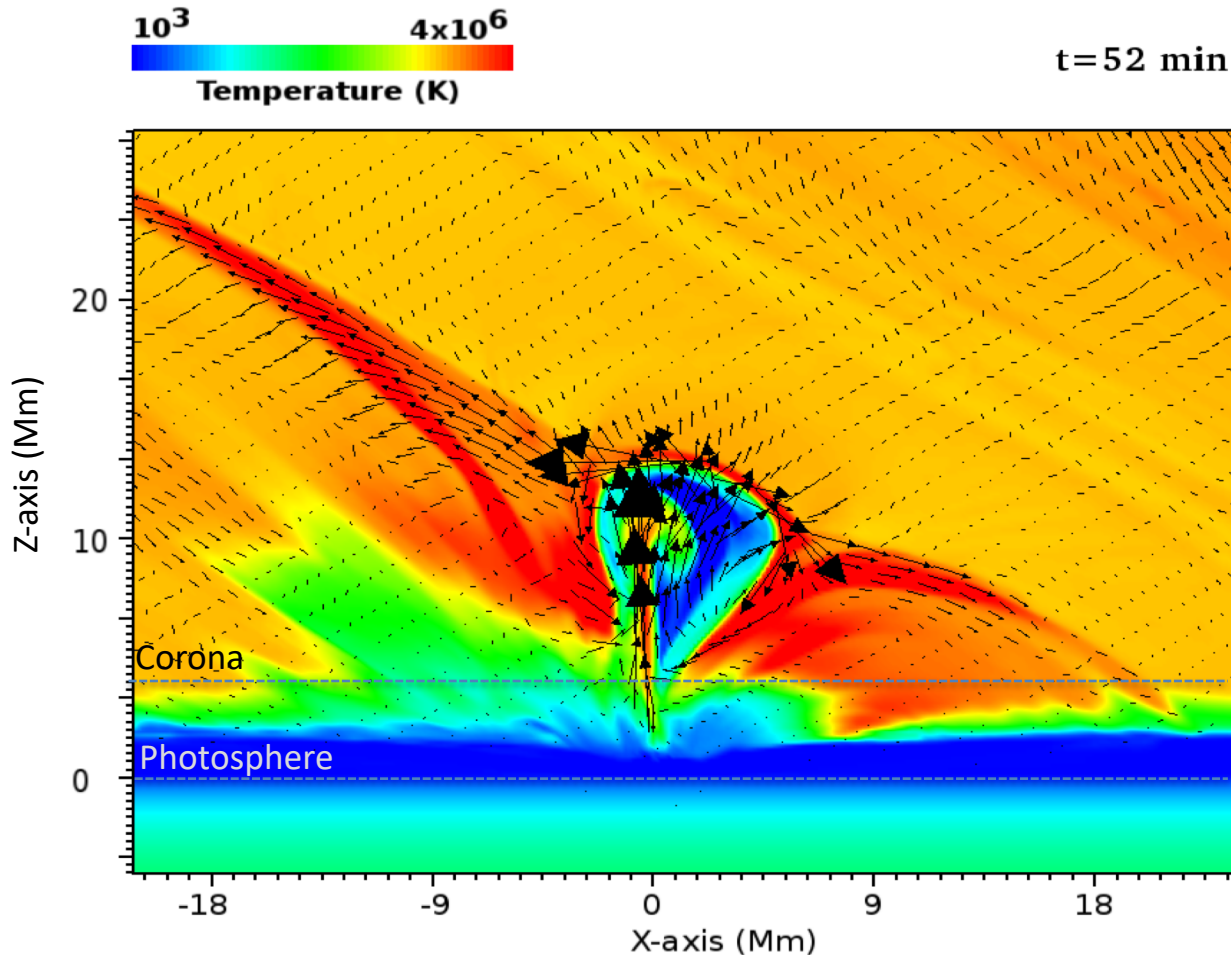
Additional heating (10-15 mK).

Wider jet's mainstream and external arcade.

TR (cool) plasma emission.

- Cool and dense material erupts. External reconnection is triggered.
- Wider external arcade.

'Blowout' jet driven by eruption - Temperature



Eruption of flux rope.

Internal arcade (5-10 mK).

Upflow/jet (400-500 km/sec).

More external reconnection.

Additional heating (10-15 mK).

Wider jet's mainstream and external arcade.

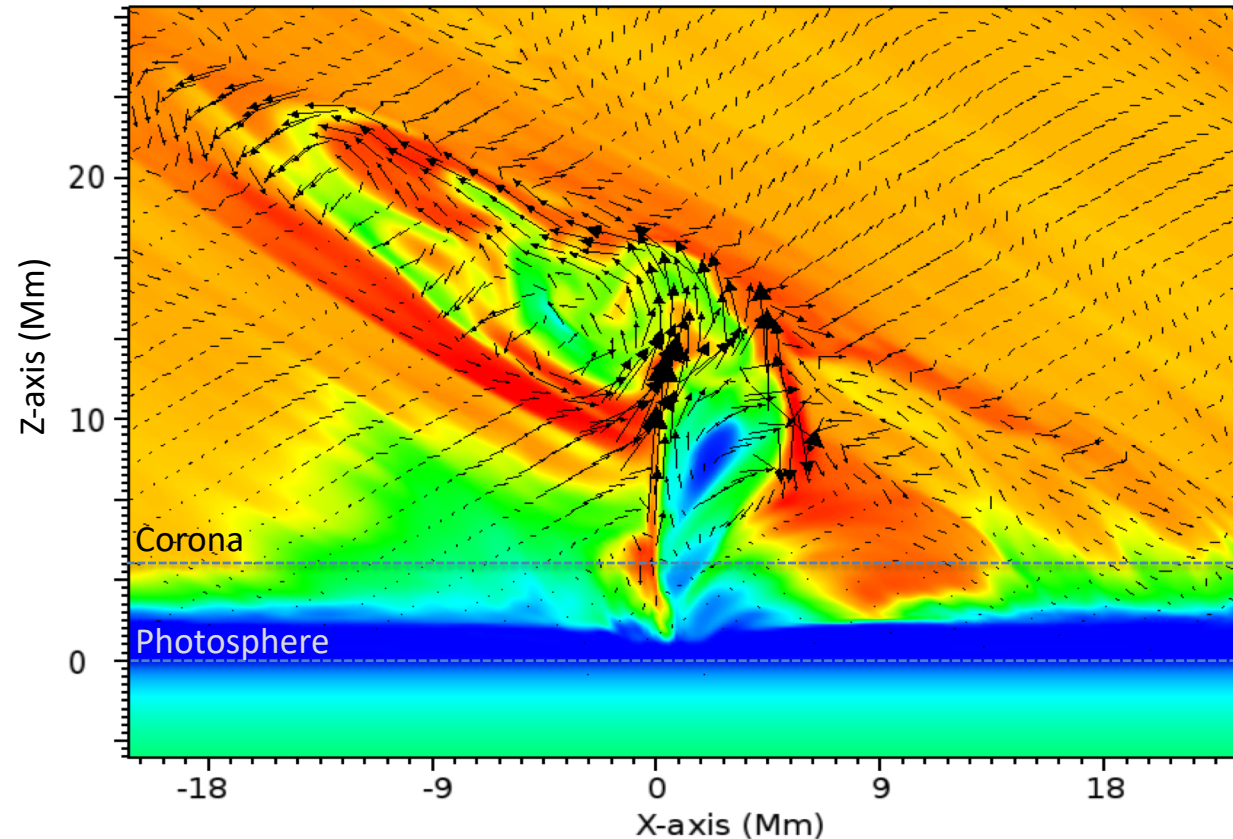
TR (cool) plasma emission.

- Internal reconnection. BP is formed.
- More heating at the external arcade, which grows in size.
- Upward channel of the jet becomes wider.

'Blowout' jet driven by eruption - Temperature

10^3 4×10^6
Temperature (K)

t = 53 min



Eruption of flux rope.

Internal arcade (5-10 mK).

Upflow/jet (400-500 km/sec).

More external reconnection.

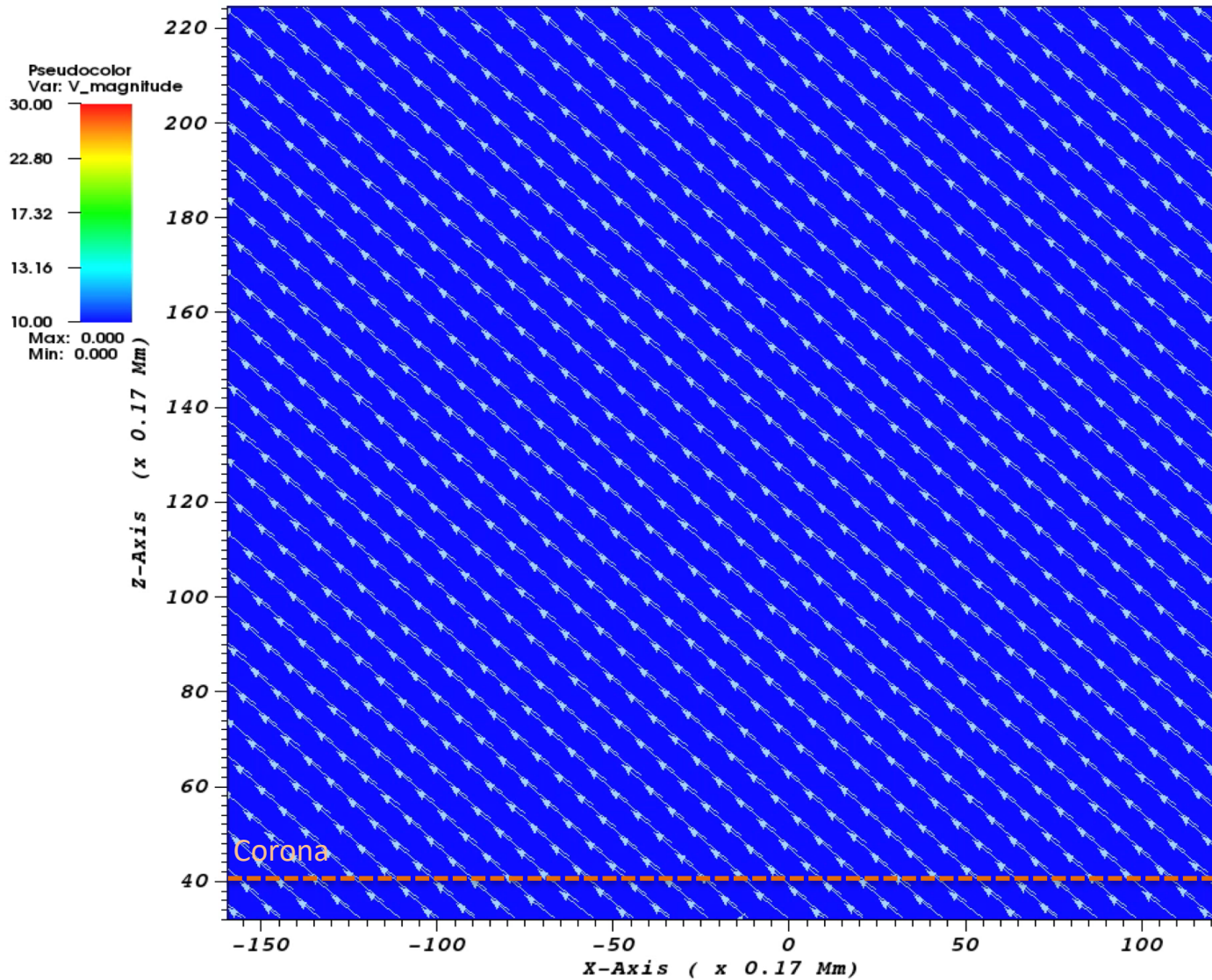
Additional heating (10-15 mK).

Wider jet's mainstream and external arcade.

TR (cool) plasma emission.

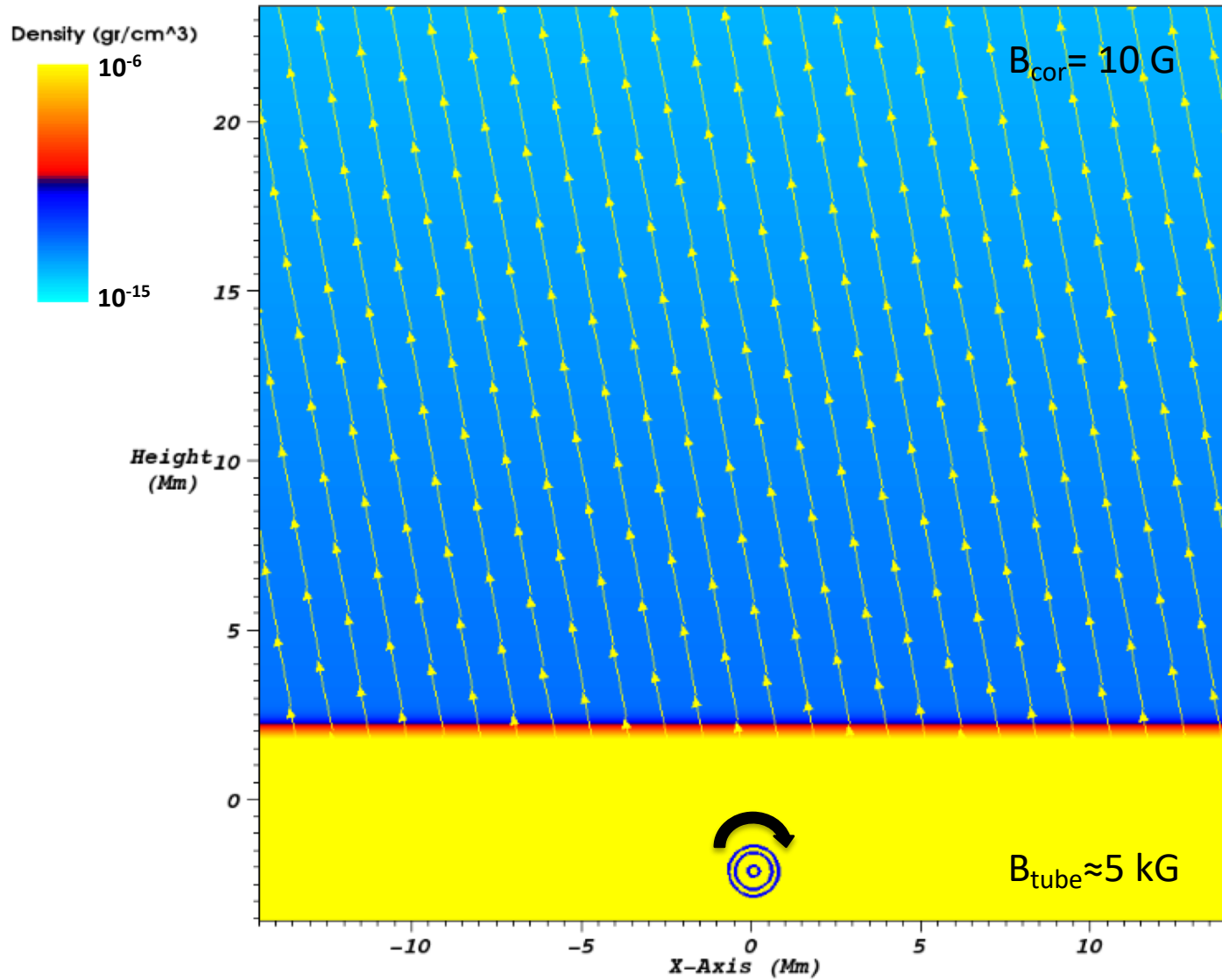
- Kinetic energy $\sim 8 \times 10^{27}$ erg
- Poynting flux per unit of surface at the top of the box $\sim 4 \times 10^5$ erg/s/cm².
- Propagation of torsional Alfvén wave, Lee, E. et.al, ApJL (2015).

Velocity (≥ 70 km/sec)



Time=0 (min)

Initial magnetic field configuration



Numerical experiments: MHD equations

$$\frac{\partial \rho}{\partial t} = -\nabla \cdot (\rho \mathbf{u}),$$

$$\frac{\partial (\rho \mathbf{u})}{\partial t} = -\nabla \cdot (\rho \mathbf{u} \otimes \mathbf{u} + \underline{\underline{\tau}}) - \nabla p + \rho \mathbf{g} + \frac{\mathbf{J}}{c} \times \mathbf{B},$$

$$\frac{\partial e}{\partial t} = -\nabla \cdot (e \mathbf{u}) - p \nabla \cdot \mathbf{u} + Q_{\text{Joule}} + Q_{\text{visc}},$$

Mass,

momentum and

energy conservation eqs.

$$\frac{\partial \mathbf{B}}{\partial t} = -c \nabla \times \mathbf{E},$$

$$\mathbf{E} = -\frac{\mathbf{u}}{c} \times \mathbf{B} + \eta \frac{\mathbf{J}}{c^2},$$

$$\mathbf{J} = \frac{c}{4\pi} \nabla \times \mathbf{B},$$

Faraday,

Ohm and

Ampere's law.

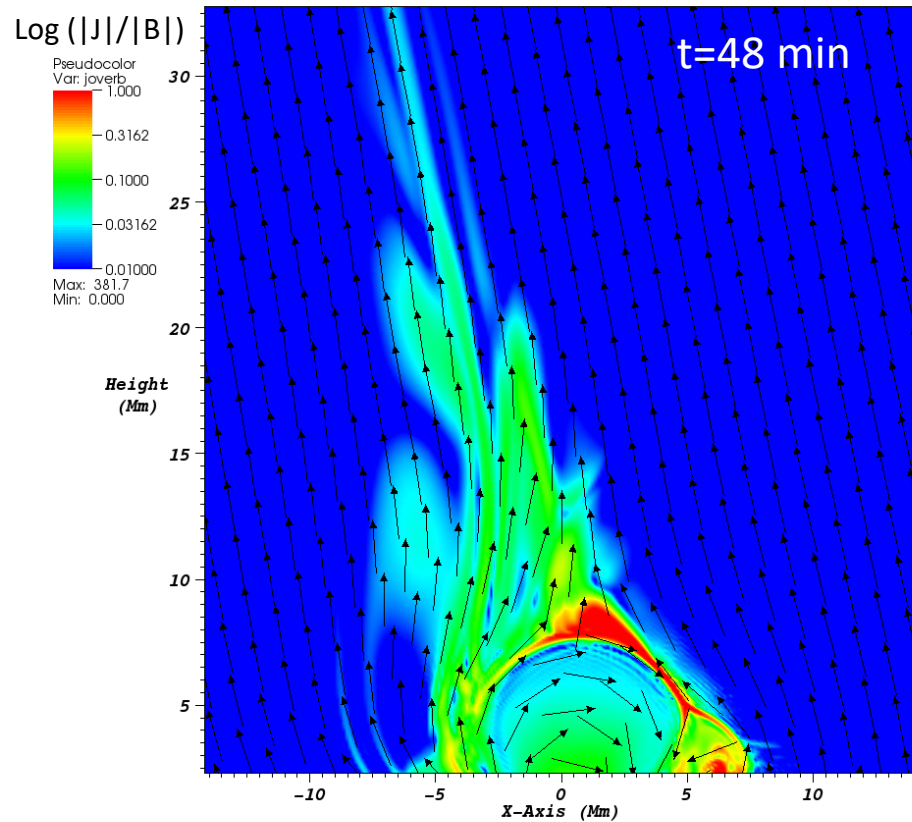
$$p = \rho T \frac{\mathcal{R}}{\bar{\mu}},$$

EOS.

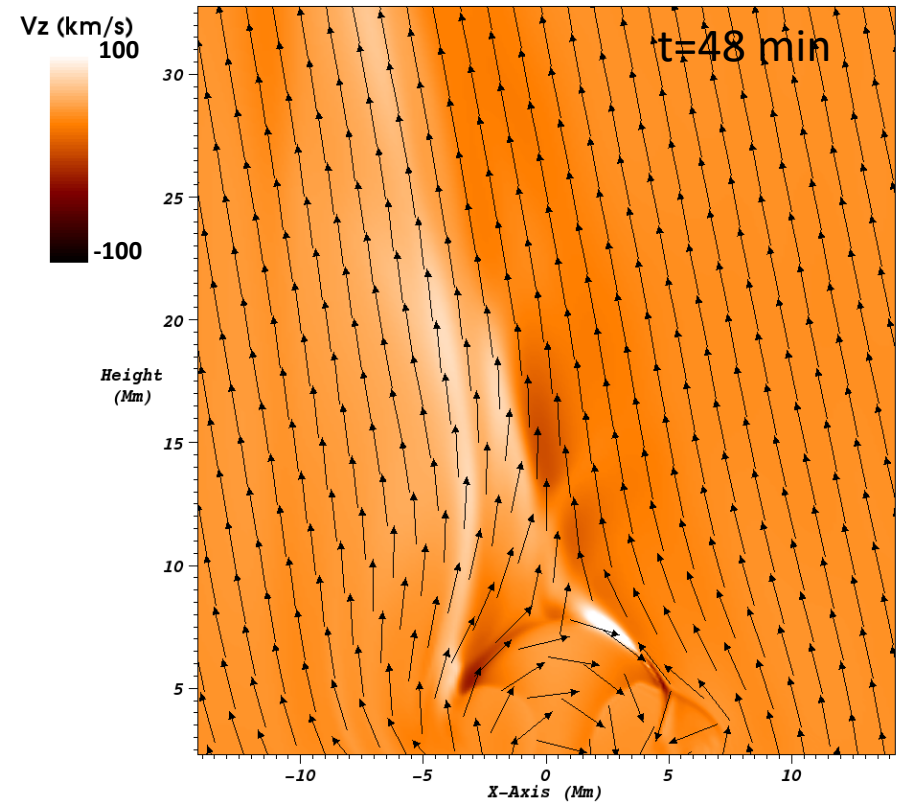
Thermodynamics: ideal gas, no heat conduction, no radiative cooling.

3D model: 'Standard' (?) reconnection jet .

Current distribution



Velocity map

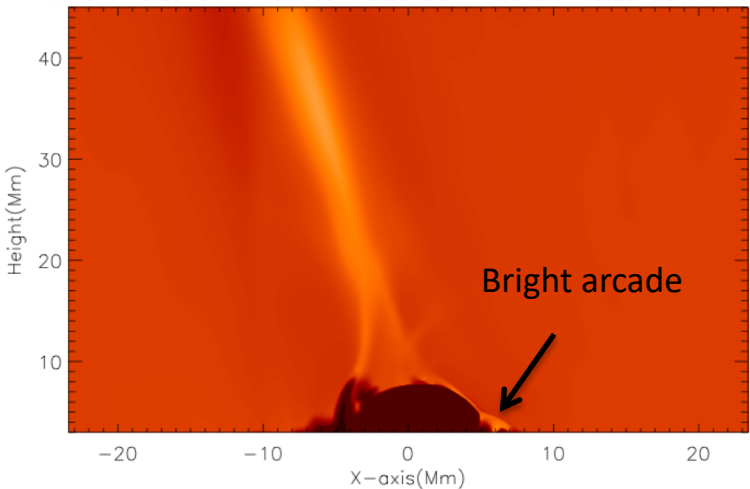


- Structure of current more complex than expected – helical jet?
- Velocity shows the inverted-Y shape of the jet as a whole.

3D model: 'Standard' (?) reconnection jet .

Temperature (K)

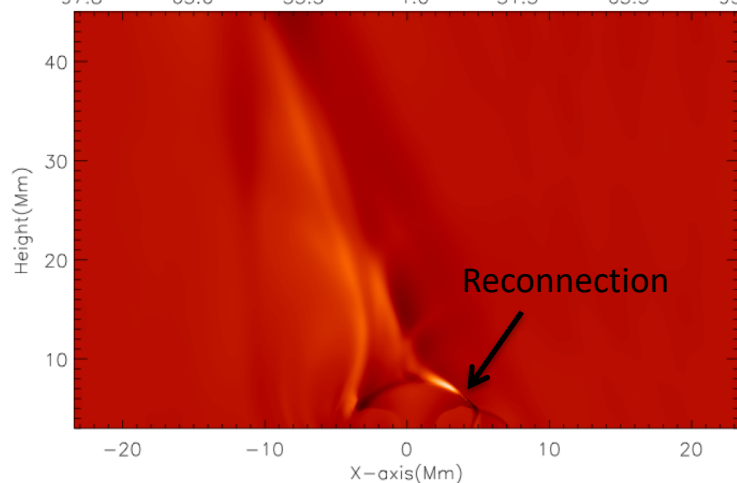
1.0e+04 3.2e+04 1.0e+05 3.2e+05 1.0e+06 3.2e+06 1.0e+07



t=48 min

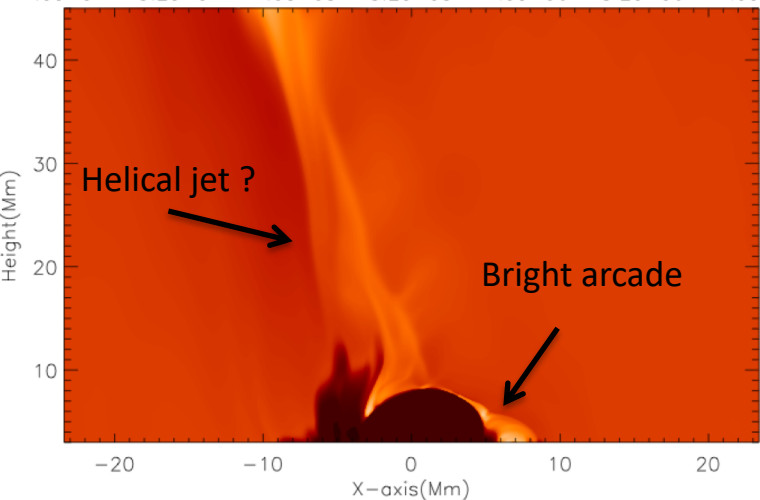
Velocity (km/sec)

-97.8 -65.6 -33.3 -1.0 31.3 63.5 95.8



Temperature (K)

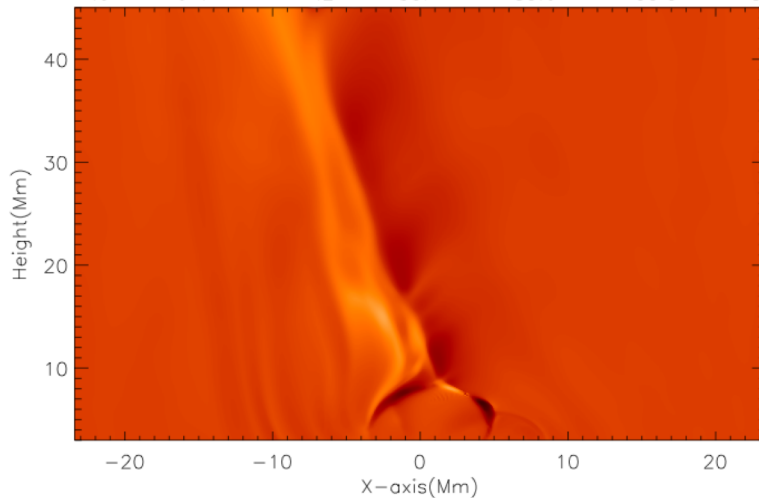
1.0e+04 3.2e+04 1.0e+05 3.2e+05 1.0e+06 3.2e+06 1.0e+07



t=52 min

Velocity (km/sec)

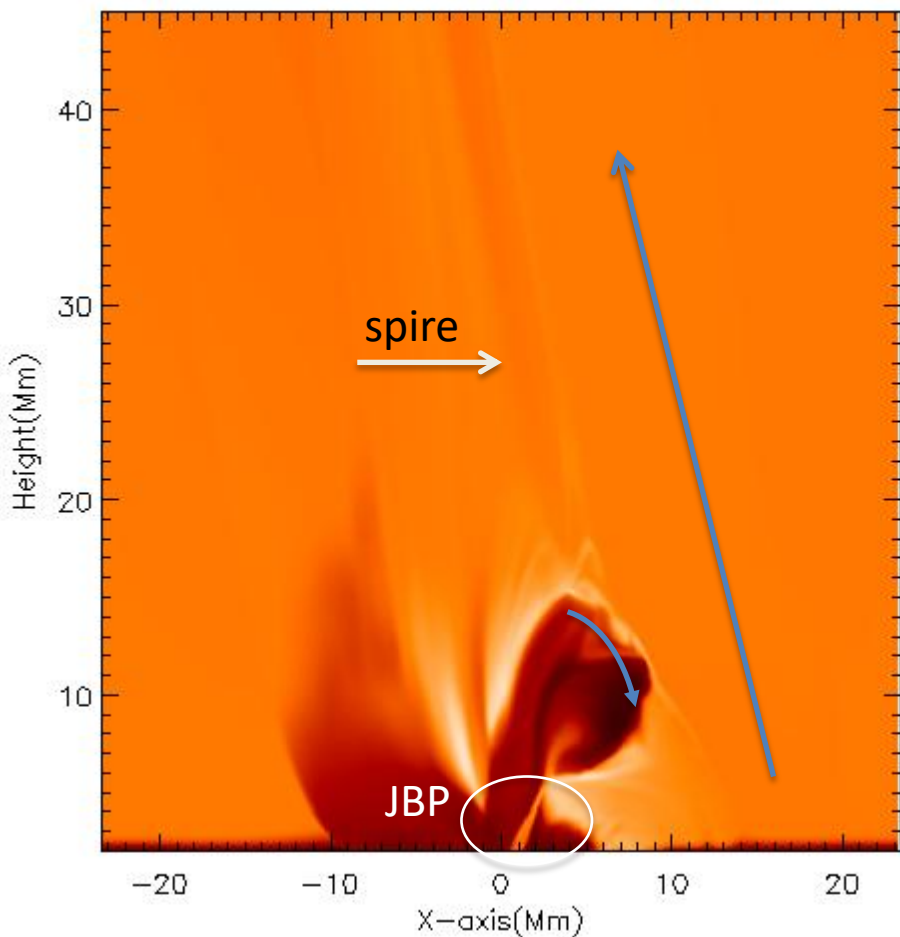
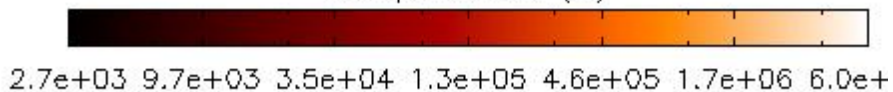
-114.0 -64.1 -14.2 35.7 85.6 135.5 185.4



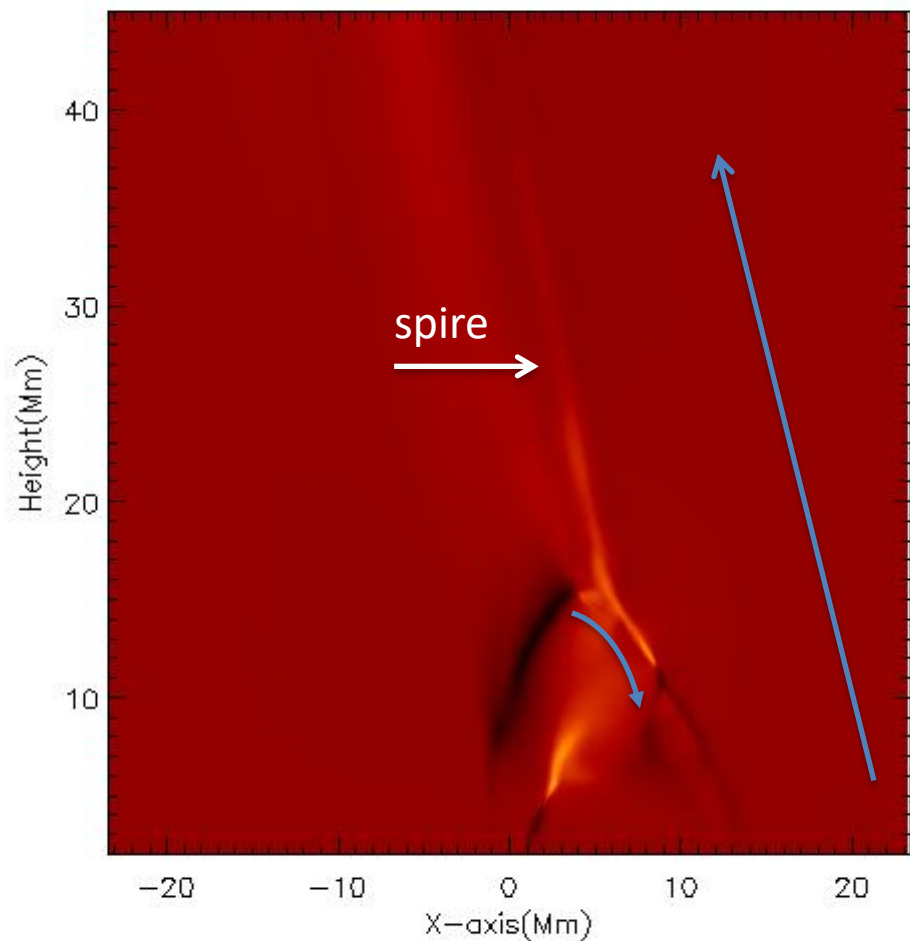
But FEM models reproduce the basic observed features!!

t=62 min

Temperature (K)



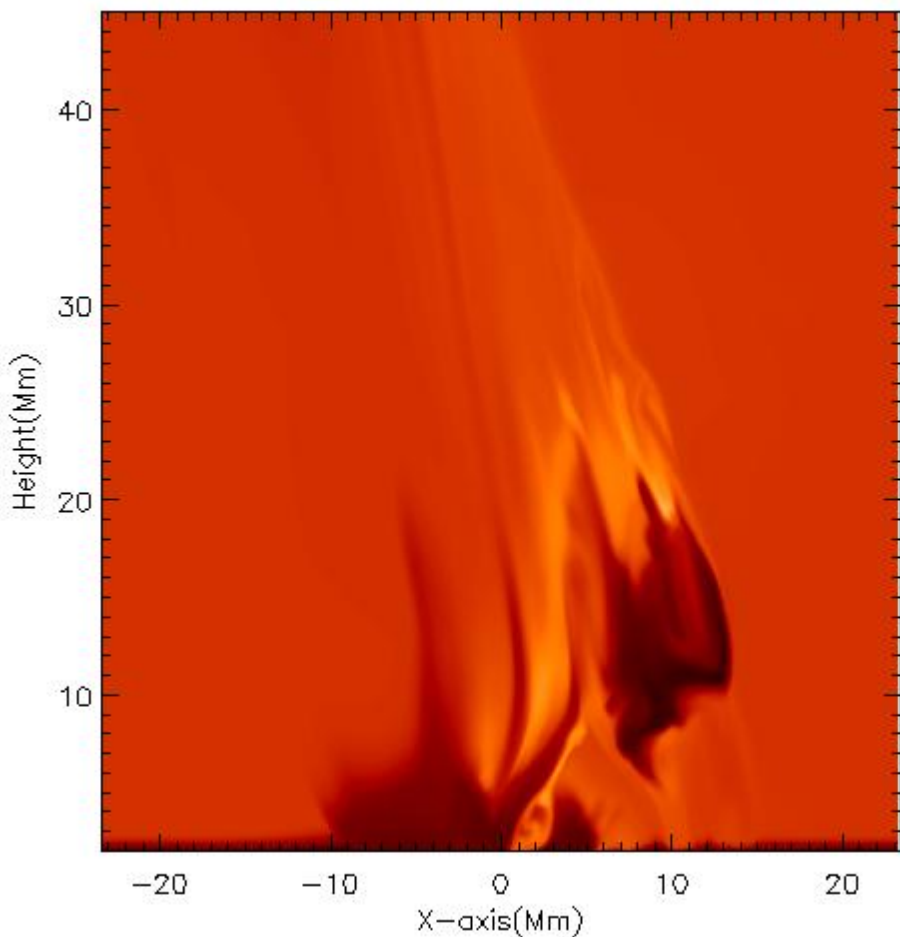
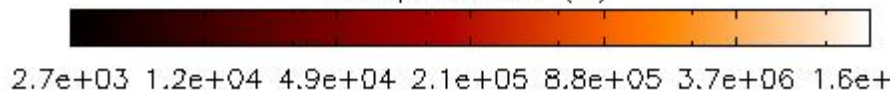
Vz(km/sec)



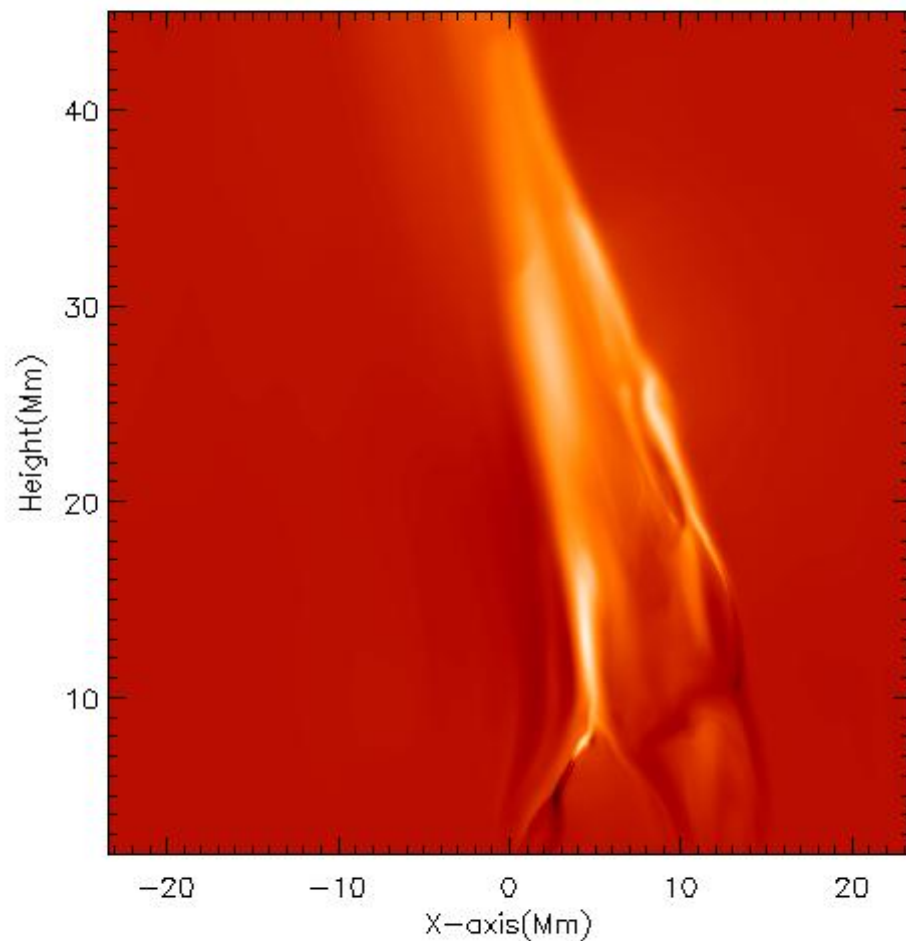
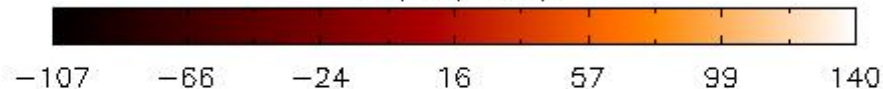
But FEM models reproduce the basic observed features!!

t=64 min

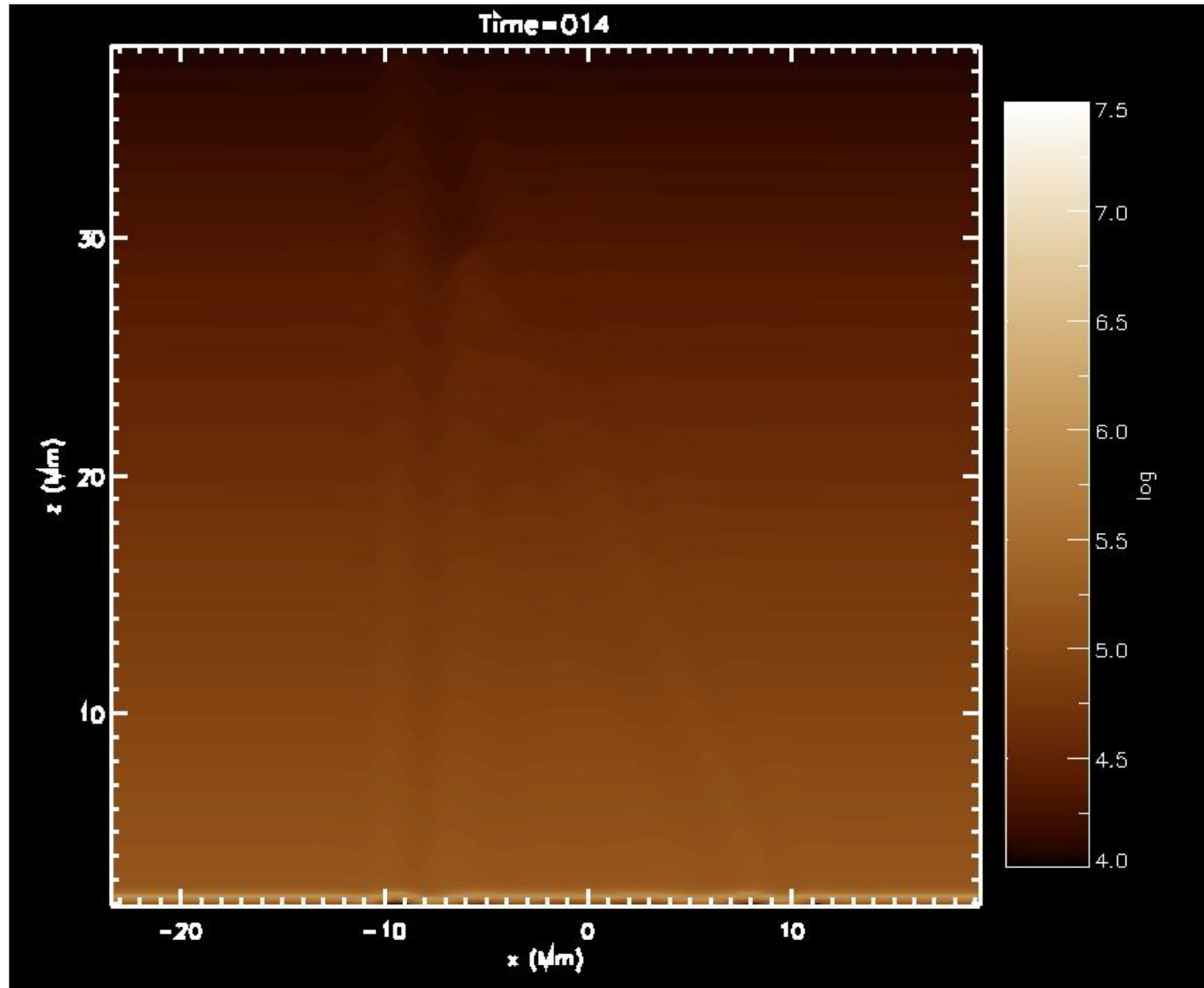
Temperature (K)



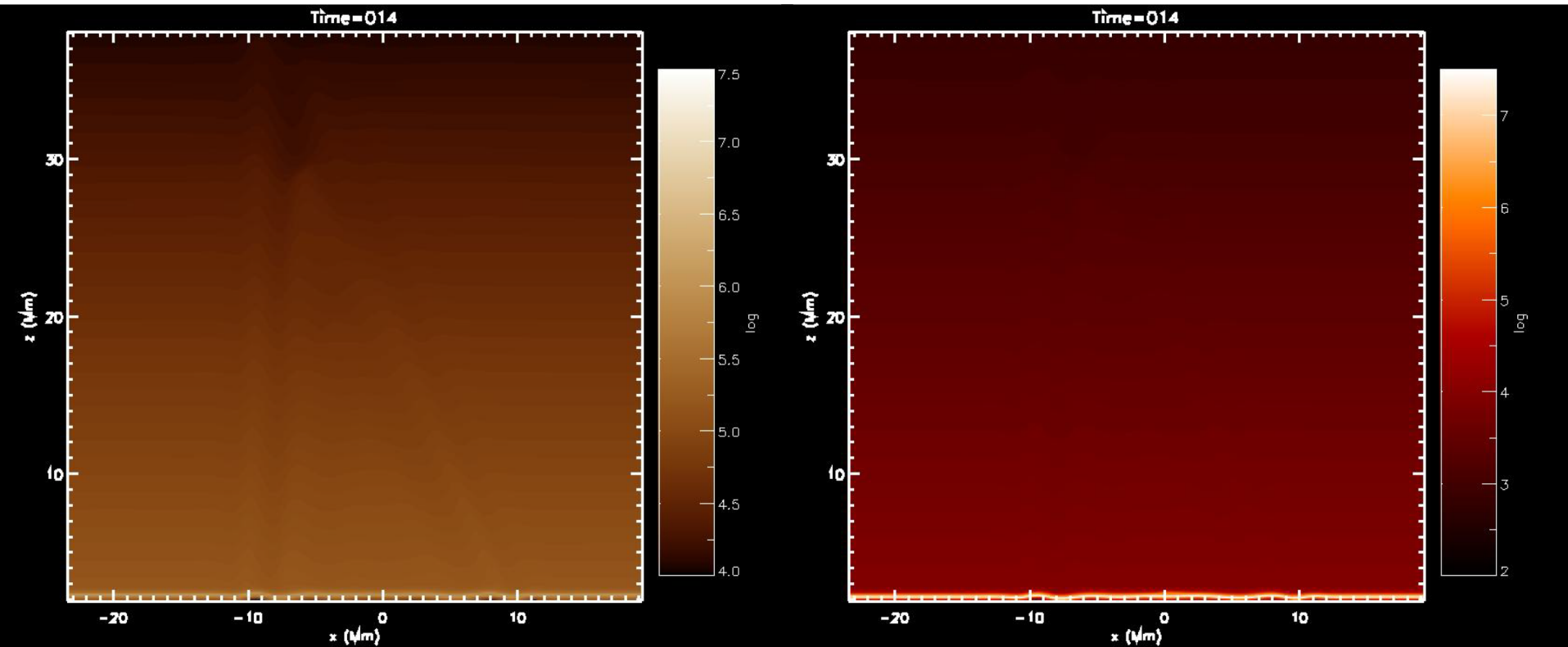
Vz(km/sec)



Pseudo-synthetic images (193 A)



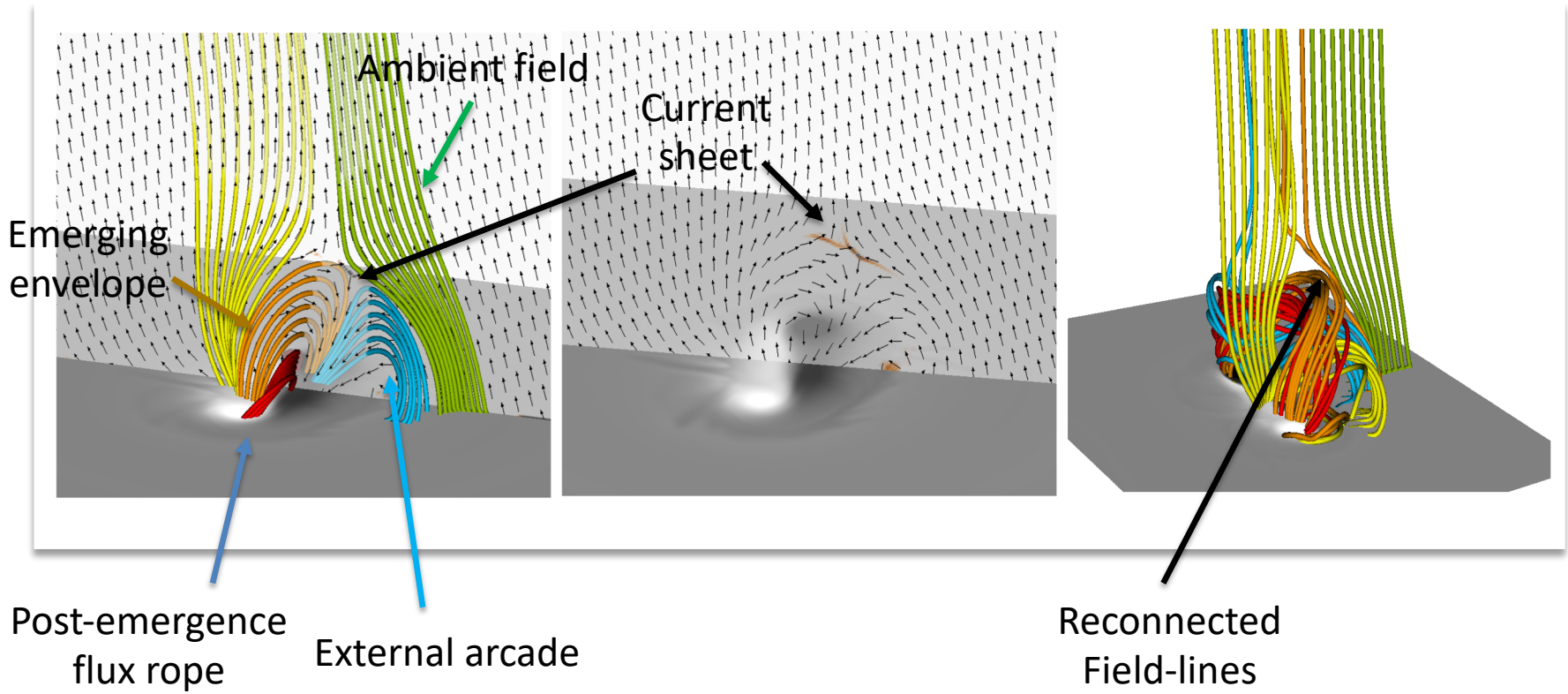
But FEM models reproduce the basic observed features!!



Work by Petros Syntelis on multi-thermal structure of blowout jets.

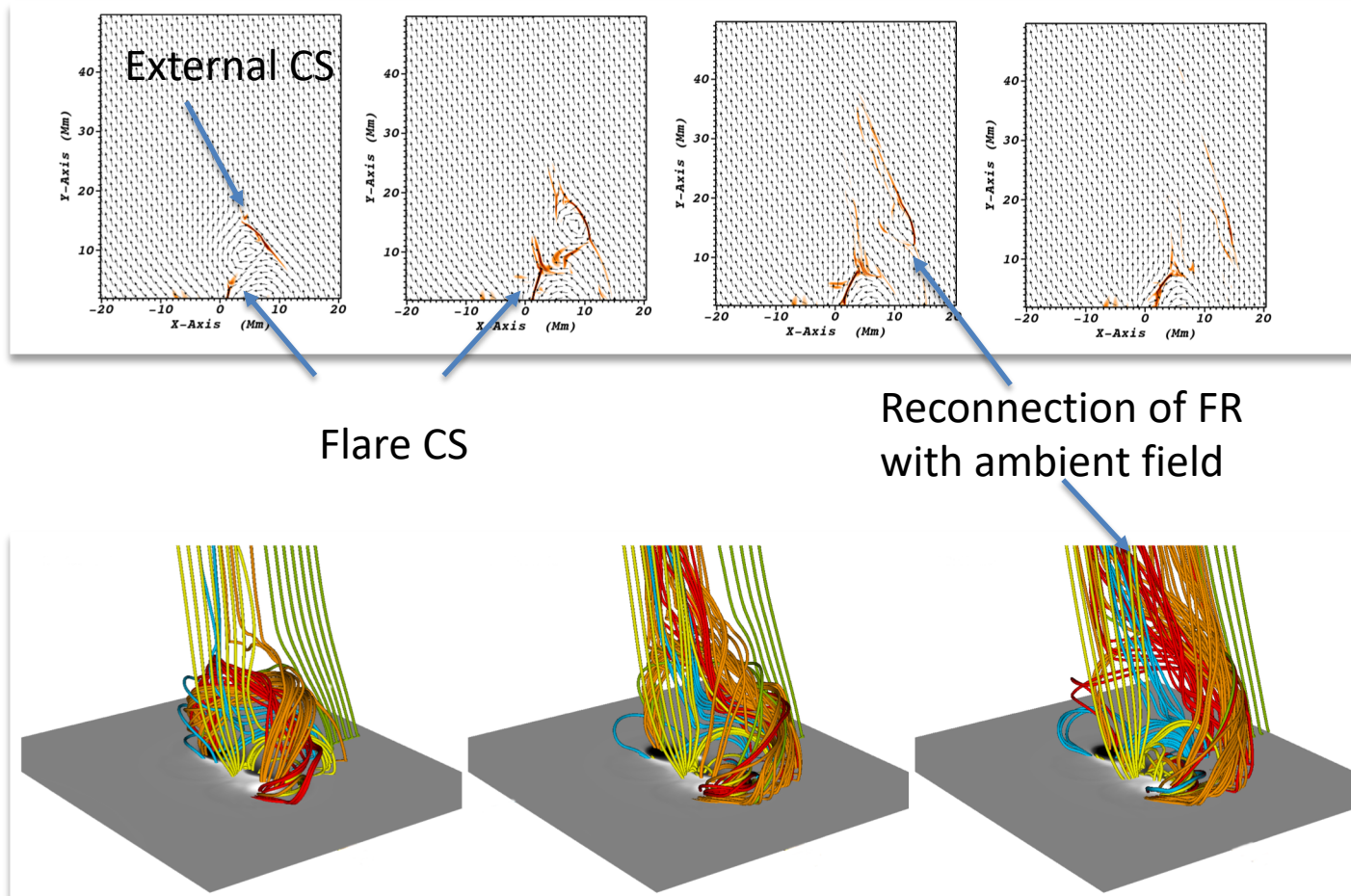
High B_0 case – Fieldline topology I

- Envelope field constantly reconnects with ambient field.
- Filament is formed due to shearing and internal reconnection.
- External reconnection constantly destabilized flux rope.



High B_0 case – Fieldline topology II

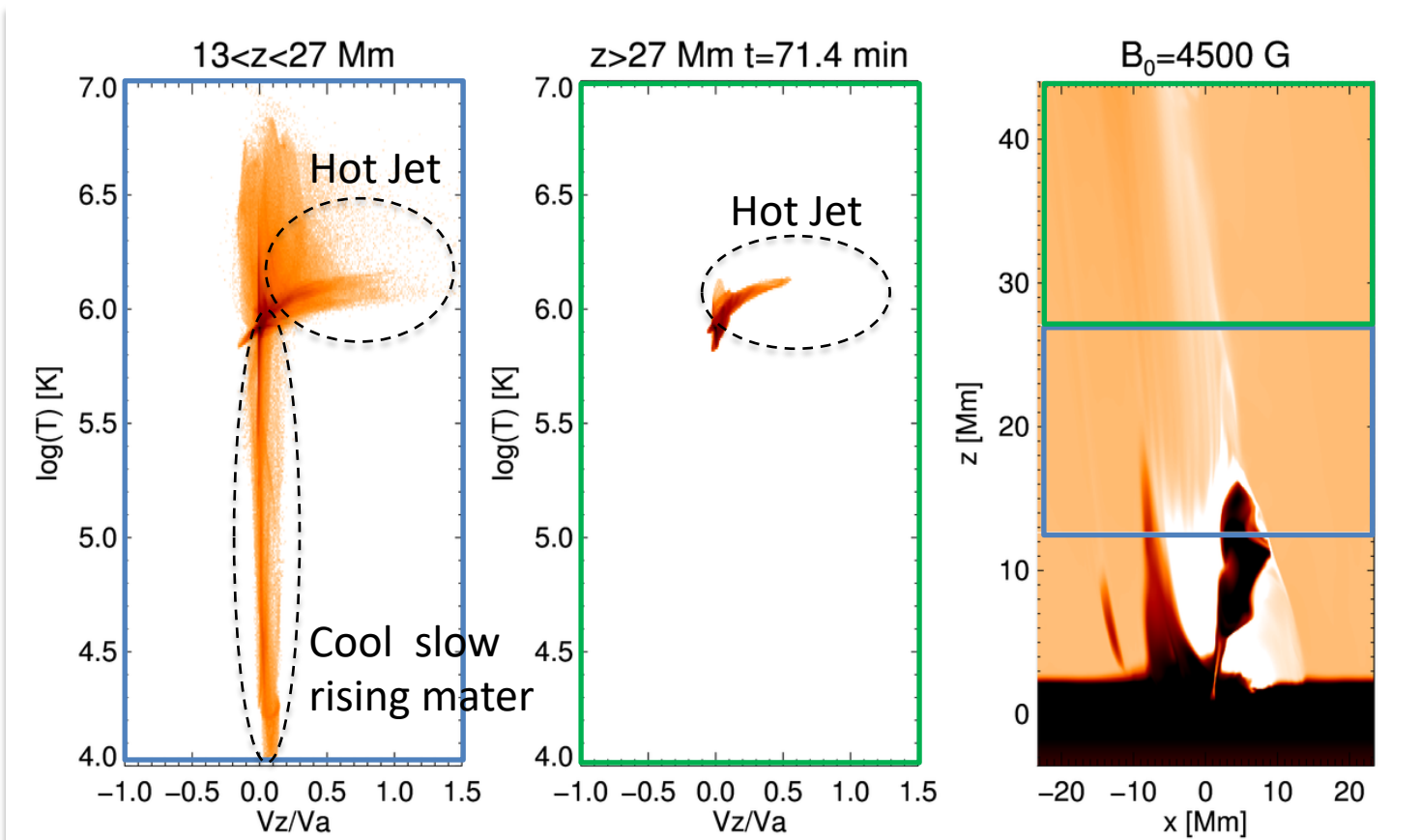
- Flare current sheet is formed
- Filament reconnects with ambient field and transfers cool plasma to ambient field (blow-out)
- Helical motions due to torsional Alfvén wave (Lee, Archontis, Hood 2015)



High B_0 case – Temperature & Energy

Before filament eruption:

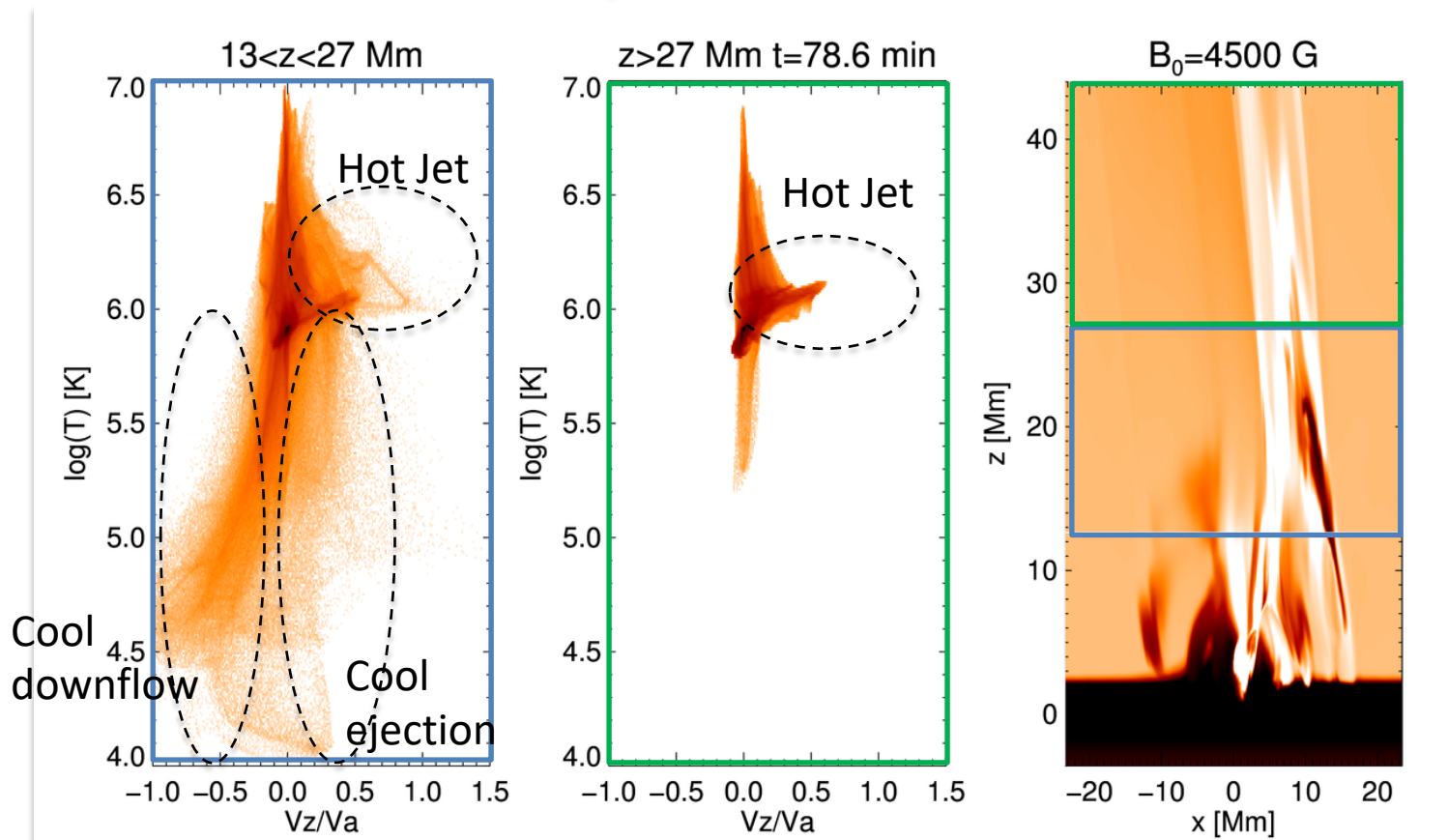
- Slow rising low lying cool filament plasma
- Fast high and low lying reconnection jet



High B_0 case – Temperature & Energy

Beginning of filament eruption:

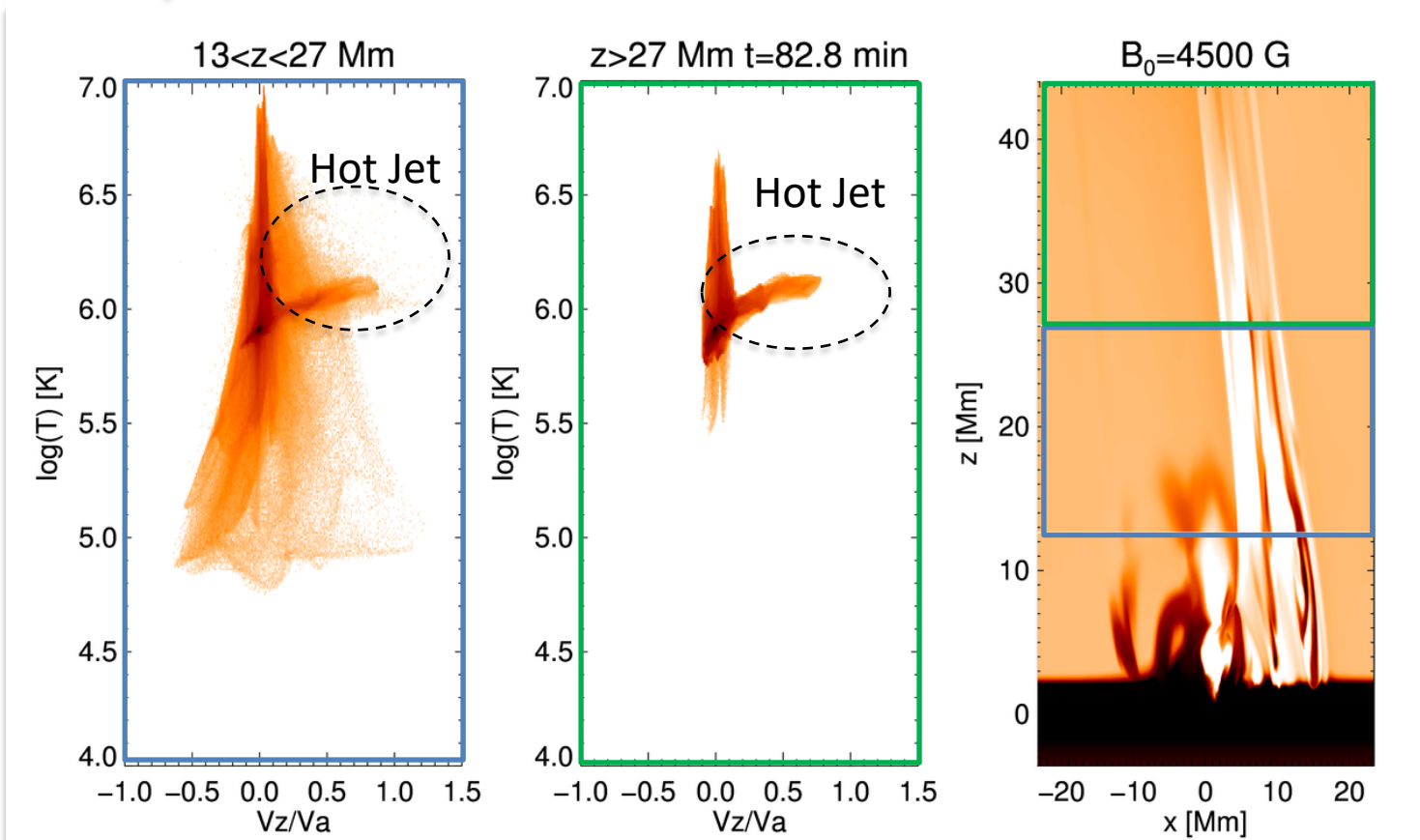
- Hot reconnection jet along the whole spire
- Cool upflows along most of the spire
- Cool downflows at the lower spire



High B_0 case – Temperature & Energy

Ending of filament:

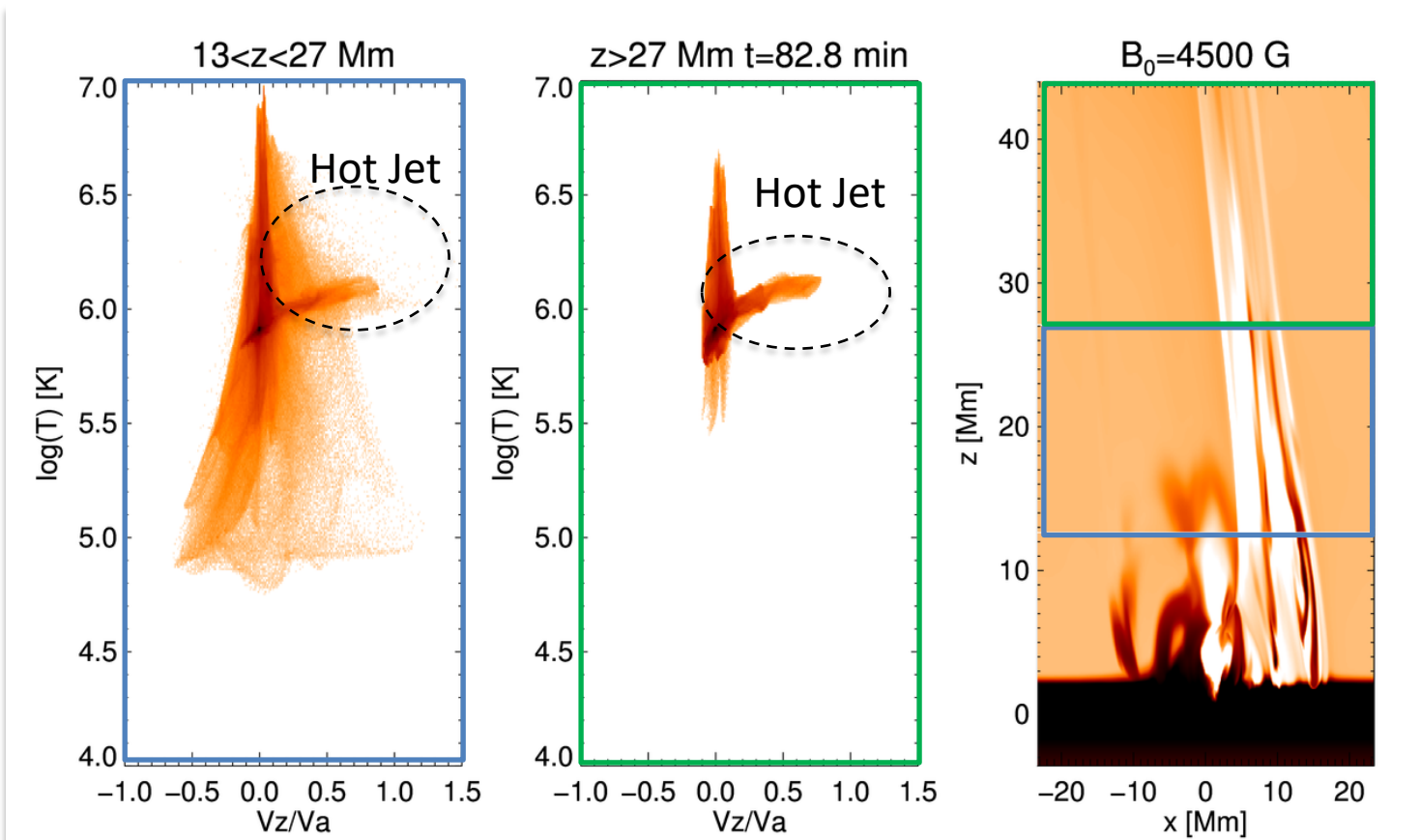
- The hot reconnection jet remain along the jet and dominates upper spire
- Cool upflows and downflows remain close to the emerging region
- Cooler plasma has drained or heated



High B_0 case – Temperature & Energy

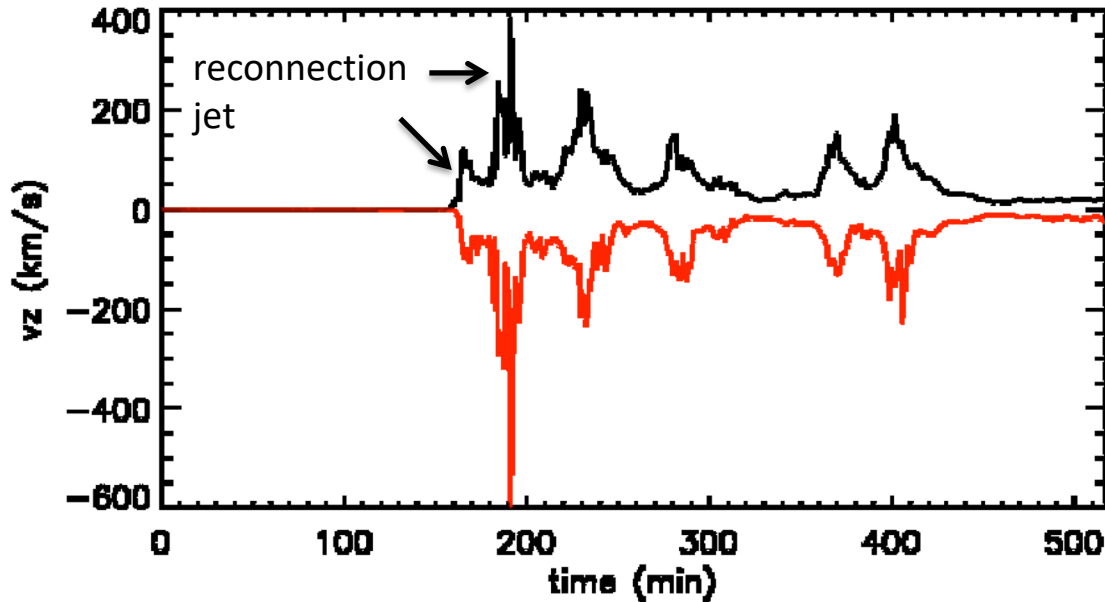
Energy scales of the jet:

- Kinetic energy $\sim 8 \times 10^{27}$ erg
- Poynting flux per unit of surface at the top of the box $\sim 4 \times 10^5$ erg/s/cm²



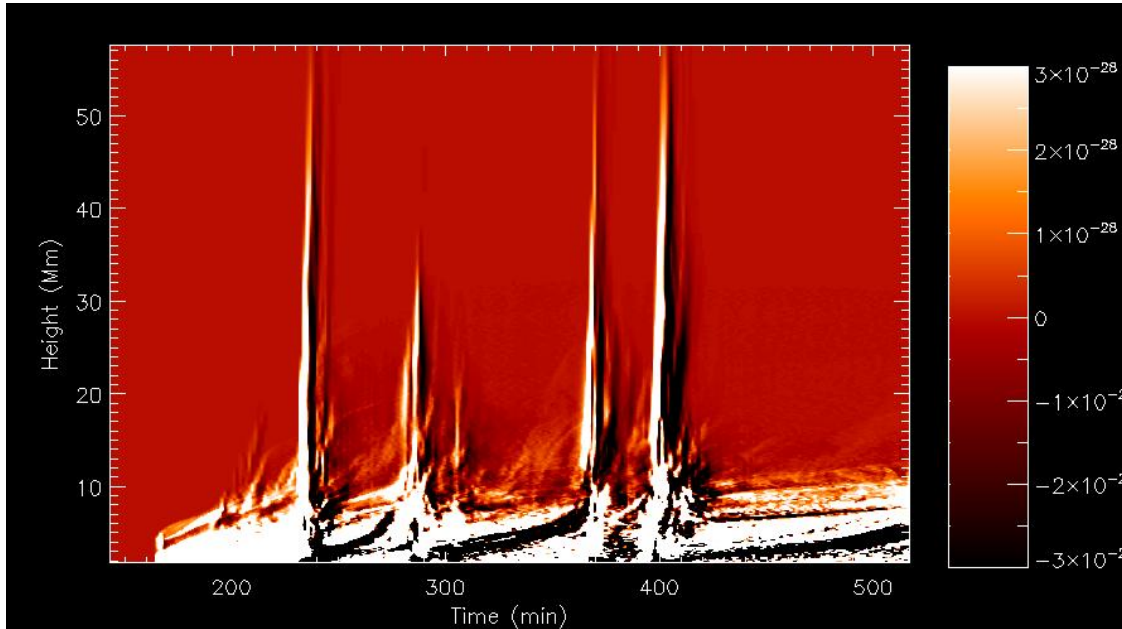
Work by Eon Lee on the
propagation of torsional Alfvén
waves along the blowout jets.

Recurrent jets



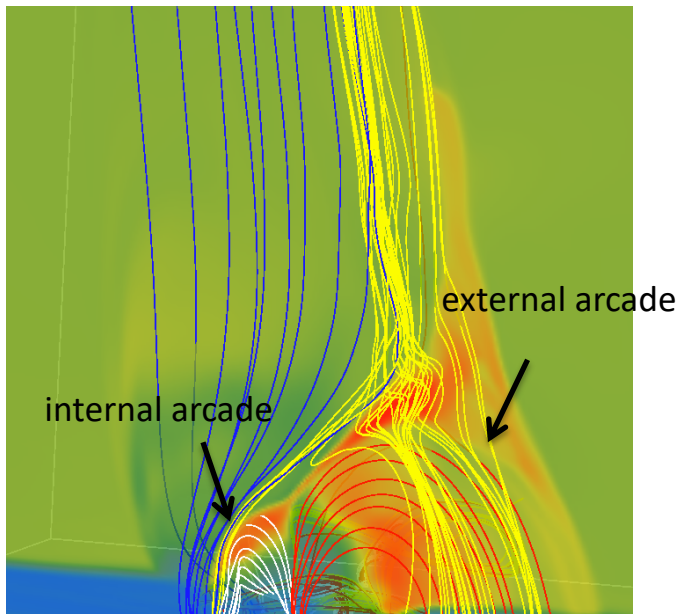
- Black – $\max v_z$
- Red – $\min v_z$
- Bidirectional flows
- 5 major events

E. J. Lee, V. Archontis, and A. W. Hood 2015 ApJL 798, L10

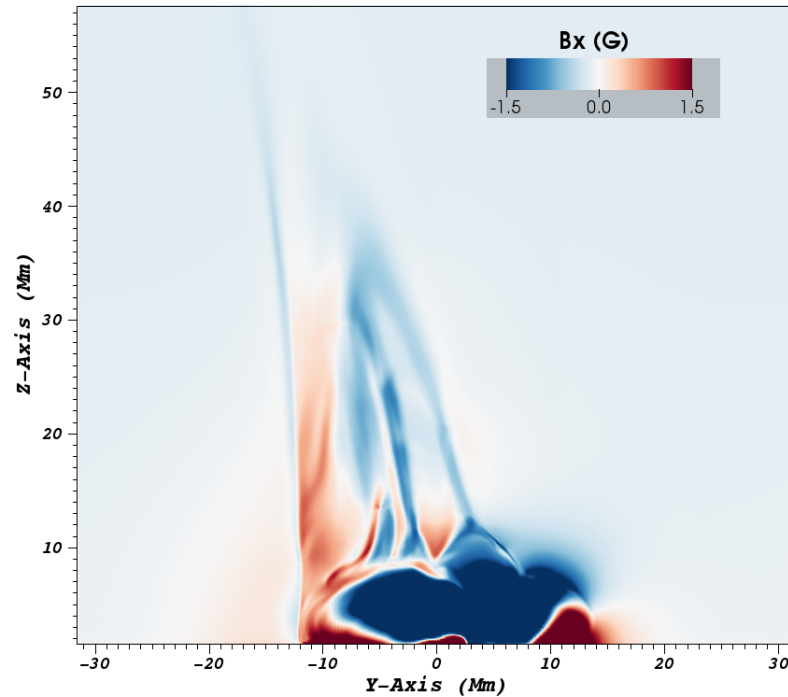
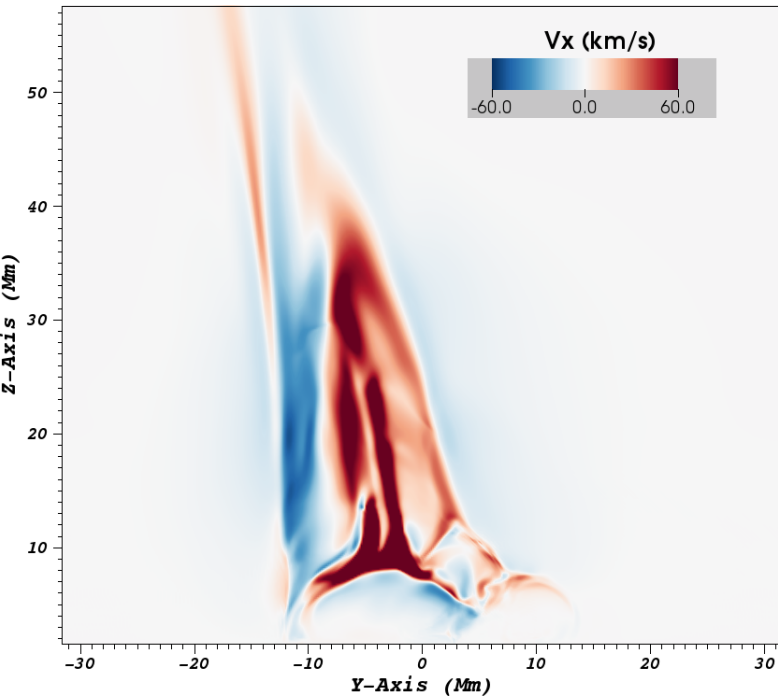


- Running difference of $\int \rho^2 dx dy, T > 8.0 \times 10^5 \text{ K}$
- 4 profound events, correspond to the 4 blowout jets
- The small spikes correspond to small reconnection jets and also pressure driven jets

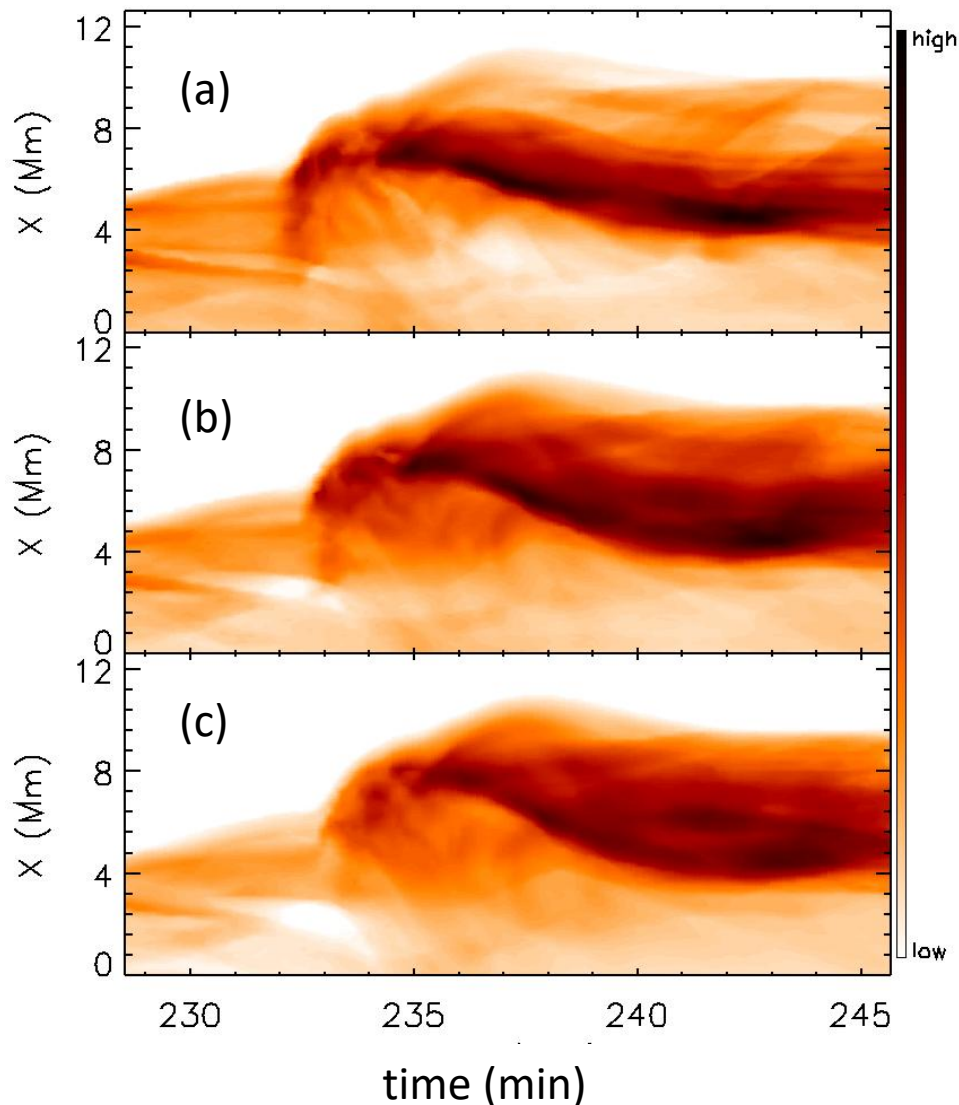
t=232.8 min



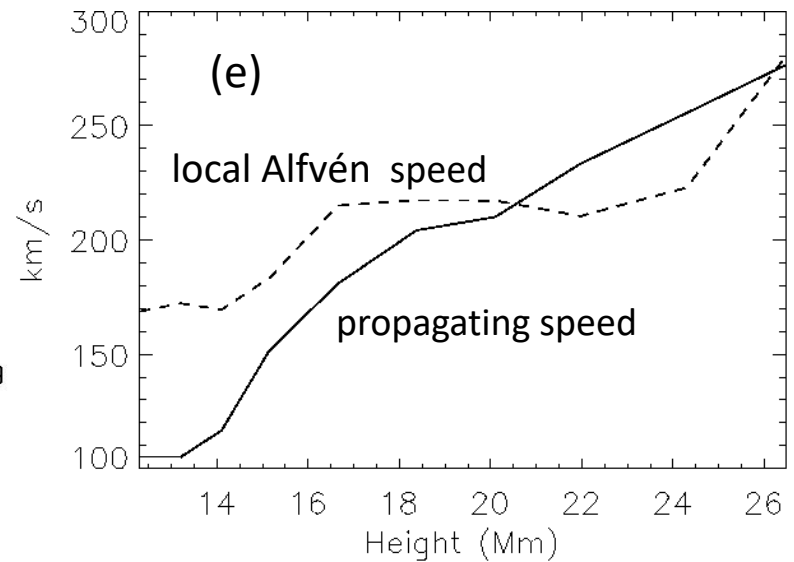
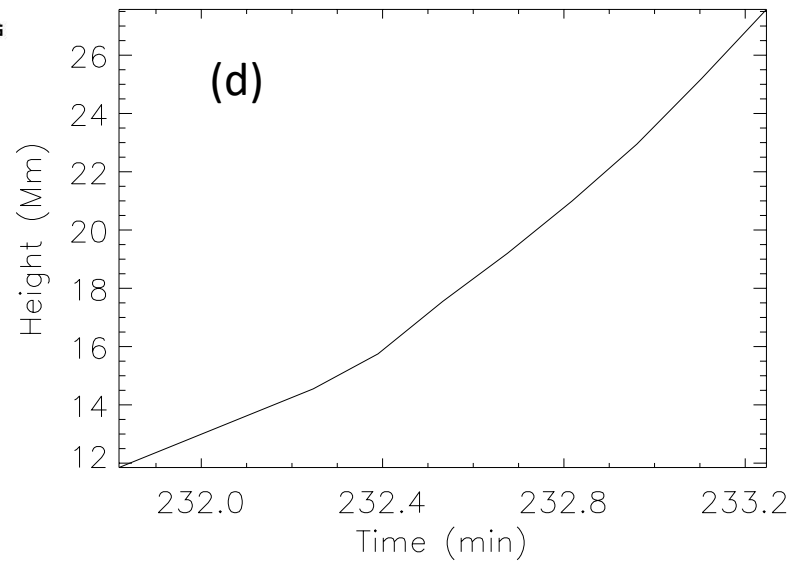
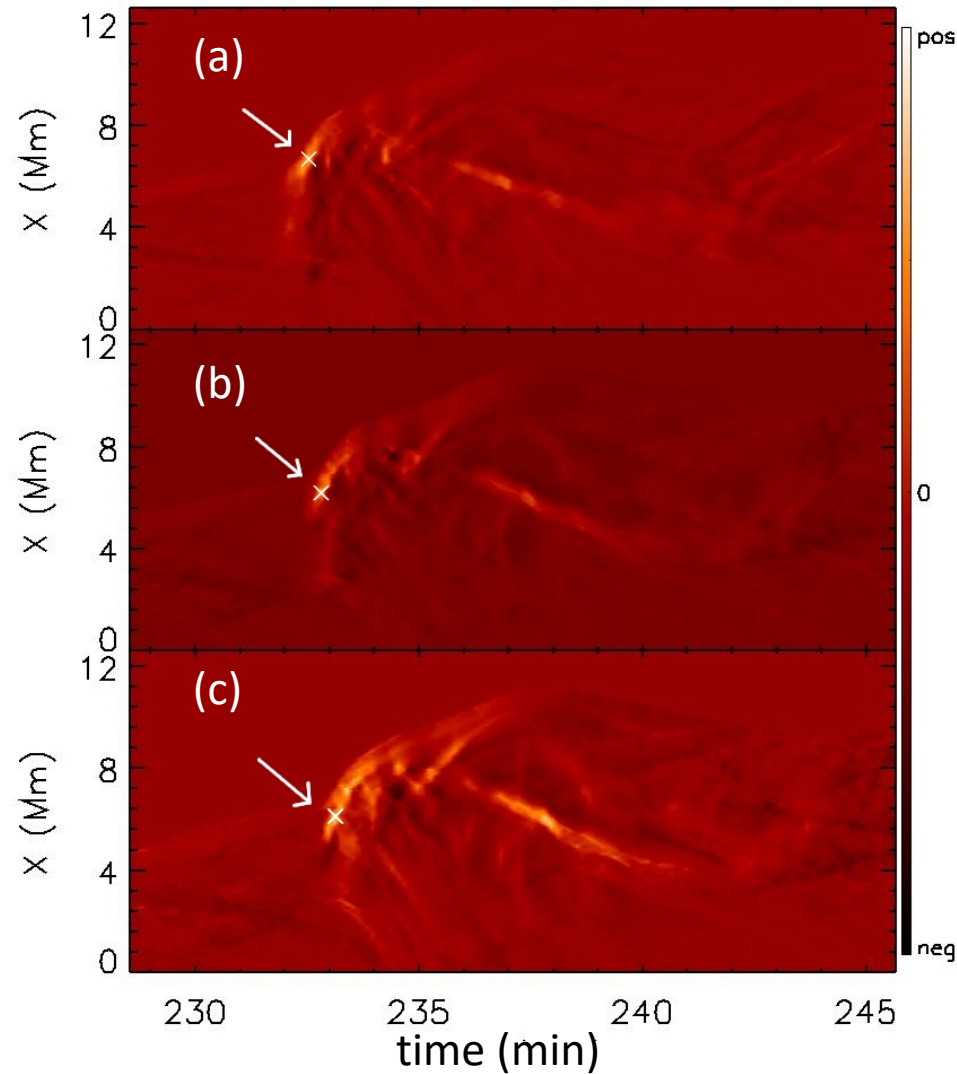
- Yellow – twisted fieldlines from blowout jet
- Blue – previously reconnected fieldlines
- Red – external arcade
- White – internal arcade
- Direction of flow (v_x) is opposite to direction of fieldlines (B_x) – untwisting of fieldlines.



Transverse movement of the jet




- Distance-time diagram of $\int \rho^2 dy$ where $6.0 \times 10^5 \text{ K} < T < 1.2 \times 10^6 \text{ K}$
- (a): $z=17 \text{ Mm}$
- (b): $z=21.5 \text{ Mm}$
- (c): $z=25 \text{ Mm}$
- Plasma moving towards +ve x , then -ve x , then back to +ve x
- Jet undergoes oscillatory motion during emission
- Transverse oscillation velocity amplitude $\approx 7 \text{ km s}^{-1}$
- Oscillation propagates from low to higher height



- (a-c): Running difference of previous 3 diagrams
- (d): Height-time profile of the front of the jet (white cross in a-c)
- (e): Propagating speed (solid line), local Alfvén speed (dashed line)
- propagating speed comparable to Alfvén speed, torsional Alfvén wave

Hinode XRT: Observation of X-Ray jets in coronal holes.



Solar-B XRT Jets
January 10, 2007